

## Tactile Feedback Using Surface Acoustic Wave

Masaya Takasaki<sup>1</sup> and Takeshi Mizuno<sup>1</sup>

<sup>1</sup>Saitama University  
E-mail: masaya@ieee.org

### Abstract

*This paper deals with tactile display using surface acoustic wave (SAW). Basic principle to indicate human tactile sensation, especially for roughness sensation, is described. The first prototype of the display and a controller are reported. A large transducer to expand the display area size is introduced. SAW indirect excitation method to solve size problem of the piezoelectric material substrate was proposed. According to the proposal a transparent SAW transducer was fabricated and installed on a LCD. With the method, fabrication of a large glass substrate transducer was also carried out.*

Keywords: Ultrasonics, Surface acoustic wave, Tactile sensation, Virtual reality

### 1. Introduction

Recently, indication of human tactile sensation attracts attentions. The indication can be applied in many fields such as virtual reality, computer interface and so on. To indicate the sensation, proposed devices have employed actuators to deform our finger skin(for example, [1]-[4]). Those actuators need some volume to install them behind the device surface touch area. On the other hand, ultrasonic vibration has been focused by some researchers to indicate the tactile sensation[5]-[9]. They have applied squeeze film effect due to ultrasonic vibration. Sometimes response of the effect is relatively slow to indicate a sharp sensation like roughness.

We focused friction control using surface acoustic wave (SAW) and applied it to the actuation in tactile display. Properties of SAW are high operating frequency of more than a few MHz, thin structure, simple fabrication, easy installation of a transducer, high energy density and so on. A thin tactile display with high performance can be developed using SAW properties. In the case of application of the friction control with SAW, fast response can be expected. Therefore, indication of roughness and its difference can be expected.

Tactile display using SAW is reported in this paper. SAW excitation method and basic structure of the display are described. Fabricated display and its demonstration are reported. To expand application, a new transducer design is proposed. Fabricated transducers according to the proposal are also reported.

### 2. Reproduction of tactile sensation

When we rub rough solid surface, microscopically, vibration is generated in our finger skin. The vibration is perceived at mechanoreceptors in the finger skin. In our brain, signals from the mechanoreceptors are processed according to the rubbing motion and perceived as a tactile sensation. In our approach, generation of the vibration in the finger was focused for tactile display. The tactile sensation of rubbing rough solid surfaces was considered to be controlled by changing the frequency and amplitude of the vibration according to the rubbing motion.

Artificial generation of the vibration in our finger skin seems to be effective to reproduce the tactile sensation, especially roughness sensation. In our research, the vibration was generated by using SAW. Generally, operating frequency of the SAW is too high (more than a few MHz) for human to perceive directly. We applied bursting SAW to excite the artificial vibration. We can expect indication of

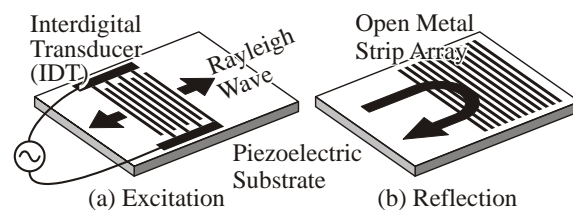


Fig. 1. Excitation and reflection of SAW

sharp sensation, because the SAW excitation response is fast enough for human perception.

### 3. Surface Acoustic Wave

Figure 1 (a) indicates the excitation of Rayleigh wave, a kind of SAW. An interdigital transducer (IDT) is arranged on a piezoelectric substrate (Single crystals are usually used for SAW devices). The IDT consists of a metal strip array. When AC driving voltage is applied to the IDT, Rayleigh wave is excited and propagates on the substrate surface in the direction indicated by the arrows in the figure. The frequency of the driving voltage is decided according to the size of the IDT, particularly pitch of the IDT electrodes. The substrate is also used as a medium on which Rayleigh wave propagates. In the case of Rayleigh wave, the vibration propagates with gathering its vibration energy of more than 90 % in the medium surface of 1 wavelength depth. Therefore, the substrate can be fixed easily, for instance, by applying cement on backside of the transducer.

Standing wave of the Rayleigh wave can be generated easily by combination of two opposed progressive waves. To excite the standing wave, two opposed IDTs or two reflectors with IDTs are required on the piezoelectric substrate surface. The reflector is configured by an open metal strip array (OMSA), as shown in Fig. 1 (b). The IDTs and the reflectors can be formed simultaneously by using a photolithography process.

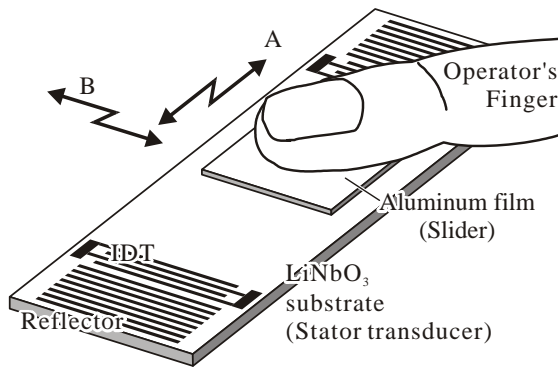


Fig. 2. Basic structure of SAW tactile display

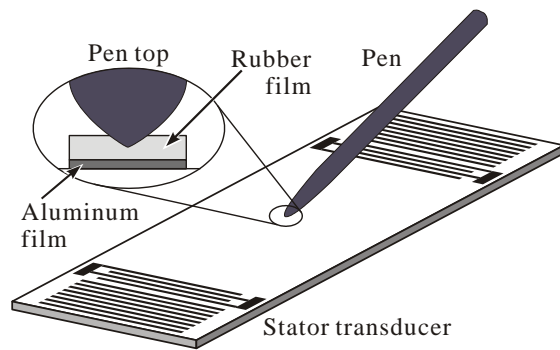


Fig. 3. Pen-tablet type SAW tactile display

### 4. Tactile Display

The schematic diagram of basic structure of the SAW tactile display is shown in Fig. 2. A display operator rubs a stator transducer through a slider, which is consisted by an aluminum film. The film enhances the friction reduction effect mentioned below and also protects operators' fingers from high power/frequency ultrasonic vibration. He/she can rub the area between the IDTs. Tactile indication principle in our research can be applied to pen-tablet type interface as shown in Fig. 3. In this set up, operators can enjoy the sensation while they draw a line with charcoal on craft paper. On the top of the pen, rubber film and the aluminum film were attached. The rubber film plays a role of finger skin in the basic configuration.

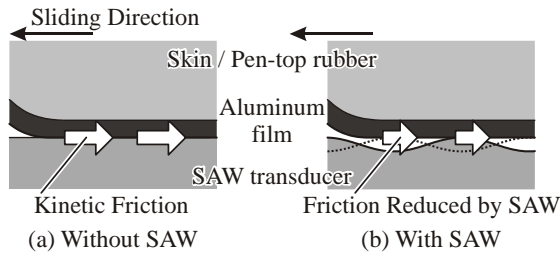
While the finger travels on the SAW transducer, it experiences kinetic friction between the slider and the transducer, as indicated by Fig. 4 (a). When an AC driving voltage is applied to the IDTs, the SAW is excited and propagates on the substrate surface then forms the standing wave. Under the rubbing motion, the friction is reduced by mechanical vibration of the SAW, as illustrated in Fig. 4 (b). With repeat of switching the SAW on and off by pulse modulated driving voltages, the friction can be switched discretely. The slider experiences the repeat of the normal friction and the reduced friction. The repeat results in the vibration under the rubbing motion. Therefore, the vibration can be produced according to the switching. To recognize the controlled friction, the operator must rub the substrate surface with his/her finger through the slider. If the amplitude of the driving voltage is modulated by analog signal, the friction can be arranged continuously. This means that amplitude modulation as well as the switching can be applied to control the vibration on the finger and the pen top.

Figure 5 indicates an example of control system for the SAW tactile display. A motion detector such as an encoder or a camera is attached to the display to detect the position of the finger/pen. Rubbing/drawing speed  $v_m$  [m/s] can be calculated from derivative of the position. Frequency and duty ratio of the control pulses to switch

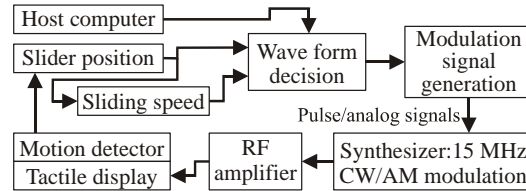
the SAW is decided according to parameters stored in the system. In our equipments, the parameters can be modified by a host computer. Typically, the frequency  $f$  is decided by the following equation.

$$f = \frac{v_m}{k_r} \tag{1}$$

where,  $k_r$  [m] was a stored parameter. Normally, the frequency is DC-1 kHz variable. Generated pulse waves are transmitted to a synthesizer and switch the driving signal of SAW. The driving signal is amplified by a RF amplifier and provided to IDTs on the SAW transducer in the tactile display. Basically, analogue signals can be applied instead of the pulse waves. In this case, the friction can be arranged precisely. Therefore, various and realistic tactile sensation can be expected. Amplitude modulation is applied instead of switching in the synthesizer.

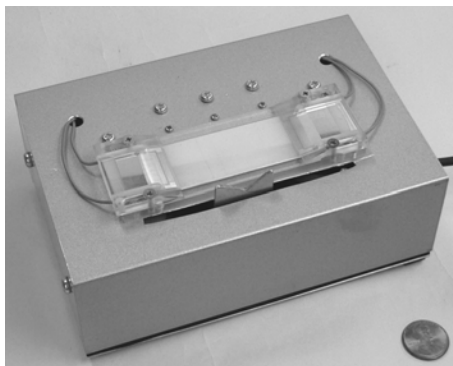


**Fig. 4.** Friction shift by switching SAW

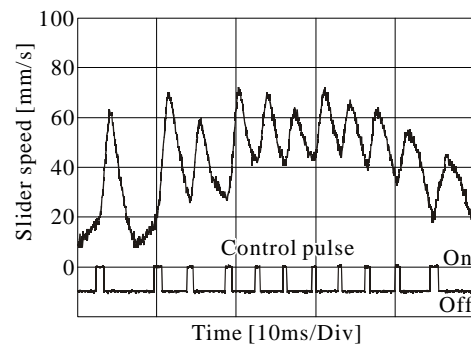


**Fig. 5.** SAW tactile display control system

A prototype of the SAW tactile display was fabricated according to the principle. Figure 6 is a photograph of the display. A  $\text{LiNbO}_3$  wafer was applied as the piezoelectric substrate. Two IDTs were arranged on the surface and two reflectors were formed behind each IDT. The electrodes were covered by acrylic resin shells. In this prototype, rubbing motion was limited in one dimension with available rubbing stroke of 50 mm. Operator's finger was guided by a linear guide with an encoder to detect the slider position. For this prototype, controlling system was embedded in a microcomputer (SH2/4075F) so that it could work at standalone situation. Under the control described above, slider speed was measured. The result of the measurement is plotted on Fig. 7. It was observed that the slider vibration frequency could be controlled according to the control pulse signal. Roughness sensation was successfully indicated.



**Fig. 6.** Prototype of SAW tactile display



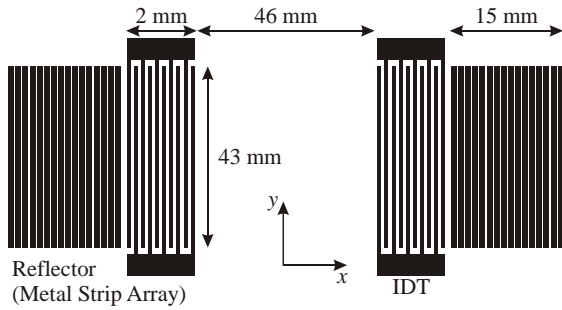
**Fig. 7.** Measurement result of slider speed

## 5. Transparent transducer

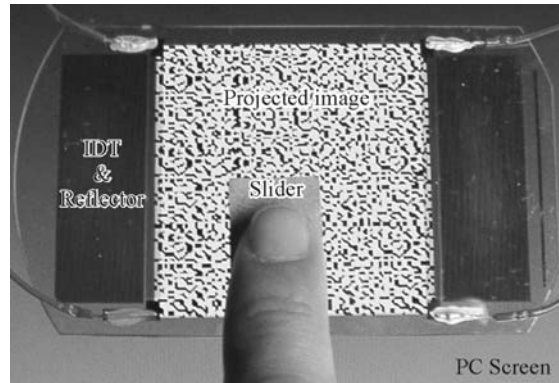
### Polished $\text{LiNbO}_3$ wafer

A  $\text{LiNbO}_3$  128° Y-cut X-prop wafer has been employed for the SAW transducer. For normal wafers of the material, only obverse surface was polished and reverse surface was grained. Since, the SAW material is typically used for signal processing for communication devices, the grain is formed to reduce noise due to scattering of waves on the reverse side. The  $\text{LiNbO}_3$  is originally transparent material. Commercially available wafers of the material, however, look like white opaque material. To achieve transparent SAW transducer, the

wafer with both surface polished (special-ordered wafer) was used as the SAW transducer. To excite standing Rayleigh wave, two IDTs were arranged on the surface, for combination of two opposed progressive waves builds standing wave, as mentioned above. Reflectors, which consist of an open metal strip array, were allocated behind the IDTs to generate the Rayleigh standing wave efficiently. Figure 8 shows a configuration of the electrodes. An IDT has 10 finger pairs and a reflector consisted of 120 metal strips. The operating frequency of 15 MHz was decided so that the all electrodes could be aligned on a 4-inch LiNbO<sub>3</sub> wafer, because electrodes area would be reduced with higher operating frequency. The fabricated transparent transducer was installed on a computer screen as shown in Fig. 9. An image was projected on the screen and was visible for operators. In this configuration, we can enjoy both visual information and tactile information.



**Fig. 8.** Configuration of the SAW transducer



**Fig. 9.** Fabricated transparent LiNbO<sub>3</sub> SAW transducer installed on PC screen

### Glass substrate transducer

For a larger SAW transducer for a large LCD, the LiNbO<sub>3</sub> wafer is not suitable as the elastic medium due to size limit for commercially available wafers, i.e. 4 inches. To overcome this limitation, we proposed a method to excite and propagate SAW on a non-piezoelectric material surface using a piezoelectric material. In this paper, the method is called “indirect excitation.” On the other hand, the conventional method (SAW is generated by the IDT and propagates on the piezoelectric material directly) is called “direct excitation.” For the indirect excitation, a combination of a piezoelectric substrate and a non-piezoelectric substrate was employed. Glass substrate was applied as the non-piezoelectric substrate. LiNbO<sub>3</sub> was applied as the piezoelectric one. The glass substrate can be machined into a desired shape, and any size can be selected. The cost of this method is more reasonable than the conventional one.

Configuration to realize the indirect excitation is shown in Fig. 10. The IDT is formed by photolithography process on the glass substrate. The LiNbO<sub>3</sub> substrate is cut into a die with the same size as crossed digital electrodes area of the IDT and contacted to the IDT. X axis of the LiNbO<sub>3</sub> is fitted perpendicular to IDT fingers. A preload is applied to the LiNbO<sub>3</sub> die and enhances acoustic connection between the glass substrate and the die. If a voltage is applied to the electrodes, electric field is generated in the die and the glass substrate, as illustrated in Fig. 11. The field yields stress distribution inside of the die because of piezoelectricity of LiNbO<sub>3</sub>. The distribution produces alternative stress on the glass substrate through the electrodes, as shown in the figure. If the voltage is alternative, the stress can couple with an acoustic wave on the substrate. With appropriate frequency for the alternative voltage, the stress can couple with Rayleigh wave.

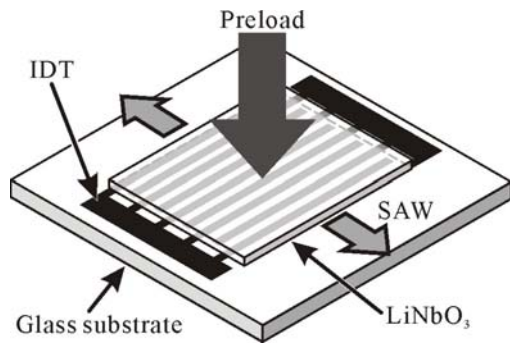


Fig. 10. Transducer structure for indirect excitation

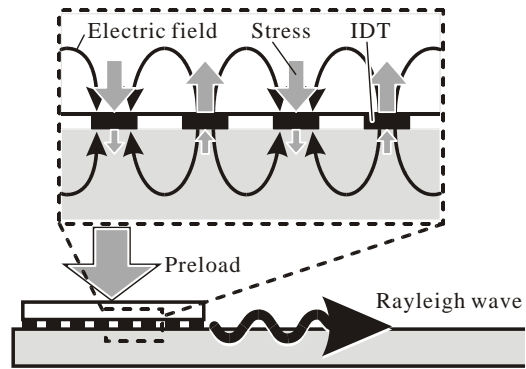


Fig. 11. Principle of indirect excitation

A glass transducer was fabricated on trial. The transducer consisted of a transparent glass substrate (a soda-lime glass) and  $\text{LiNbO}_3$   $128^\circ$  Y-cut X-prop dies. The glass substrate SAW transducer was assembled. For each wafer, the preload was provided by the combination of a beam and coil springs. The preload was measured by strain gauges on the beam. Dimension of the glass transducer was  $100 \times 20 \times 3 \text{ mm}^3$ . Dimension of the  $\text{LiNbO}_3$  dies was  $12 \times 8 \times 1 \text{ mm}^3$ . The dies were approximately in the same size as the fingers area of the IDT. Rubbing stroke on this apparatus was about 70 mm. For demonstration, an LCD was equipped under the transparent glass transducer to display visual information, as shown in Fig. 12. On the LCD, 4 sections in different colors were projected. The controller could set a different roughness setting for each section. We could feel roughness sensation and experience as if to rub the colored images with roughness directly.

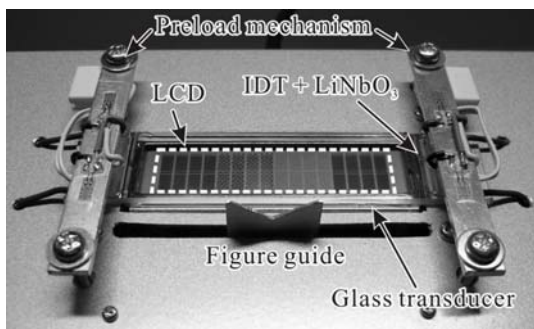


Fig. 12. Glass substrate transducer installed on an LCD

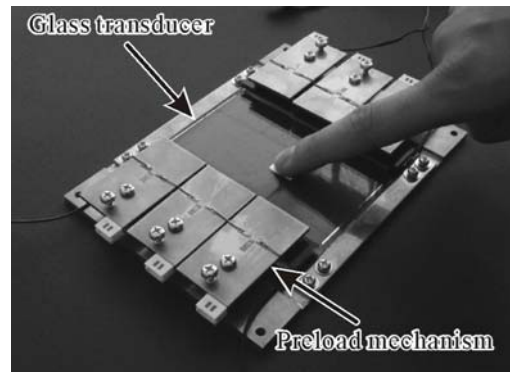


Fig. 13. SAW tactile display using a large glass transducer

The combination of glass substrate and  $\text{LiNbO}_3$   $128^\circ$  Y-cut X-prop dies was used as a large SAW glass transducer. To excite standing wave, two IDTs were arranged on the surface, since combination of two opposed progressive waves builds standing wave. Figure 13 is the photograph of the glass transducer fabricated on trial. The transducer consisted of the transparent glass substrate (a soda-lime glass) and 6 dies of the  $\text{LiNbO}_3$   $128^\circ$  Y-cut X-prop single crystal. Dimension of the glass transducer was  $100 \times 100 \times 3 \text{ mm}^3$ . The IDT has 20 finger pairs. The operating frequency of 5 MHz was decided so that the all electrodes could be aligned on the substrate. The electrodes were formed on a glass substrate by aluminum evaporation and photolithography. Rubbing area of this apparatus was  $90 \times 60 \text{ mm}^2$ . Dimension of the IDT was  $90 \times 16 \times 1 \text{ mm}^2$ . These IDTs were larger than the conventional one. The glass substrate SAW transducer was assembled. For each die, the preload was provided by plate springs and was measured independently by a strain gauge on each of them. To cover whole area of the IDT, 3 dies of  $\text{LiNbO}_3$  with the dimension of  $30 \times 16 \times 2 \text{ mm}^3$  were used for each. The preload was approximately 25 N.

To investigate the indirect excitation on the large glass substrate transducer, frequency response of admittance was measured by using a precision impedance analyzer (Agilent 4294A). The conductance curve had some peaks at 4.74MHz(7.0 mS), 4.83MHz(7.3 mS) and 4.94MHz(13.1 mS). The maximum value was 13.10 mS at

4.94 MHz. The glass substrate transducer was driven at the frequency. With the controller mentioned above, roughness sensation could be indicated successfully.

## 6. Summary

We proposed a method to indicate human tactile sensation, especially for roughness sensation. The method applies friction control with ultrasonic vibration. The controlled friction was utilized to excite mechanical vibration on operator's finger skin. A prototype using LiNbO<sub>3</sub> substrate was fabricated and indicated the roughness sensation successfully.

To solve the size limit of the LiNbO<sub>3</sub> wafer, Indirect excitation using combination of the large size glass substrate and the LiNbO<sub>3</sub> dies was proposed. A large glass transducer was fabricated and two dimensional SAW tactile display could indicate the roughness sensation successfully.

## 7. Acknowledgement

This work was partially supported by Grant-in-Aid for Young Scientists (A), JSPS KAKENHI Grant Number 23680010.

## References

- [1] R. D. Howe, et. al., "Remote Palpation Technology," *IEEE Eng. In Medicine and Biology*, Vol.14, No.3, pp. 318-323, 1995.
- [2] M. Shinohara, et. al., "Three-Dimensional Tactile Display for the Blind," *IEEE Trans. Rehabilitation Eng.*, Vol. 6, No. 3 pp. 249-256, 1998.
- [3] M. Konyo, et. al., "Tactile Feeling Display for Touch of Cloth Using Soft High Polymer Gel Actuators," *Trans. Virtual Reality Society of Japan*, Vol. 6, No. 4, pp.323-328, 2001 (in Japanese).
- [4] S. Tsuchiya, et. al., "Vib-Touch: Virtual Active Touch Interface for Handheld Devices," *Proc. IEEE RO-MAN*, pp. 7-12, 2009.
- [5] T. Watanabe, et. al., "A Method for Controlling Tactile Sensation of Surface Roughness Using Ultrasonic Vibration," *Proc. IEEE ICRA*, pp. 1134-1139, 1995.
- [6] M. Biet, et. al., "Squeeze Film Effect for the Design of an Ultrasonic Tactile Plate," *IEEE Trans. UFFC*, Vol. 54, No. 12 pp. 2678 – 2688, 2007.
- [7] M. Biet, et. al., "Using an Ultrasonic Transducer: Evidence for an Anisotropic Deprivation of Frictional Cues in Microtexture Perception," *Proc. World Haptics Conf.*, 2007.
- [8] L. Winfield, et. al., "TPaD: Tactile Pattern Display Through Variable Friction Reduction," *Proc. World Haptics Conf.*, 2007.
- [9] D. Nicholas, et. al., "Friction Measurements on a Large Area TPaD," *Proc. Haptics Symp.*, pp. 317 – 320, 2010.

## Investigation of the Effect of Composite Bed on Milling Machine to Reduce Chatter

Adib Bin Rashid<sup>1</sup>, Hasibul Shams<sup>1</sup>, Abdur Rashid Tipu<sup>2</sup>, Mohammad Reyad Arefin<sup>1</sup>

<sup>1</sup>Department of Mechanical and Chemical Engineering,

<sup>2</sup>Department of Technical & Vocational Education

Islamic University of Technology (IUT), Dhaka, Bangladesh

E-mail: [adib\\_iut2009@yahoo.com](mailto:adib_iut2009@yahoo.com)

### Abstract

*In general machine tool structure like lathe, milling machine, broaching, and grinding machine etc are subjected to regular unwanted vibration. This machine tool vibration or chatter are deleterious to machining operation. It result unwanted surface roughness of machined parts, shorter tool life and excessive noise, hence are to be necessarily damped out. This paper shows a systematic process of reducing vibration by using damping material. In this paper, Glass fiber polestar is used as damping material with varying thickness. An end milling operation is carried out and the vibration signal is recorded on the screen of digital phosphorus storage oscilloscope. The signal and the RMS amplitude, frequency and time period of vibration are recorded. The experiment is repeated for different number of piece of material. The surface roughness of the machined surfaces is checked by Surface profilometer. It is observed that the vibration amplitude, surface roughness decreases with the increases in a optimum number of layers of damping material.*

**Keywords:** Milling machine, vibration or chatter, surface roughness, oscilloscope, Surface profilometer

### 1. Introduction

The function of the machine tool is to produce a work piece of the required geometric form with an acceptable surface finish at high rate of production in the most economic way [1]. In fact, general purpose machine tools. CNC lathes and machining centers are designed to cope with low cutting speeds with high cutting forces as well as high cutting speeds with low cutting forces. Machine tools structure must possess high dumping, high static and dynamic stiffness. High cutting speeds and feeds are essential requirement of a machine tool to accomplish this basic function. Therefore, the material for the machine tool structure should have high static stiffness and damping in its property to improve both the static and dynamic performance. This static stiffness of a machine tool can be increased by using either higher modulus material or more material in the structure of a machine tool. However, it is difficult to increase the dynamic stiffness of machine tools with these methods because the damping of machine tool structure cannot be increased by increasing the static stiffness. Sometimes high specific stiffness is more important than stiffness to increase the natural frequency of the vibration of the machine tool structure in high speed machining [2]. Often the most economic way of improving a machine tool with high resonance peaks is to increase the damping rather than static stiffness even though it is not easy to increase the damping of the machine tool structure. The chatter is a nuisance to the metal cutting process and can occur on any chip producing tool. Chatter or self-excited vibrant occurs when the width of cut or cutting speed exceeds the stability limit of machine tool [3, 4]. The effects of chatter are all adverse affecting surface finish, dimensional accuracy, tool life and machine life [5]. When the machine tool is operated without any vibration or chatter, the damping of the machine tool plays no important role in machining. However, the machine tool structure has several resonant frequencies because of its continuous structural elements. If the damping is too small to dissipate the vibration energy of the machine tool, the resonant vibration occurs when the frequency of machining operation approaches one of the natural frequencies of the machine tool structure. Therefore the material for the machine tool structure should have static stiffness and damping in its property to improve both the static and the dynamic performance.

## 1.1 Review on research done in damping of composite materials

Bert [6] and Nashif al.[7] had done survey on the damping capacity of fiber reinforced composites and found out that composite materials generally exhibit higher damping than structural metallic materials. Chandra et al.[8] has done research on damping in fiber reinforced composite materials.

Composite damping mechanisms and methodology applicable to damping analysis is described and had presented damping studies involving macro mechanical, micromechanical and Viscoelastic approaches. Gibson et al.[9] and Sun et al.[10,11] assumed viscoelasticity to describe the behavior of material dumping components. The concept of specific damping capacity (SDS) was adopted in the damped vibration analysis by Adams and his co workers [12-13].Morison[14] and Kinera et al.[15].

## 1.2 Chatter in the milling machine

The milling operation is a cutting process using a rotating cutter with one or more teeth. An important feature is that the action of each cutting edge is intermittent and cuts less than half of the cutter revolution, producing varying but periodic chip thickness and an impact when the edge touches the work piece. The tooth is heated and stressed during the cutting part of the cycle, followed by a period when it is unstressed and allowed to cool. The consequences and thermal and mechanical fatigue of the material and vibrations, which are of two kinds: forced vibrations, caused by periodic cutting forces acting in the machine structure and chatter vibrations, which may be explained by two distinct mechanism, called “mode coupling” and “regeneration waviness”, explained in Tobias(1965),Koenigsberger & Tlusty(1967) and Budak & Altintas(1995).

The mode coupling chatter occurs when forced vibrations are present in two directions in the plane of cut. The regenerative chatter is a self excitation mechanism associated with the phase shift between vibrations waves left on both sides of the chip and happens earlier than the mode coupling chatter in most machining cases, as explained by Altintas(2000).In milling, one of the machine tool work piece system structural modes is initially excited by cutting forces. The waved surface left by a previous tooth is removed during the succeeding revolution, which also leaves a wavy surface due to structural vibrations. The cutting forces become oscillatory whose magnitude depends on the instantaneous chip dynamic thickness, which is a function of phase shift between inner and outer chip surface. The cutting forces can grow until the system becomes unstable and the chatter vibrations increase in a point when the cutter jumps out of the cut or cracks due the excessive forces involved. These vibrations produce poor surface finishing, noise and reduce the life of the cutter. In order to avoid these undesirable effects, the feed rate and the depth of the cut are chosen at conservative values, reducing the productivity.

## 1.3 Instrumentation

The following equipment is needed in recording the amplitude, frequency, period of the vibrations during the machining operation

- (1) Power supply unit
- (2) Vibration pick-up
- (3) Digital Storage oscilloscope



(A)Oscilloscope



(B)Vibration measuring probe



(C) Power supply unit



## 1.4 Composite used in the work is Glass fiber polyester

Fiberglass is made from extremely fine fibers of glass. It is used as a reinforced agent for many polymer products; the resulting composite material, properly known as fiber-reinforced polymer (FRP) or glass-reinforced plastics (GRP), is called “fiberglass” in popular usage. Uses for regular fiberglass include mats, thermal insulation, electrical insulation, reinforcement of various materials, tent poles, sound absorption, heat and corrosion-resistant fabrics, high –strength fabrics, pole vault poles, arrows, bows and crossbows, translucent roofing panels, automobile bodies, hockey sticks, surfboards, boat hulls, and paper honeycomb.

Polyester is a category of polymers which contain the ester functional group in their main chain. Although there are many types of polyester, the term “polyester” as a specific material most commonly refers to polyethylene. Depending on the chemical structure polyester can be a thermoplastic or thermo set; however the most common polyesters are thermoplastics. Polyesters are used to make “plastic” bottles, films, tarpaulin, canoes, liquid crystal displays, holograms filters, dielectric film for capacitor, film insulation for wire and insulating tapes.

## 2. Experimental Procedure

The work specimen of 70mm x 55mm x 15 mm is a mild steel square plate. The glass fiber e polyester composite plates are thoroughly cleanse and polished. Plates are fixed on to a bench vice and the edges are filed to clear off the irregularities. All the plates are made to the exact dimensions for the ease of the further operations. All the plates are carefully made homogeneously similar to avoid interfacial vibrations and slipping. The work piece is then mounted onto the layered sheets of composites and tightly clamped. Initially mild steel plate is machined with no layer under it .A contact type magnetic base vibration pickup connected to a digital phosphor storage oscilloscope of Tektronix 4000 series is placed on the mild steel during the machining operation. The response signals with respect to amplitude, time period.RMS amplitude and frequency are recorded and stored on the screen of the storage oscilloscope. The number of layers is increased to 7 layers and the observations are recorded. The experiments are conducted for 0, 1,2,3,4,5,6,7 numbers of layers respectively. Finally mild steel plate is machined with no layer under it and the readings are noted and compared.

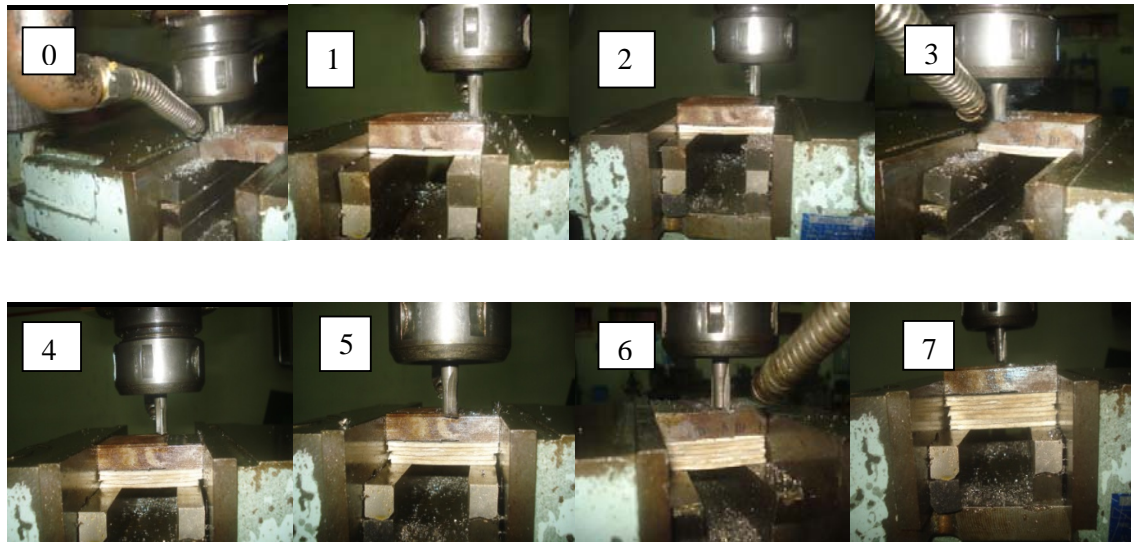


Figure 1. Experiment proceed on increasing the number of damping material

An End milling cutting operation with constant feed of 16mm/min and depth of cut if .02mm is performed during all the experiments. An oil-water emulsion made from animal fat is used as a cutting fluid.

The surface roughness of the job pieces are measured on Surface profilometer .The microscopic view of the surfaces are shown in the Figure-2. The value of Signal Amplitude(mV), Time period( $10^{-6}$  s), Frequency(KHz), RMS amplitude (mV), Surface roughness for different cutting conditions are tabulated in the Table-1

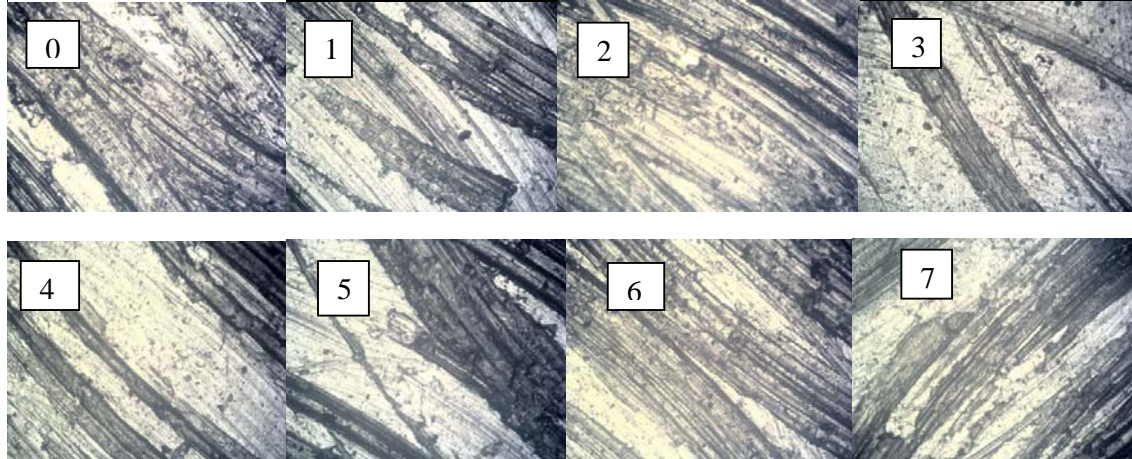


Figure-2: Microscopic view of surface produced on different condition

**Table 1. Signal Amplitude(mV), Time period( $10^{-6}$  s), Frequency(KHz), RMS amplitude (mV), Surface roughness for different cutting condition**

No of plates	Signal Amplitude(mV)	Time period( $10^{-6}$ s)	Frequency(KHz)	RMS amplitude (mV)	Surface roughness
0	65.6	437.5	2.286	14.1	0.96
1	52.1	468	2.09	11.5	0.925
2	45.8	503.8	1.87	10.2	0.88
3	39	569.4	1.65	9.4	0.83
<b>4</b>	<b>33.6</b>	<b>692.5</b>	<b>1.444</b>	<b>8.06</b>	<b>0.80</b>
5	36.2	745.9	1.49	8.9	0.82
6	47.2	799.2	1.55	10.3	0.87
7	53.9	827	1.72	10.7	0.91

### 3. Conclusion

The above result shows the variation of signal amplitude with respect to number of layers for different combinations of composites. It is observed that when the numbers of layers are increased, the signal amplitude has decreased. The maximum amplitude is obtained when no composite material was used indicating that the

presence of composite material decreases the vibration amplitude and increases counter vibration characteristics of the system. This shows that with increase in the plates the damping can be increased but only to a certain limit. Also by analyzing the surface roughness on Surface profilometer it is observed the same result. Hence optimum level of plates is to be decided to profitably damp out the vibrations.

#### 4. References

- [1] The Machine Tool Industry Research Association, A Dynamic Performance Test for Lathes, July, 1-86, (1971).
- [2] Welbourn , D.B. and Smith, J.D., "Machine Tool Dynamics, Cambridge University Press, Chap.1, Chap.5, Chap.8, (1970).
- [3] Koenigsberger, F. and Tlusty, J., "Machine Tool Structure". Pergamon Press, Vol.1, Sect.2, (1970).
- [4] Cook, N.H., "Manufacturing Analysis, Addison-Wesley Publishing Company, Chap.3, Chap.7. , (1986).
- [5] Merritt, H.E. , "Theory of Self-Excited Machine Tool Chatter", Journal of Engineering for Industry. Transactions of ASME, 447-454 (1965).
- [6] Bert, C.W., "Composite materials: A survey or the damping capacity of fiber reinforced composites in damping applications for vibration control", AMD-Vol. 38. (1980).
- [7] Nashif , A.D, Jones, D.I.G and Henderson, J.P. Vibration Damping, Wiley, New York, (1985).
- [8] Chandra, R., Singh S.P, and Gupta.K Damping studies in fiber-reinforced composites-a review. Composite Structs, 46(1), 41-51, (1999).
- [9] Gibson, R.F., Chaturvedi, S.K. and Sun, C.T., "Complex moduli of aligned discontinuous fiber-reinforced polymer composites", J. Mater Sci., Vol. 17. pp. 3499-3509 (1982).
- [10] Gibson, R.F., Chaturvedi, S.K. and Sun, C.T., "Internal damping of short- fiber reinforced polymer matrix composites", Comput. Struct 20, pp. 391-401, (1985).
- [11] Sun, C.T., Wu, J.K. and Gibson, R.F., "Prediction of material damping of laminated polymer matrix composites". J. Mater. Sci. 22, pp. 1006-1012, (1987).
- [12] Adams, R.D. and Bacon, D.G.C, "Effect of fiber orientation and laminate geometry on dynamic properties of CFRP , J Compos.Mater. 7, pp. 402-428, (1973).
- [13] Lin D.X, Ni R.G and Adams R.D, "Prediction and measurement of the vibrational damping parameters of carbon and glass fiber-reinforced plastics plates", J. Composite. Materials. 18, pp. 132-152 (1984).
- [14] Ni R.G and Adams R.D., "A rational method for obtaining the dynamic mechanical properties of lamina for predicting the stiffness and damping of laminated plates and beams", Composites 15, pp. 193-199, (1984).
- [15] Morison W.D, "The prediction of material damping of laminated composites". Can. Aeronaut. Space J. 28, pp. 372-382, (1982).

## Imaging Problem of a Low Cost Finger Print Sensor & Adjusting Various Parameters for Its Improvement

Amit Roy\*, Md. Rokunuzzaman, S. M. Rasid, Md. M. Hasan, S. M. Rasid, G. Azam, B. K. Sarker

Department of Mechanical Engineering  
Rajshahi University of Engineering & Technology, Rajshahi-6204, Bangladesh

\*E-mail: [royamit.me@gmail.com](mailto:royamit.me@gmail.com)

### Abstract

*The diffusion of mobile cameras and webcams is rapidly growing. Unfortunately, images produced by these kinds of sensors during the acquisition of human fingertips are very different from the images obtained by dedicated fingerprint sensors, especially as quality is concerned. One critical issue regarding the protection of confidential information or valuable items is to determine the identity of a person. Biometrics is supposed to offer this security in a user-friendly and secure way. One problem however is that there are ways to compromise systems based on biometric verification. Some of these biometrical features have known vulnerabilities. Persons with similar facial characteristics, e.g. identical twins, can fool face recognition system. It is also stated that identical twins have similar fingerprints due to the fact that they have fingerprints that belong in the same class. Recognition of a finger prints it is necessary to get better image quality of finger print to get better image. So designed a low cost finger print sensor & adjusted its various parameters to improve finger print image quality. We used optical finger print reader using a low cost webcam for capturing image. Image saved in computer. Edge was determined from image using visual C++ program of different person. The result of this experiment was not found very well because it is a big experiment & its program is very difficult. There are many programs we had done for finding better image. We had used image loading program, capturing program, image saving program, zoom in program etc.*

**Keywords:** webcams, finger print sensor, biometrics.

### 1. Introduction

The possibility to obtain fingerprint images by using low cost cameras and off-the-shelf webcams has a great practical importance since nowadays fingerprint biometrics can be successfully achieved only by using dedicated sensors. The diffusion of general purpose cameras is rapidly growing, and they can be found easily on laptops and cellular phones. Unfortunately, the images of human fingerprints acquired from these kinds of sensors are very different from the images obtained by dedicated fingerprint sensors. In order to exploit the paramount variety of techniques now available in the literature to achieve verification and recognition by fingerprint biometrics it is important to process the camera image of the fingerprints so that they are as similar as possible to the images produced by dedicated sensors. The approach that we propose aims to allow for using the webcams as an interoperable device for fingerprint biometrics. For example, the proposed approach allows for exploiting a webcam as a fingerprint biometric sensor on a personal computer in case of a dedicated sensor is not available or a dedicated sensor is not required by the desired security level for the envisioned application.

There are different types [2] of techniques for finger print processes are optical readers, electro-optical readers, capacitance base finger print sensor, silicon chips, TFT base finger print sensor, RF field - AC capacitance base finger print sensor, RF field - AC capacitance Resistive membrane on silicon, TFT, Tactile MEMS, thermal base finger print sensor and ultra-sound base finger print sensor.

All the above technique is used for finger print image processing. To get better recognition of finger print, it is necessary to get better image quality of finger print. There are different kinds of pattern given below-



Fig 1.1: The arch pattern.



Fig 1.2: The loop pattern.



Fig 1.3: The whorl pattern

The major Minutia features of fingerprint ridges are: ridge ending, bifurcation, and short ridge. The ridge ending is the point at which a ridge terminates. Bifurcations are points at which a single ridge splits into two ridges. Short ridges (or dots) are ridges which are significantly shorter than the average ridge length on the fingerprint. Minutiae and patterns are very important in the analysis of fingerprints since no two fingers have been shown to be identical.

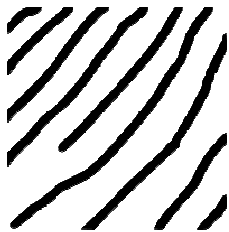


Fig-1.4: Ridge ending



Fig-1.5: Bifurcation

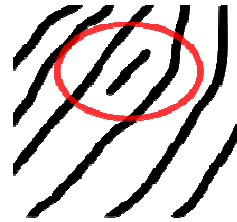


Fig1.6: Short Ridge (Dot)

## **2. Methods and tools used:**

Optical fingerprint imaging involves capturing a simple image of the print using visible light. This type of sensor is, in essence, a specialized web camera. The top layer of the sensor, where the finger is placed, is known as the finger tip rest surface. In this time three type of illuminator we are use. This type of illuminator is used in illuminates the finger tip rest surface. The web cam focus length is fixed. When the programming is run then the finger image capture automatically and saved. In this time, the image processing steps are image noise reduction and enhancement.

### **2.1 Main components of setup**

1. Glass Box
2. Web Camera
3. Computer
4. LED Light
5. Illuminator variable circuitry

### **Sensor design**

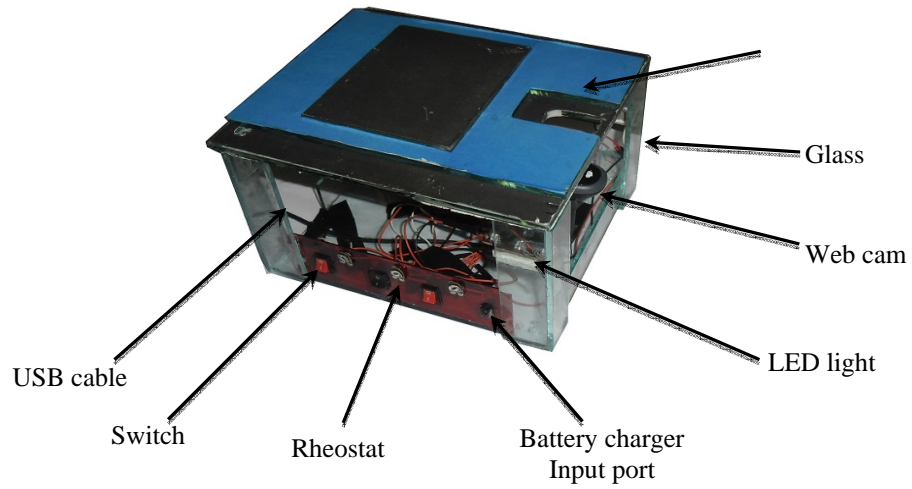


Figure 2: Sensor Design

### 3.1 Experimental setup:

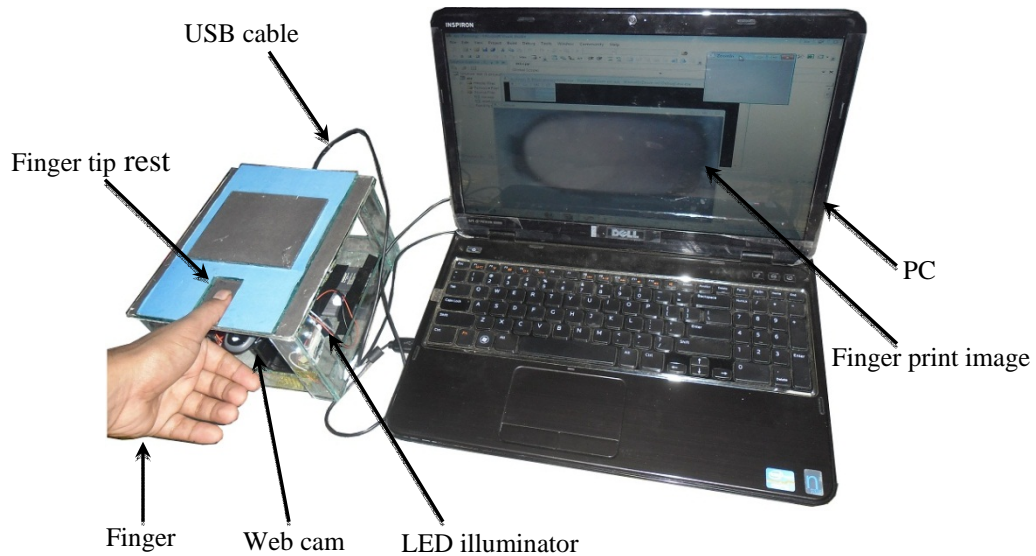


Figure 3: Experimental setup for fingerprint sensor

### 3.2 Working principle of the project

There was Logitech C110 for this project. It was a 1.3 megapixels device that had optical fingerprint reader.

Finger tip image was stored in a computer by changing different parameter of illuminator. There were three illuminators such as- illuminator 1, illuminator 2 & illuminator 3. The image was captured by changing different condition of illuminator & different condition i.e. day & night. The changing condition of illuminator is low, high & medium.

The fingerprint open source fingerprint recognition library was used to handle image capture, enrollment and improve image quality. As stated in the current model is that a fingerprint was enrolled and the pre-stored finger tip image quality was improved by using Gaussian filter & image equalizes histogram.

A small application was written to initialize the device and capture the image using fingerprint open source library functions. We had to resolve Linux-compilation, link-load errors. These errors were due to the way which static and dynamic libraries have to specified for compilation and linking an application.

Capturing Image was stored using C++ program in computer.

### 3.3 Experimental scenario

The main function of the sensor is used for capturing finger print tip image. We captured finger tip image of different person for saving computer in different condition.

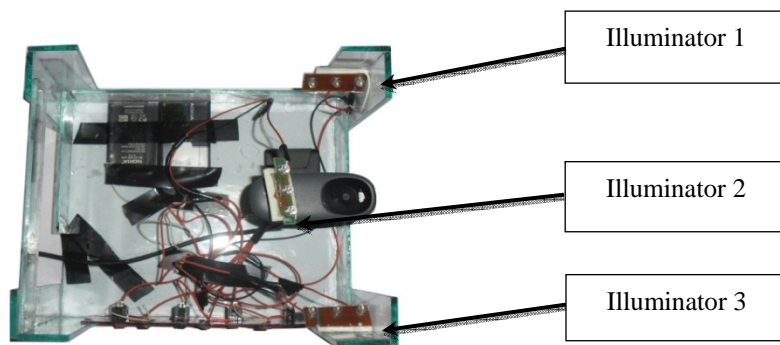


Fig3: Internal view of finger print sensor

## 4. Methodology

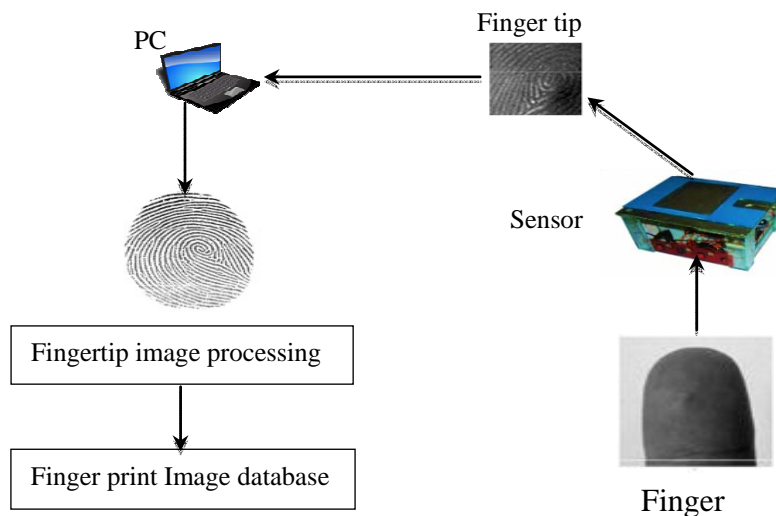


Figure 4: System fingerprint image processing

## 5.1 Experimental data

Table 1: Image Captured by Webcam in night


















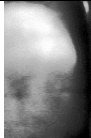
No. of Obs.	Illumination of Light			Finger Tip Image	
	Illuminator1	Illuminator 2	Illuminator 3	Person-1	Person-2
01	Low	Low	Low		
02	Low	Low	Medium		
03	Low	Medium	Medium		
04	Medium	Medium	Medium		
05	High	Medium	Medium		
06	High	High	Medium		
07	High	High	High		

Table 2: Finger Crop Image

No. of Obs.	Illumination Of light			Person 1		Person 2	
	Illuminator 1	Illuminator 2	Illuminator 3	Finger Tip Image	Crop Image	Finger Tip Image	Crop Image
01	Low	Low	Low				



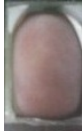


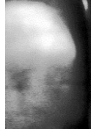
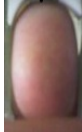

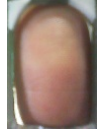




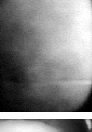


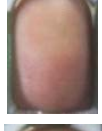
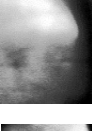

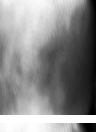
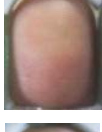


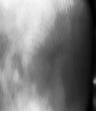
















02	Low	Low	Medium				
03	Low	Medium	Medium				
04	Medium	Medium	Medium				
05	High	Medium	Medium				
06	High	High	Medium				
07	High	High	High				
08	Low	High	High				
09	Low	Low	High				
10	High	Low	Medium				

Table3: Image captured in day light

No. of Obs.	Illumination of Light			Finger Tip Image	
	Illuminator1	Illuminator 2	Illuminator 3	Person 1	Person 2
01	Low	Low	Low		









02	Low	Medium	Medium		
03	Low	Medium	High		
04	Medium	Medium	High		
05	High	High	High		

Table4: Finger Gray Image





















No. of Obs.	Illumination of light			Person 1		Person 2	
	Illuminator 1	Illuminator 2	Illuminator 3	Finger Tip Image	Finger Tip Gray Image	Finger Tip Image	Finger Tip Gray Image
01	Low	Low	Low				
02	Low	Low	Medium				
03	Low	Medium	Medium				
04	Medium	Medium	Medium				
05	High	Medium	Medium				

Table5: Finger crop image & gray image in day

No. of Obs.	Illumination of Light			Person 1		Person 2	
	Illuminator 1	Illuminator 2	Illuminator 3	Crop Image	Gray Image	Crop Image	Gray Image
01	Low	Low	Low				
02	Low	Medium	Medium				
03	Low	Medium	High				
04	Medium	Medium	High				
05	High	High	High				

## 6. Results

Table 6: The good image was found below this following condition

No. of Obs.	Illumination of Light			Finger tip image	
	Illuminator 1	Illuminator 2	Illuminator 3	Person 1	Person 2
01	High	Medium	Medium		
02	Low	Medium	High		
03	Medium	Medium	High		
04	High	High	High		

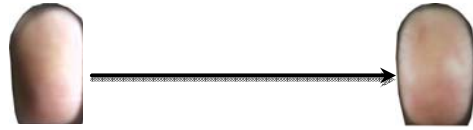


Fig 6.1: Noise image

Fig 6.2: Good image

## 7. Conclusion

In this experiment we used different types of C++ program for getting good & improve image. The C++ program such as Image loading program, Image capturing and saving program, Image resize program.

Image converts to gray, Image smoothing program, Images zoom in program, Image ROI program, Image background remover program, Image cropped program, Image histogram equalize program. At first loaded image, then captured and saved the image in a computer. We resized this image and converted into gray image, then smoothing in the gray image. Now we removed the back ground for finding good image. But in this process there was much noise in the image. Then we try to reduce the noise, so we used zoom in function for seeing this image in large form. Then we enhanced the image, but in this case we did not get good minutiae. Again we used ROI program, then cropped and histogram equalize program. In this case, we got improve image compared to previous image. But this image was also noise. So finally we captured image by changing the parameter of illumination i.e. low, medium & high. We captured image in day light & night by changing parameter of illuminator. The captured image was nice in day light than night. These images can be used for finger print recognition but it is need further process.

In this project the proper illumination system development has been found difficult for this application, because the environment condition for illumination causes some spots in the images. For noise removal of the images we have used Gaussian Filter. We have also used Histogram Equalization for image contrast of the image.

## References

- [1] G. Bradski, A. Kaehler, "*Learning OpenCV: Computer Vision with the OpenCV Library*", O'Reilly Media (publisher), 2008.
- [2] Jain, L.C. et al. Langenburg, Glenn (January 24, 2005), "*fingerprints similar to those of his or her parents in any discernable way?*" Are one's retrieved 28, August 2010.
- [3] Thornton, John (May 9, 2000). "*Latent Fingerprints, Setting Standards in the Comparison and Identification*". 84<sup>th</sup> Annual Training Conference of the California State Division of IAI, retrieved 30 August 2010.
- [4] Mamdar, Subhra; Dhulipala, Venkata (2008), "*Biometric Security Using FingerFingerprint Recognition(PDF)*", University of California, San Diego. P.3 retrieved 30, August 2010.
- [5] Meghdadi, Majid; Jalilzadeh, Saeed, "*Algidity and Acceptability of the 7th WSEAS International Conference on Mathematical Methods and Computational Techniques In Electrical Engineering World Scientific and Engineering Academy and Society*"
- [6] Dalong Li Simske, S. Mersereau, R.M.M., "*Blind image deconvolution using constrained variance maximization*", Signals, Systems and Computers, Vol. 2, 2004, pp. 1762-1765.

## **Design and Implementation of a Remote Controlled Robotic Arm Based on Industrial Application Perspective**

Md. Bony Amin<sup>1</sup>, G.M. Sultan Mahmud Rana<sup>2</sup>, Abdullah-Al-Farabi<sup>1</sup>,  
A.M.M. Nazmul Ahsan<sup>1</sup>, Md. Ahasan Habib<sup>1</sup>

<sup>1</sup>Department of Industrial Engineering and Management, Khulna University of Engineering & Technology,  
Khulna-9203, Bangladesh

<sup>2</sup>Department of Mechanical Engineering, Khulna University of Engineering & Technology, Khulna-9203,  
Bangladesh

E-mail: bony\_kuet\_ipe@hotmail.com, gsmrana@gmail.com, alfarabi41@hotmail.com,  
ahsan.ipe@gmail.com, shiplu04\_ipe@yahoo.com

### **Abstract**

*This paper describes an implementation of a remote controlled robotic arm with six degrees of freedom which is able to pick an object with a specific weight and can place them in a desired location. The method of design of the remote controlled robotic arm consists of two stages. First stage is the construction of the mechanical structure following modular concept with six degrees of freedom and the second is to design the interface of components of the robotic arm to control it via a wireless joystick. To ensure ease of use, wireless system is introduced in this robotic arm. This kind of the arm can be applied in industrial sectors where automaton is profoundly needed.*

*Keywords: Automation, AVR Microcontroller, Arduino, Mobile robot, Ease of use, Modular design, Ease of maintenance, Wireless, Joystick.*

### **1. Introduction**

As technology increases, robots not only become self-sufficient through autonomous behavior but actually manipulate the world around them. Robots are capable of amazing feats of strength, speed, and seemingly intelligent decisions; however, this last ability is entirely dependent upon the continuing development of machine intelligence and logical routines [1]. Industrial robots should perform complex tasks in the minimum possible cycle time in order to obtain high productivity. Robotic arm is one of the key developments in the field of industrial robotics. This paper describes design and implementation of a remote controlled robotic arm with six degrees of freedom which is able to pick an object with a specific weight and can place it at a desired location. The programming of the arm is done on an ATMEGA-328P Microcontroller using Arduino programming. The input is given using a wireless joystick that is also programmed with an ATMEGA-8 Microcontroller. To ensure ease of use, wireless system is introduced in this robotic arm. The wireless system is implemented using wireless transceiver.

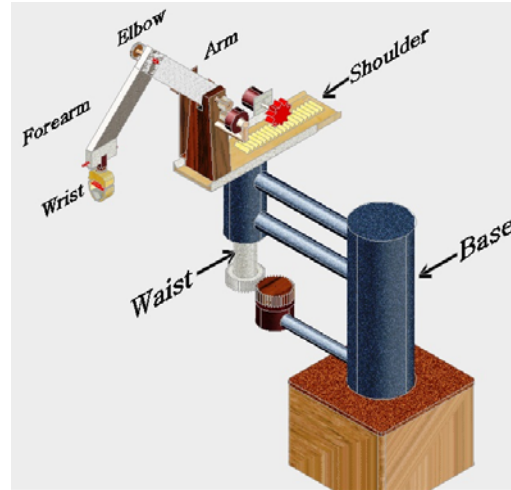
### **2. Design of the Robotic Arm**

The design methodology of the remote controlled robotic arm consists of two stages. First stage is the construction of the mechanical structure following modular concept with six degrees of freedom and the second is to design the interface of components of the robotic arm to control it via a wireless joystick. The robotic arm movement depends upon the angular movement of the joint. Joint movement determines the required power. The joint movement must be adjusted to stay within the power available on the robotic system to be used. Friction must also be considered in relation to robotic arm movement [2].

#### **2.1 Mechanical structure of robotic arm**

The robotic arm described in this paper consists of two basic elements, a basic structure and a wrist. The basic

structure consists of base, waist, shoulder, arm, elbow and forearm which are the first five links (bodies) of this robotic arm and the other link is called its wrist or hand (Figure 1). A robot link is a solid mechanical structure which connects two joints. The main purpose of robot links is to maintain a fixed relationship between the joints at its ends [3]. A robot manipulator consists of links connected by joints driven by separate motors. The wrist is designed for orienting the end effector to do a task or to grasp an object. Rotating motion of wrist enables this robotic arm to grasp an object from different angle.



**Fig. 1.** Basic structure of the robotic arm.

It is shown that maintenance difficulty arrives seriously after completing the manufacturing process of a robotic arm for the absence of modular concept in its design. Modular design is a form of standardization. Modules represent groupings of component parts into subassemblies, usually where individual parts lose their separate identity. One advantage of modular design of equipment compared with nonmodular design is that failures are often easier to diagnose and remedy because there are fewer pieces to investigate. Similar advantages are found in ease of repair and replacement; the faulty module is conveniently removed and replaced with a good one [4].

## 2.2 Degree of freedom

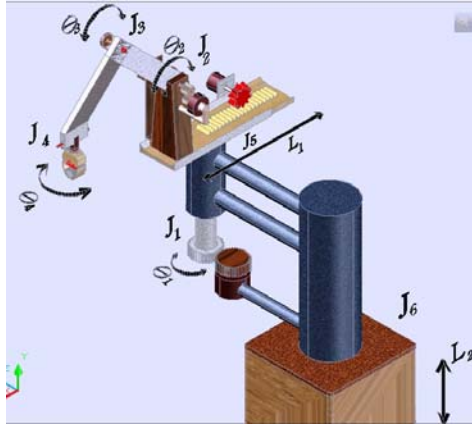
Robotic systems are characterized by their degrees of freedom (DOF) [2]. Each degree of freedom is a joint on the arm, a place where it can bend or rotate or translate. One can typically identify the number of degrees of freedom by the number of actuators on the robot arm. Each degree requires an actuator, often an encoder, and exponentially complicated algorithms and cost. The robotic arm described in this paper has six degrees of freedom as shown in figure 2. Link 1 ( $J_1$ ) allows waist rotation ( $\Theta_1$ ) about y-axis, link 2 ( $J_2$ ) allows arm rotation ( $\Theta_2$ ) about an axis which is perpendicular to the y-axis that means z-axis, link 3 ( $J_3$ ) allows rotation ( $\Theta_3$ ) of forearm along elbow about an axis which is parallel to the z axis, link 4 ( $J_4$ ) allows rotation ( $\Theta_4$ ) of wrist along y-axis, link 5 ( $J_5$ ) allows a linear movement ( $L_1$ ) of shoulder along x-axis and link 6 ( $J_6$ ) allows upward and downward movement ( $L_2$ ) of base along an axis which is parallel to the z-axis.

## 2.3 Overview of links

- Link 1: At  $J_1$ , waist is adjusted into the hollow cylindrical portion of base. Two tapered bearing has used to facilitate the rotation of waist into the hollow cylinder.
- Link 2: At  $J_2$ , two gears are coupled. A motor has used for the angular movement of arm using gears as power transmission medium.
- Link 3: At  $J_3$ , for the angular movement of forearm, power is transmitted through chain & sprocket system. The motor which is used for the angular movement of forearm, has been in such a way that it's shaft meet at the same level to the motor shaft which is used for link 2.
- Link 4: At  $J_4$ , wrist can be rotate as requirement to grasp an object. A small ball bearing has used here to facilitate wrist rotation.
- Link 5: At  $J_5$ , shoulder can be moved through the waist with sliding motion. Here rack & pinion are used as

the power transmission medium.

- Link 6: At  $J_6$ , base can be moved to upward and downward direction along with slots into the rectangular box. To facilitate this vertical motion an automotive lifting system has used at  $J_6$ .



**Fig. 2.** Robotic arm with six degree of freedom

## 2.4 Robot workspace (Work Volume)

The robot workspace (sometimes known as reachable space) is a collection of points that the end effector (gripper) can reach. The workspace is dependent on the DOF angle/translation limitations, the arm link lengths, the angle at which something must be picked up at, etc. The workspace is highly dependent on the robot configuration. The table below describes the workspace for the designed robotic arm.

**Table 1.** Movement range of basic structure

Structure	Movement type	Maximum allowable movement
Waist	Rotation( $\Theta_1$ )	$0 < \Theta_1 \leq 360^\circ$
Arm	Rotation( $\Theta_2$ )	$0 < \Theta_2 \leq 180^\circ$
Forearm	Rotation( $\Theta_3$ )	$0 < \Theta_3 \leq 200^\circ$
Wrist	Rotation( $\Theta_4$ )	$0 < \Theta_4 \leq 360^\circ$
Shoulder	Linear( $L_1$ )	$0 < L_1 \leq 8$ inch
Base	Linear( $L_2$ )	$0 < L_2 \leq 12$ inch

## 2.5 Ease of maintenance

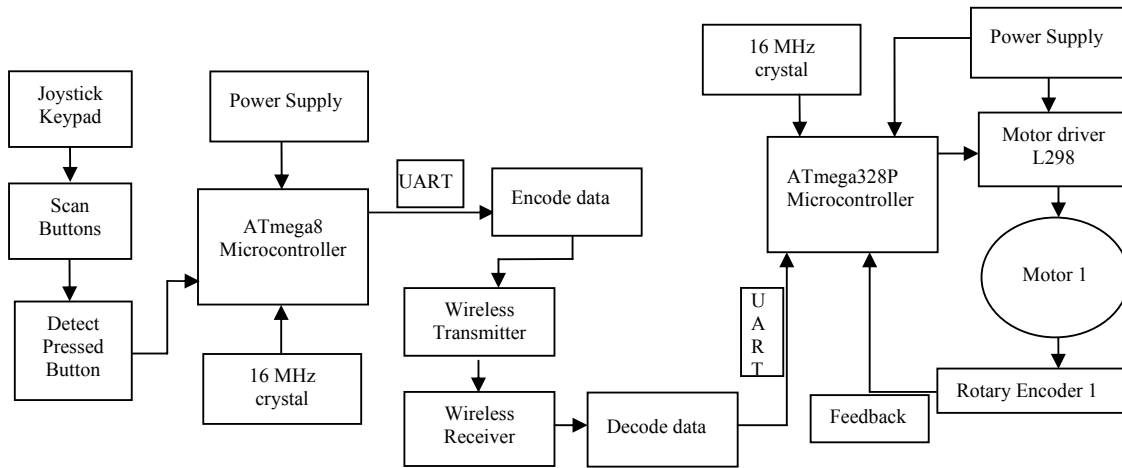
During operation with heavy load any portion of this robotic arm may be hampered or needed to be upgraded. Because of modular design every portion of the structure of this robotic arm is independent. As a result skilled person is not necessary for the reassembling or assembling the total structure of this robotic arm. For these reason it is very easy for someone to work with any portion of the structure without disturbing other portion. Efficient design of this robotic arm enables one to lubricate it properly without any complexity. The design of this robotic arm also facilitates the scope if any upgrades are needed for the robotic arm to cope with any new advanced process layout or to facilitate production work [10].

## 3. Implementation Process

The implementation process consists of two parts, the first one is designing the motherboard for the robotic arm to control the motor and the second one is designing the wireless control interface for the wireless joystick to operate the robotic arm remotely.

### 3.1 Robot motherboard

The theory behind control systems and how they control motors and other devices is the foundation of all modern electromechanical systems. Using control system mathematics and theory, we can design systems that do nearly anything we want, to the granularity that we desire, in the amount of time that we desire. Control system theory can be broadly broken up into two major categories: open loop control and closed loop controls. Open loop control is by far the simpler of the two types of control theory. In open loop control, there is some sort of input signal (digital or analog), which passes through amplifiers to produce the proper output and then it passed out from the system. Open loop controls have no feedback and require returning input to zero before the output return to zero. In general open loop control means send electrical signals to an actuator to perform a certain action, like connecting a motor to a battery. In this scheme of control, there is no any other mean for controller to make sure that the task was performed correctly and it often needs human intervention to obtain accurate results. A very simple example of open loop control is the remote controller of an RC toy car. The human have to constantly check the position and the velocity of the car to adapt to the situation and move the car to the desired place. We have employed the advanced close loop control system [7] to operate the motors for our robotic arm. Closed- loop control system is implemented using a common communication medium (wired or wireless), network quality strongly influences the performance of the control solution. Specifically, time delays governed by deterministic and stochastic processes are often introduced by the network [8]. In closed loop control, the system is self-adjusting. Data do not flow one way. It may pass back from a specific amplifier (such as velocity or position) to the start of the control system, telling it to adjust itself accordingly .Many physical systems have closed loop control at the lowest level since the data about velocity and current position modify the output (also position) at a consistent rate. We need some mean of gaining information about the rotation of the shaft like the number of revolutions executed per second, or even the precise angle of the shaft. This source of information about the shaft of the motor is called “feed-back” because it sends back information from the controlled actuator to the controller. It is clear that the closed loop system is more complicated because it needs a 'shaft encoder' which is a devise that will translate the rotation of the shaft into electrical signals that can be communicated to the controller. Ploplys et al.[9] Implements a closed- loop control solution for an inverted pendulum using a wireless sensor network communicating upon the IEEE 802.11 b communication standard.



**Fig. 3.** Closed loop motor control via wireless joystick.

The close loop motor control block diagram is shown in the figure 3 above. The heart of this control system is the ATmega328P microcontroller. The wireless receiver module receives the wave signal transmitted by the wireless joystick transmitter module. Then the module decodes the wave signal and sends to the ATmega328P microcontroller through UART. UART is stands for Universal Asynchronous Receiver Transmitter. It is widely used as protocol for communicating with the microcontroller. Then the microcontroller sends the motor controlling signal to the L298 motor driver IC according to received wireless signal. The motor control circuit is shown in figure 4. The rotary encoder is attached with each motor, which sends clock pulse to the microcontroller when the motor shat rotate. The number of pulse send by the rotary encoder for each motor in one revolution of motor shaft is fixed. By counting the number of pulse the microcontroller calculate the current position of the arm internally and if any error found with the position of the arm and receiver module received position then the position is fixed by sending the necessary signal to the motor driver. In this way the close loop control system is applied effectively to control the position of the arm.



### 3.2 Programming platform

Arduino, an open-source electronics prototyping platform, has been used for Programming the robotic arm and the Arduino UNO board has been used for our Robotic arm motherboard. The Arduino Uno is a microcontroller board based on the ATmega328P [5]. It has 14 digital input/output pins of which (6 can be used as Pulse Width Modulation (PWM) outputs), 6 analog inputs, a 16 MHz ceramic resonator, a USB connection, a power jack, an ICSP header, and a reset button. There is also a free Arduino IDE for Programming the Arduino board that has been used for compiling and uploading the hex code to the microcontroller. The Programming language used in Arduino IDE is C++.

### 3.3 Wireless joystick

Joystick circuit diagram is shown in figure 5. Radio Frequency (RF) Transceiver Module has been used for wireless communication. A RF Module is a small electronic circuit used to transmit and/or receive radio signals on one of a number of carrier frequencies. RF Modules are widely used in electronic design owing to the difficulty of designing radio circuitry and it is very cheap to buy from market. Good electronic radio design is notoriously complex because of the sensitivity of radio circuits and the accuracy of components and layouts required achieving operation on a specific frequency [9].

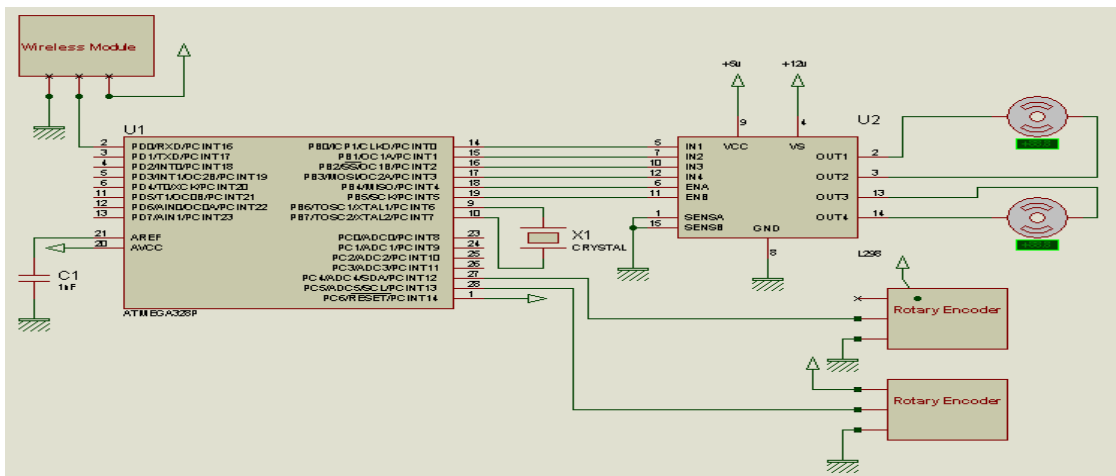


Fig. 4. Motor control circuit diagram.

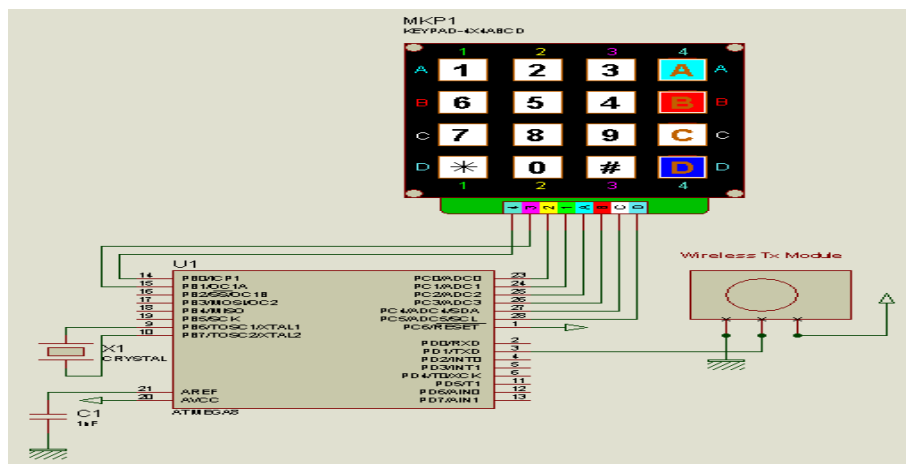


Fig. 5. Joystick circuit diagram.

ATmega8 microcontroller is used in joystick to send the wireless signal to the robot [5] [6]. The microcontroller scans continuously the keypad and detects the pressed button. The joystick is able to detect multiple key presses at the same time. After detecting the buttons which are pressed down, microcontroller encode the key pressed data and send it to the wireless transmitter module. The transmitter transmits the data in the form of wave.

#### 4. Results & Discussions

The photographic view of our implemented remote controlled robotic arm is shown in figure 6. It is able to lift the objects of medium weight up to 1.6 pound. Three contributions of our work are: (i) This can be employed in places where precision and accuracy is required, (ii) This robot can also be employed where human hand cannot penetrate. (iii) These robots have a wide range of applications such as pick and place.

This robot arm can be used for various applications, few of them are: (i) To lift objects, (ii) To lift nuclear wastes without harming the humans, (iii) Prototype for a Bomb disposal robot.



**Fig. 6.** Robotic arm lifting objects of average

#### 5. Conclusion & Future work

Our robot developed with an implementation of Arduino Uno microcontroller board based on the ATmega328P, can be guided with six degrees of freedom. We used geared motors for their high torque at low speeds, in exchange for a highly-reduced brushless or brushed motor. These design tradeoffs were chosen for the envisioned target application of robots interacting with unstructured environments such as a typical home or workplace, where the safety of intrinsic mechanical compliance is an important design consideration. These robots have a wide range of industrial and medical applications such as pick and place robots, surgical robots etc. This robotic arm so far designed is able to lift the objects. In order to extend it to some extent, more advanced tools and material are to be used for mounting the tools which are grasped by mechanical grippers include the spot or arc welding gun, spray painting gun, drilling spindle, grinder wire brushes, and heating torches. Then it will be fit for paints, ceramics, and foundry shop as well as for automotive industry.

#### 6. References

- [1] C.C. Kemp, A. Edsinger, and E. Torres-Jara, "Challenges for robot manipulation in human environments [Grand challenges of robotics]", *IEEE Robotics and Automation Magazine*, Vol. 14, No. 1, pp. 20–29, 2007.
- [2] V.K. Banga, J. Kaur, R. Kumar, and Y. Singh, "Modeling and Simulation of Robotic Arm Movement using Soft Computing", *World Academy of Science, Engineering and Technology*, Vol. 51, pp. 616-619, 2011.
- [3] Prof. Said M. Megahed, "MDP646: ROBOTICS ENGINEERING", Part I-Module#3: 2- Robot Mechanical Structure and Tooling.
- [4] J. Heizer, and B. Render, Principles of Operations Management, *Pearson College Div.*, 4<sup>th</sup> Edition, 2000.
- [5] C. Hernández, R. Poot, L. Narváez, E. Llanes, and V. Chi, "Design and Implementation of a System for Wireless Control of a Robot", *International Journal of Computer Science Issues*, Vol. 7, No. 5, pp. 191-197, 2010.
- [6] K. Brahmani, K.S. Roy, and M. Ali, "Arm 7 Based Robotic Arm Control By Electronic Gesture Recognition Unit Using Mems", *International Journal of Engineering Trends and Technology*, Vol. 4, No. 4, pp. 1245-1248, 2013.
- [7] J.P. Lynch, Y. Wang, R.A. Swartz, K.C. Lu, and C.H. Loh, "Implementation of a closed-loop structural control system using wireless sensor networks", *Structural Control and Health Monitoring*, Vol. 15, pp. 518 -539, 2008.
- [8] Lian FL, Moyné J, Tilbury DM. "Network design consideration for distributed control systems". *IEEE Transactions on Control Systems Technology* 2002; 10(2):297–307.

- [9] Ploplys NJ, Kawka PA, Alleyne AG. "Closed-loop control over wireless networks". *IEEE Control Systems Magazine* 2004; 24(3):58–71.
- [10] Karl T Ulrich, Steven D Eppinger and Anita Goyal, *Product Design & Development*, *McGraw-Hill Book Company*, 4th edition. pp -182-183, 2009.

## Hand Gesture Recognition by Artificial Neural Network

Soumen paul<sup>1</sup>, Md. Abu Shahab Mollah<sup>2</sup>, Rajibuzzaman<sup>3</sup>, Tanvir Ahmad<sup>4</sup>, Kazi Toufiqur Rahman<sup>5</sup>

<sup>1,3</sup>Khulna University of Engineering & Technology, Khulna-9203, Bangladesh

<sup>2,4</sup>Ahsanullah University of Science & Technology, Dhaka, Bangladesh

<sup>5</sup>Daffodil International University, Dhaka, Bangladesh

E-mail: sowmen\_paul@yahoo.com, shahabee\_06@yahoo.com, tanvir\_165@yahoo.com, jewelee87@yahoo.com

### Abstract

*This paper represents hand gesture recognition with artificial neural network. Visual Interpretation of gestures can be useful in accomplishing natural Human Computer Interactions (HCI). In this paper we proposed a method for recognizing hand gestures. We have designed a system which can identify specific hand gestures and use them to convey information. In this system we select the feature vectors by Biorthogonal Wavelet Transform. We have used supervised feed-forward neural network based training and Scaled conjugate gradient Backpropagation algorithm for classifying hand gestures into ten categories: A,B,C,D,G,H,I,L,V,Y. This system gives us good performance for recognizing the gestures. We can get up to 82% correct results on a particular gesture set.*

Keywords: ANN, HMM, Radon Transformation, Human Computer Interaction, SCG.

### 1. Introduction

With the development of ubiquitous computing, computer is becoming more and more important in our daily life. Computer applications require more and more unrestricted interaction between human and computers. Hand gesture is frequently used in people's daily life. A gesture is spatio-temporal pattern, which may be static or dynamic or both. One of the most structured sets of gestures belongs to sign language. In sign language, each gesture has an assigned meaning (or meanings). It involves relative flexure of the user's fingers and consists of information that is often too abstract to be interpreted by a machine. Applications of hand gesture recognition widely range from teleoperated control to medicine. For instance, transform of human hand motion for telemanipulation is especially important in hazardous environment. Another important application of hand gesture recognition is to improve the quality of life of the deaf or non-vocal persons through a hand-gesture to speech system. Due to congenital malfunction, disease, head injuries, or virus infections, deaf or non-vocal individuals are unable to communicate with hearing people through speech. Deaf or non-vocal persons use sign language or hand gestures to express themselves. However, most hearing people do not have the special sign language expertise. This is a major barrier between these two groups in daily communication. To overcome this barrier to help those people to integrate into society is a very challenging research area.

The first gestures that were applied to computer interactions date back to the PhD work of Ivan Sutherland [1], who demonstrated Sketchpad, an early form of stroke-based gestures using a light pen to manipulate graphical objects on a tablet display. This form of gesturing has since received widespread acceptance in the human-computer interaction (HCI) community. In the last decade, several methods of potential applications [2], [3], [4] in the advanced gesture interfaces have been suggested but these differ from one to another in their models. Some of these models are Neural Network [2], Fuzzy Systems [3] and HMM [4], [5], [6], [7]. Viola uses integral images as Haar wavelet features in rapid object detection [8]. Integral images allow for the fast implementation of box type convolution filters, which makes very fast feature extraction. Farid Parvini and Dennis McLeod presented hand gesture recognition by feature subset selection utilizing Bio-Mechanical characteristics [9]. Hasanuzzaman et al. [10] presented a real-time hand gesture recognition system using skin color segmentation and multiple-feature based template matching techniques. In their method, the three largest skin-like regions are segmented from the input images by skin color segmentation technique from YIQ color space and they are compared for feature based template matching using a combination of two features correlation coefficient and

minimum (Manhattan distance) distance qualifier. Ho-Sub et al. [11] introduced a hand gesture recognition method, which used the combined features of location, angle and velocity to determine the discrete vector that is used as input to HMMs. This method runs over the alphabets (A-Z), numbers (0-9) and six edit commands. Wu [12] developed a hand gesture recognition system for media player control. The system firstly separated the left arm by background subtraction and detected the straight line by both Hough transform and Radon transform.

In this paper we proposed a system where we select the feature vectors by Biorthogonal Wavelet Transformation for recognizing static hand gestures. Here a supervised feed forward neural network has been used with Scaled conjugate gradient Backpropagation learning with a hidden layer having the output nodes representing classes of static hand gesture classification.

## 2. System Overview

We propose an automatic system that recognizes static hand gesture for alphabets (A,B,C,D,G,H,I,L,V,Y) using Biorthogonal Wavelet Transform. In particular, the proposed system consists of several steps. In the first step images are at first read and then pre-processed. Then noise is removed from the image by using filters. In the next step the proposed method detect the edge from the images and then compute *projections* of an image along specified directions by RT (Radon Transformation). After that, the Biorthogonal Wavelet Transformation is performed on the projections of an image which we get from the RT (Radon Transformation). Then the gestures are trained by supervised feed-forward neural network and then testing is performed. After the completion of testing period the gestures are recognized.

## 3. Feature Extraction Algorithms

In our proposed system 3 feature extraction algorithms are used. All the algorithms are necessary for recognizing the gestures appropriately.

### I. Canny Edge detection Algorithm:

The Canny algorithm uses an optimal edge detector based on a set of criteria which include finding the most edges by minimizing the error rate, marking edges as closely as possible to the actual edges to maximize localization, and marking edges only once when a single edge exists for minimal response. According to Canny, the optimal filter that meets all three criteria above can be efficiently approximated using the first derivative of a Gaussian function.

$$G(x, y) = \frac{1}{2\pi\sigma^2} e^{-\frac{x^2+y^2}{2\sigma^2}} \dots\dots\dots (3.1)$$

$$\frac{\partial G(x,y)}{\partial x} \propto x e^{-\frac{x^2+y^2}{2\sigma^2}} \dots\dots\dots (3.2)$$

$$\frac{\partial G(x,y)}{\partial y} \propto y e^{-\frac{x^2+y^2}{2\sigma^2}} \dots\dots\dots (3.3)$$

The first stage involves smoothing the image by convolving with a Gaussian filter. This is followed by finding the gradient of the image by feeding the smoothed image through a convolution. The 2-D convolution operation is described in the following equation.

$$I'(x, y) = g(k, l) \times I(x, y) \\ = \sum_{k=-N}^N \sum_{l=-N}^N g(k, l) I(x - k, y - l) \dots\dots\dots (3.4)$$

Where:  $g(k, l)$  = convolution kernel

$I(x, y)$  = original image

$I'(x, y)$  = filtered image

$2N + 1$  = size of convolution kernel

### II. Radon Transformation:

In mathematics, the Radon transform in two dimensions, named after the Austrian mathematician Johann Radon, is the integral transform consisting of the integral of a function over straight lines. The transform was introduced by Johann Radon (1917). Radon further included formulas for the transform in three-dimensions, in which the integral is taken over planes.

Applying the Radon transform on an image  $f(x, y)$  for a given set of angles can be thought of as computing the projection of the image along the given angles. The resulting projection is the sum of the intensities of the pixels in each direction, i.e. a line integral. The result is a new image  $R(\rho, \theta)$ . This can be written mathematically by defining

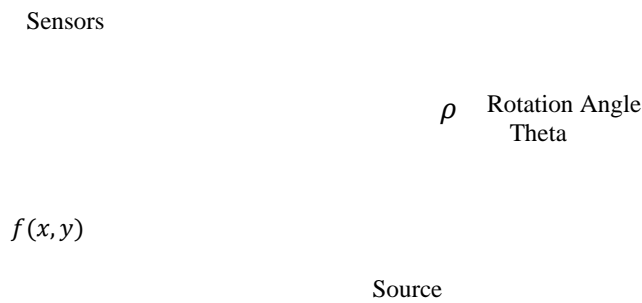
$$\rho = x \cos \theta + y \sin \theta \dots\dots\dots (3.5)$$

after which the Radon Transformation can be written as

$$R(\rho, \theta) = \int_{-\infty}^{\infty} \int_{-\infty}^{\infty} f(x, y) \delta(\rho - x \cos \theta - y \sin \theta) dx dy \dots\dots\dots (3.6)$$

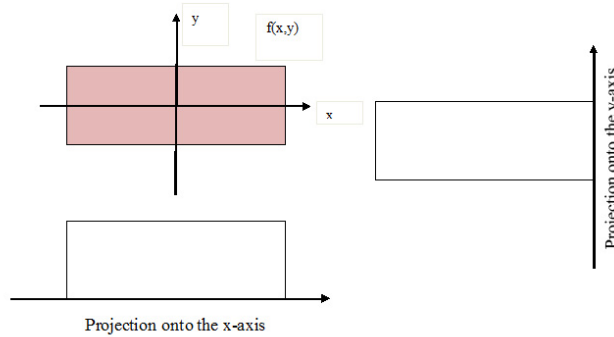
Here,  $\delta$  is dirac delta function.

A projection of a two-dimensional function  $f(x, y)$  is a set of line integrals. The *radon* function computes the line integrals from multiple sources along parallel paths, or *beams*, in a certain direction. The beams are spaced 1 pixel unit apart. To represent an image, the *radon* function takes multiple, parallel-beam projections of the image from different angles by rotating the source around the centre of the image. The following figure 1 shows a single projection at a specified rotation angle.



**Fig.1.** Parallel-Beam Projection at Rotation Angle Theta

For example, the line integral of  $f(x, y)$  in the vertical direction is the projection of  $f(x, y)$  onto the x-axis; the line integral in the horizontal direction is the projection of  $f(x, y)$  onto the y-axis. The following figure shows horizontal and vertical projections for a simple two-dimensional function.



**Fig.2.** Horizontal and Vertical Projections of a Simple Function

### III. Biorthogonal Wavelet:

A biorthogonal wavelet is a wavelet where the associated wavelet transform is invertible but not necessarily orthogonal. Designing Biorthogonal wavelets allows more degrees of freedom than orthogonal wavelets. One additional degree of freedom is the possibility to construct symmetric wavelet functions. The first example of biorthogonal wavelet basis was constructed by Tchamitchian (1987). Before discuss about the biorthogonal wavelet, we will review briefly on orthogonal wavelet.

### 4. Hand Gesture Recognition System

Hand Gesture Recognition is a complex but one of the benchmark problem in pattern recognition research. In our proposed technique two major steps are to simulate- Image processing and neural network construction. As MATLAB contains *image processing toolbox* and *neural network toolbox* as well, so to perform this work MATLAB was chosen.

The total work is performed in several steps which are image pre-processing, feature extraction, training by neural network, testing and finally recognizing the hand gesture. The whole process can be demonstrated by the following block diagram.

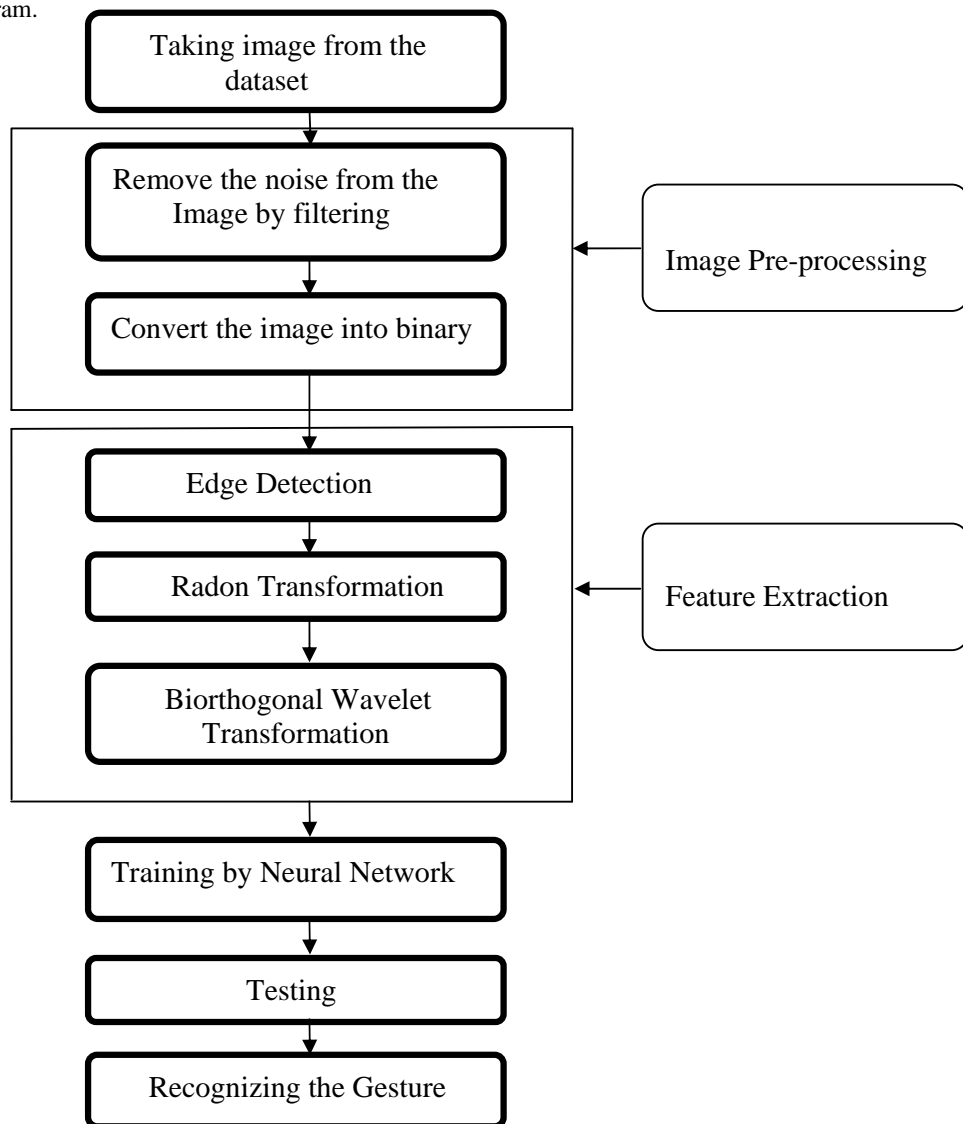


Fig.3. Block diagram of Hand Gesture Recognition System

## I. Image Pre-processing:

Before feature extraction of an image, image pre-processing is a necessary step. Image pre-processing is used for operations on images at the lowest level of abstraction. The pre-processing do not increase image information content but decrease it if entropy is an information measure. For example as Histogram equalization, it modifies the brightness and contrast of the image, making the image look clearer.

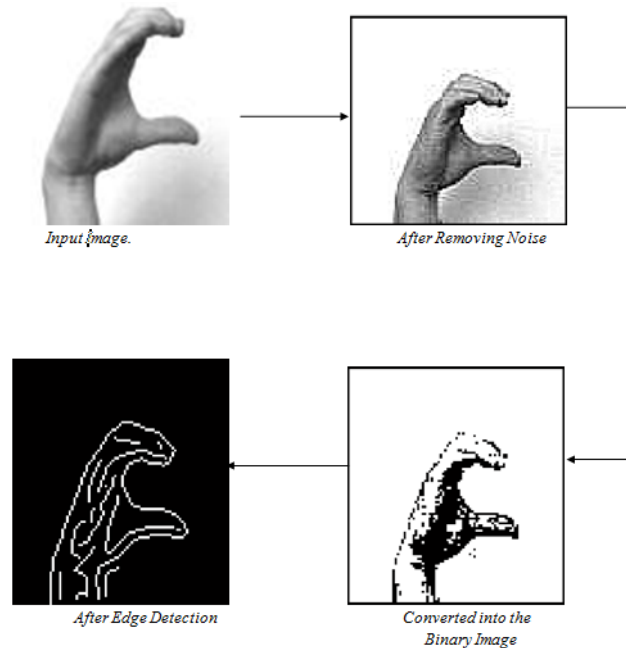
In our proposed system image pre-processing is combined of several steps. Our image database [14] was already in the gray scale format, so we did not need to convert in gray scale format. Considering the uniform background is white, first of all we resize all the images. Then we remove the noise from them by Gaussian lowpass filter using gaussian function and *imfilter* function. Converting the images into the binary scale by *im2bw* function we finished our image pre-processing task.

## II. Feature Extraction:

Feature Extraction is a very important task for any system based on artificial neural network. Selecting good feature increase performance of the system. In our proposed system feature extraction is done by the following three steps.

A. **Edge Detection:** In an image, an edge is a curve that follows a path of rapid change in image intensity. Edges are often associated with the boundaries of objects in a scene. Edge detection is used to identify the edges in an image.

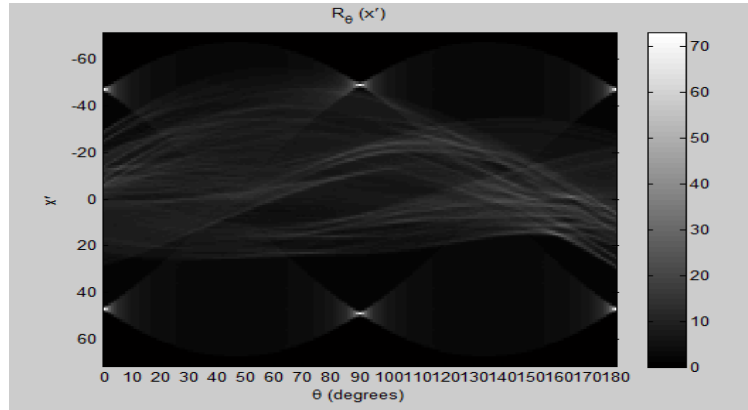
In this system we detect the edges of an image by Canny edge detection algorithm, because this edge detector performs better than reference algorithms.



**Fig. 4.** Edge detection by Canny Edge Detection Algorithm

B. **Radon Transformation:** After the detecting the edges of the image, computation of the multiple parallel-beam projections of the image from different angles by rotating the source from  $0^\circ$  to  $180^\circ$  was performed around the center of the image.

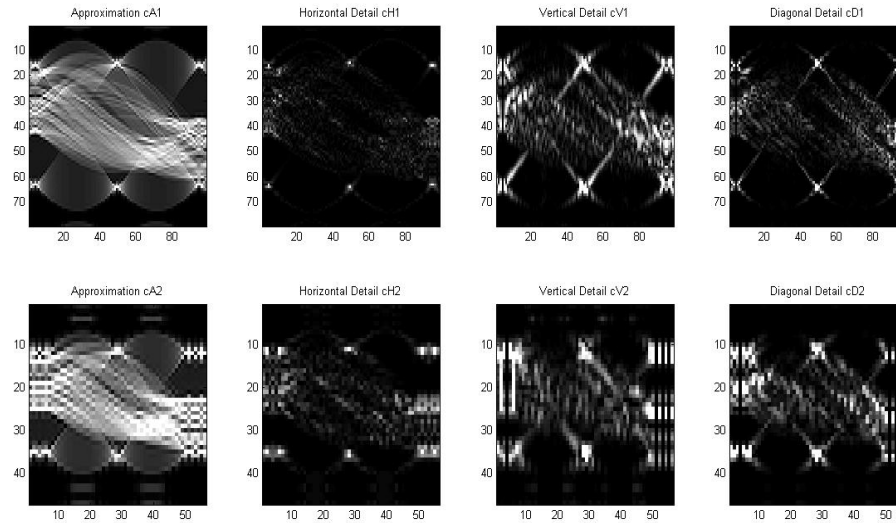




**Fig. 5.** Plotting of Radon Transformation of an image at angles from 0° to 180°.

In Figure 5 we see that some sine waves appears, it is because the Radon transform of a Dirac delta function( $\delta$ ) is a distribution supported on the graph of a sine wave. Consequently the Radon transform of a number of small objects appears graphically as a number of blurred sine waves with different amplitudes and phases. For that reason the Radon transform data is often called a *sinogram*.

**C. Biorthogonal Wavelet Transform:** By performing biorthogonal wavelet transformation on the computed projection which we obtained from the Radon Transformation, the final feature for our recognition system is selected. We used biorthogonal wavelet 3.7 in this system.



**Fig.6.** After Biorthogonal wavelet transform

### **III. Training By Neural Network:**

For training the feature by neural network, the most important portion is that to create a neural network first and to feed the inputs in that network. In MATLAB for creating a feedforward neural network a built-in function named *newff* was used here. For training the network with scaled conjugate gradient backpropagation *trainscg* function is used as a network training function.

The performance function is specified according to error calculation. In our program we used *mse* (*mean squared error*) performance function. The error is calculated as the difference between the target output and the network output. Then the mean squared error is calculated.

$$mse = \frac{1}{Q} \sum_{k=1}^Q e(k)^2 = \frac{1}{Q} \sum_{k=1}^Q (t(k) - a(k))^2 \dots \dots \dots (4.1)$$

A very important term for the learning procedure is Epoch. The term epoch means a single pass through the entire learning process. When the input vector is pass through the learning procedure the entire process then said to be an epoch. In our program the maximum number of epoch is assigned to 10000. More epochs consume more time for learning. If the number of epoch is less, the learning might be incomplete. Then the probability of error increases.

The following parameters we have used for neural network in our program

Number of epoch: 10,000

Number of hidden neurons: 10

Performance Goal: 0.00001

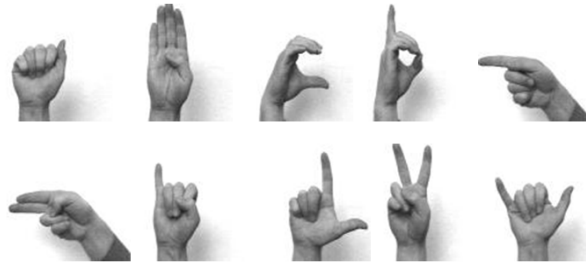
Learning rate: 0.1

Epochs between showing progress: 50

Training Time: 2s

### 5. Experimental Result:

The proposed method was tested on five different users showing ten gestures such as A,B,C,D,G,H,I,L,V,Y. Table 1 shows the recognition results of 10 gestures of 5 users.

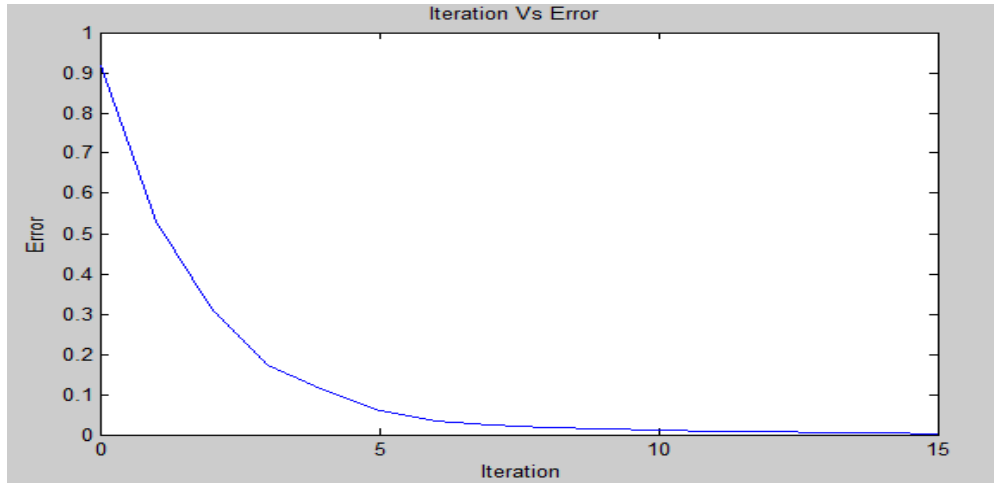


**Fig.7.** Finger spelled Alphabet (Top row [A, B, C, D, and G], Bottom row [H, I, L, V, Y]).

**Table 1:** Recognition rate of hand gestures using proposed method for 10 gestures and 5 users

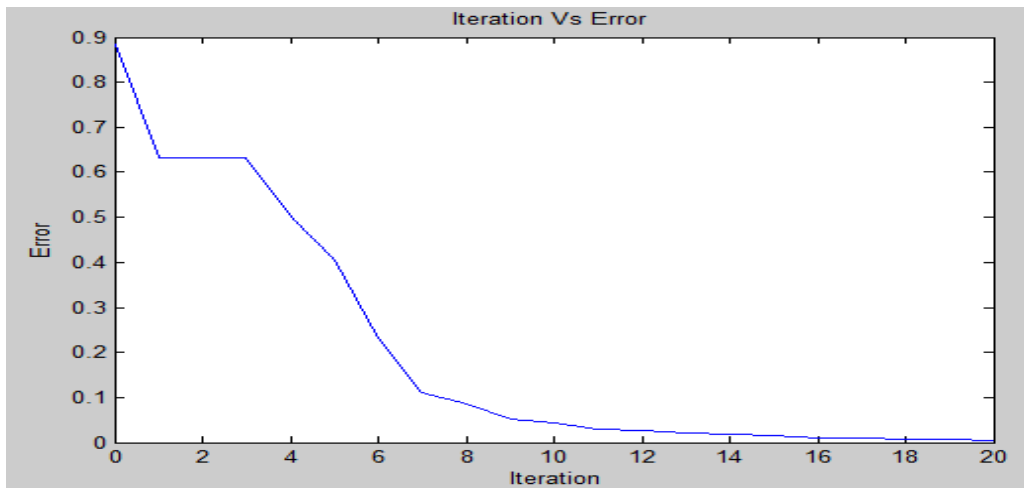
Gesture	A	B	C	D	G	H	I	L	V	Y	%
User											
1	9/10 (90%)	8/10 (80%)	7/10 (70%)	7/10 (70%)	7/10 (70%)	6/10 (60%)	8/10 (80%)	8/10 (80%)	6/10 (60%)	6/10 (60%)	72%
2	8/10 (80%)	6/10 (60%)	8/10 (80%)	7/10 (70%)	7/10 (70%)	8/10 (80%)	8/10 (80%)	5/10 (50%)	7/10 (70%)	8/10 (80%)	72%
3	8/10 (80%)	5/10 (50%)	6/10 (70%)	8/10 (80%)	9/10 (90%)	8/10 (80%)	6/10 (60%)	6/10 (60%)	8/10 (80%)	7/10 (70%)	71%
4	9/10 (90%)	10/10 (100%)	10/10 (100%)	7/10 (70%)	7/10 (70%)	9/10 (90%)	5/10 (50%)	6/10 (60%)	7/10 (70%)	6/10 (60%)	76%
5	7/10 (70%)	6/10 (60%)	9/10 (90%)	5/10 (50%)	9/10 (90%)	8/10 (80%)	9/10 (90%)	8/10 (80%)	6/10 (60%)	7/10 (70%)	74%
Total	82%	70%	80%	68%	78%	78%	72%	66%	68%	68%	

We have plotted the Iteration versus Error Curve for the different users of 10 gestures.



**Fig.8.** Iteration versus error curve for user 1

The Fig.8 shows that with iteration the error reduces. For other users the error also reduces as the iteration increases. For convenience here another curve is shown for user 3.



**Fig.9.** Iteration versus error curve for user 3

## 6. Discussion:

Artificial Neural Networks (ANN) has been applied to an increasing number of real-world problems of considerable complexity. Their most important advantage is in solving problems that are too complex for conventional technologies, i.e., problems that do not have an algorithmic solution or for which an algorithmic solution is too complex to be found. Here we applied ANNs to the problem of differentiating between the 10 static hand gestures with very good results. In order to achieve high accurate result; we applied radon transformation and biorthogonal wavelet transformation for selecting the feature. For faster training we used scaled conjugate gradient backpropagation. The accuracy can be achieved up to 82% for a particular gesture set.

## 7. Future Work:

We only recognized and classify the static hand gestures, so dynamic hand gesture recognition will be more useful for any of this related applications. The future work also will focus on the advanced feature-level algorithms for improving more accuracy of hand gesture recognition

## 8. References:

- [1] Sutherland, I. E. Sketchpad: “*A man-machine graphical communication system*”. In: Proceedings of the AFIPS Spring Joint Computer Conference 23. pp. 329–346,1963.
- [2] X. Deyou, “*A Network Approach for Hand Gesture Recognition in Virtual Reality Driving Training System of SPG*”, International Conference ICPR, pp. 519-522, 2006.
- [3] E. Holden, R. Owens and G. Roy, “*Hand Movement Classification Using Adaptive Fuzzy Expert System*”, Journal of Expert Systems, Vol. 9(4), pp. 465-480, 1996.
- [4] M. Elmezain, A. Al-Hamadi and B. Michaelis, “*Real-Time Capable System for Hand Gesture Recognition Using Hidden Markov Models in Stereo Color Image Sequences*”, Journal of WSCG, Vol. 16, pp. 65-72, 2008.
- [5] M. Elmezain, A. Al-Hamadi and B. Michaelis, “*A Novel System for Automatic Hand Gesture Spotting and Recognition in Stereo Color Image Sequences*”. Journal of WSCG, Vol.17, No. 1, pp. 89-96, 2009.
- [6] M. Elmezain, A. Al-Hamadi, J. Appenrodt and B. Michaelis, “*A Hidden Markov Model-Based Continuous Gesture Recognition System for Hand Motion Trajectory*”. International Conference on Pattern Recognition (ICPR), pp. 519-522, 2008.
- [7] M. Elmezain, A. Al-Hamadi and B. Michaelis, “*Spatio- Temporal Feature Extraction-Based Hand Gesture Recognition for Isolated American Sign Language and Arabic Numbers*”. IEEE Symposium on ISPA, pp. 254-259, 2009.
- [8] P. Viola and M Jones, “*Rapid object detection using a boosted cascade of simple features.*” in Proceedings of Computer Vision and Pattern Recognition. Hawaii,U.S., 2001, pp. 511–518.
- [9] Farid Parvini and Dennis McLeod, “*Feature Subset Selection Utilizing BioMechanical Characteristics for Hand Gesture Recognition*” 978-1-4244-4134-1/09/ 2009 IEEE.
- [10] Md. Hasanuzzaman, V. Ampornaramveth, Tao Zhang, M.A. Bhuiyan ,Y. Shirai and H. Ueno, “*Real-time Vision-based Gesture Recognition for Human Robot Interaction*”. In the Proceedings of the IEEE International Conference on Robotics and Biomimetics, Shenyang China ,2004.
- [11] Y. Ho-Sub, S. Jung, J. B. Young and S. Y. Hyun, “*Hand Gesture Recognition using Combined Features of Location,Angle and Velocity*”, Journal of Pattern Recognition, Vol. 34(7), pp. 1491-1501, 2001.
- [12] Y. M. Wu, “*The implementation of gesture recognition for media player system.*” Master Thesis of the Department of Electrical Engineering, National Taiwan University of Science and Technology, Taipei, Taiwan, 2009.
- [13] Martin Fodsllette Moller. “*A Scaled Conjugate Gradient Algorithm For Fast Supervised Learning. Neural Networks, 6:525-533, 1993*”.
- [14] Sebastien Marcel – “*Gesture Database Web Page.htm*”
- [15] “*Digital image processing using Matlab*” by Rafael C. Gonzalez, Richard E. Woods, Steven L. Eddins.
- [16] “*Neural Networks*” by Simon Haykin. “<http://ece2day.blogspot.com/2012/10/neural-networks-comprehensive.html>”.
- [17] “[http://cas.ensmp.fr/~chaplais/wavetour\\_presentation/Wavetour\\_presentation\\_US.html](http://cas.ensmp.fr/~chaplais/wavetour_presentation/Wavetour_presentation_US.html).”
- [18] “*Hand Pose Estimation for American Sign Language Recognition*” by Jason Isaacs and Simon Foo ,2004 IEEE
- [19] Duong Van Hieu; Supot Nitsuwat “*Image Preprocessing and Trajectory Feature Extraction based on Hidden Markov Models for Sign Language Recognition*”, Ninth ACIS International Conference on Software Engineering, Artificial Intelligence, Networking, and Parallel/Distributed Computing,2008,Phuket, Thailand.
- [20] Mahmoud Elmezain, Ayoub Al-Hamadi, Bernd Michaelis “*Improving Hand Gesture Recognition Using 3D Combined Features*”, 2009 Second International Conference on Machine Vision, 28-30 Dec.2009,Dubai,pp. 128-132.

## Effect of Frequency and Amplitude of Vibration on Ring-Traveller Friction of Ring Spinning Frame

Dr. Hosne Ara Begum<sup>1</sup>, Prof. Dr. Md. Maksud Helali<sup>2</sup>, Dr. Abu Bakr Siddique<sup>3</sup>

<sup>1</sup> Assistant professor Department of Yarn Manufacturing, Bangladesh University of Textiles, Tejgaon, Dhaka-1208, Bangladesh

<sup>2</sup> Department of Mechanical Engineering, Bangladesh University of Engineering and Technology, Dhaka-1000, Bangladesh

<sup>3</sup> Associate professor, Department of Textile Engineering, Primeasia University, Dhaka-1213

E-mail: [hosneara1968@gmail.com](mailto:hosneara1968@gmail.com)

### Abstract

The purpose of this paper is to investigate experimentally the effect of frequency and amplitude of vibration on yarn tension as well as the friction of ring-traveller. An external vibration generating facilities is created and placed in a miniature ring spinning frame to generate and apply vibration to ring. The experimental miniature ring spinning frame has the facility to vary the spindle speed, frequency and amplitude of vibration. During the experiment, the spindle speeds vary 12000 – 8000 r.p.m. The amplitude of vibration for this work was varied 0 mm to 1.25mm and frequency varied 0-800 Hz. Studied have shown that ring-traveller friction is influenced by the variation of the amplitude and frequency of vibration. Results are compared with different parameters of vibration status respective to spindle speed. It was found that yarn tension and friction between ring and traveller was depending on the parameters of vibration.

**Keywords:** Friction, Vibration, Frequency, Amplitude, Ring, Traveller and Yarn tension

### 1. Introduction

Ring spinning is a popular spinning system for making spun yarn from cotton, wool and different man-made staple fiber in the textile industry. According to strength of product (yarn), this system is best and this system is flexible and most widely used spun yarn manufacturing system. But low productivity is one of the remarkable limitations of this system due to the limited speed (max 40meter/sec) of traveller. Traveller speed is limited for high friction between ring and traveller, which increase the temperature of traveller and finally it breaks.[1-4]

The co-efficient of friction between the contacting surfaces depends on type of material, surface characteristics and conditions, relative motion and vibration etc.[5-8] Vibration may increase or decrease friction depending on surface characteristics, area of contact, sliding velocity, contact pressure and temperature etc. [9-15] It is known that frictional force may increases or decreases depending also on the vibration parameters. It can be noted that there are no established correlation between co-efficient of friction and vibration related parameters. Considering the above findings and lack of correlation, the present research was aimed to study the effect of frequency and amplitude of vibration on yarn tension and as well as friction between ring and traveller of a ring spinning frame.

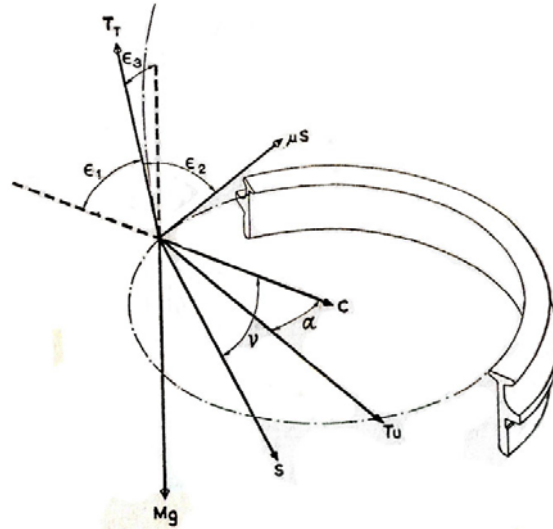
### 2. Theoretical Analysis

The forces acting at the traveller on the contact of ring owing to its rotational motion with the tension of yarn is analyzed and at the condition of equilibrium in the three orthogonal directions is founded the following three equations:-

$$C = T_U \cos \alpha + S \cos \nu - T_T \cos \varepsilon_1 \quad (1)$$

$$\mu S + T_T \cos \varepsilon_2 = T_U \sin \alpha \quad (2)$$

$$T_T \cos \varepsilon_3 = S \sin \nu + Mg \quad (3)$$



**Fig. 1.** Forces acting on traveller

Here  $C = MR\omega^2$  is the centripetal force required to keep the traveller rotating  $R$  = is the radius of rotation of the center of gravity of the traveller,  $M$  = mass of the traveller

$T_U$  = yarn tension at traveller in the package side,  $\mu$  = the co-efficient of friction between ring and traveller,  $\alpha$  = the winding angle,  $S$  = the normal reaction between ring and traveller

At equilibrium condition and simplification of equation no.1, 2 and 3 with different logical assumption, the following equation is found

$$T_T \cong a\mu C \quad (4)$$

But  $C$  is always constant for same spindle speed and traveller weight

So it can be written

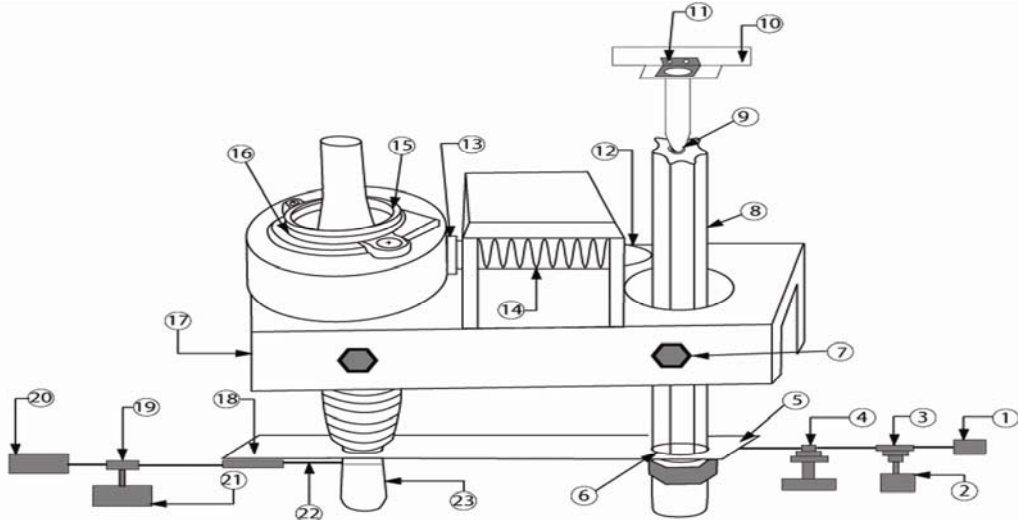
$$T_T \approx a\mu \quad (5)$$

Now it is clear that Yarn tension depends on ring traveller and yarn traveller friction.

### 3. Experimental setup

An experimental set-up was designed and fabricated such that it can transmit vibration to the existing ring of a spinning frame. In this set up (Figure.2) the to and fro motion along the radial direction of an arm is used to vibrate the ring base. The construction and working principle of the set-up is given bellow.

1= variable frequency drive, 2 = Motor, 3,4 = Step pulley , 5= Bobbin rail, 6 = Bolt, 7= Nut, 8 = Fluted spindle, 9 = Fluted spindle supporter, 10= Connector with frame, 11= Supporter attachment, 12= To and fro motion transferring arm, 13= Nut, 14= Helical Spring, 15= Ring 16= Ring fitting frame, 17 = Ring rail, 18 =Bobbin rail, 19= Motor pulley, 20= Variable frequency drive, 21= Motor.



**Fig. 2.** Schematic diagram of the experimental set-up [16]

A spindle with corrugated surface (fluted spindle) is designed and fabricated in such a way, that it can be placed at the normal position of the spindle with existing facilities. To rotate this fluted spindle, power is transferred through flexible belt from step pulley arrangement of a motor. The motor is mounted vertically on an isolated place having rubber damper. In addition to step pulley, a variable frequency drive (an electronic speed control unit) is used to vary the speed of the motor as required.

A to and fro motion transmitting arm is placed between fluted spindle and the ring base. During rotation of the fluted spindle, to and fro motion is created to the contacting arm which finally becomes a vibration to the ring base.

The Spindle of the ring spinning machine rotates from the power of main drive through belt. A variable frequency drive is also connected with this main motor to rotate the spindle at variable speed.

The parameters of spinning are taken, which are mention in. (table-1) and during experiment the following measurements (table-2) are recorded:-

**Table. 1** Experimental condition

Name of the Parameter	Selected material and value for experiment
Type of fiber	Polyester multifilament and cotton fiber
Yarn count (Ne)	10 and 20
Twist per inch	14 and 18
Ring diameter(mm)	45
Traveller weight	0.045- 0.049 gm

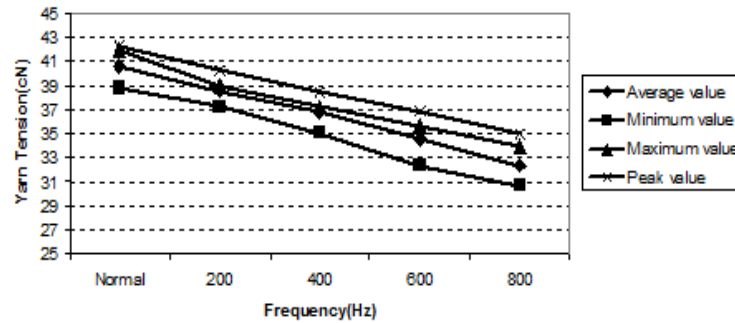
**Table. 2** Measuring instrument and measurement

Name of the Measuring Instrument	Parameters measured/Calculate
Vibration Measuring Meter METRIX Instrument Co	Displacement and Velocity of vibration
Yarn Tension Measuring Meter SCHMIDT, Germany	Yarn Tension (Average, Minimum, Maximum and Peak value)
Digital Tachometer	Spindle speed

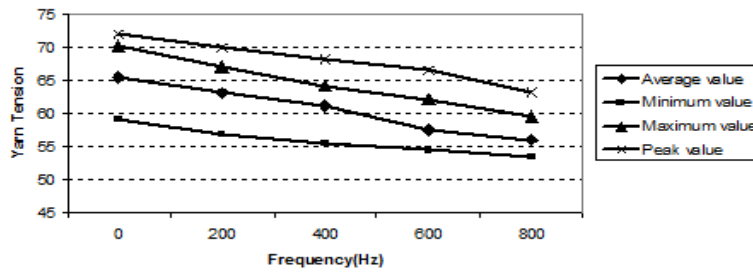
## 4. Results and Discussions

### 4.1 Effect of Frequency of Vibration on Yarn Tension

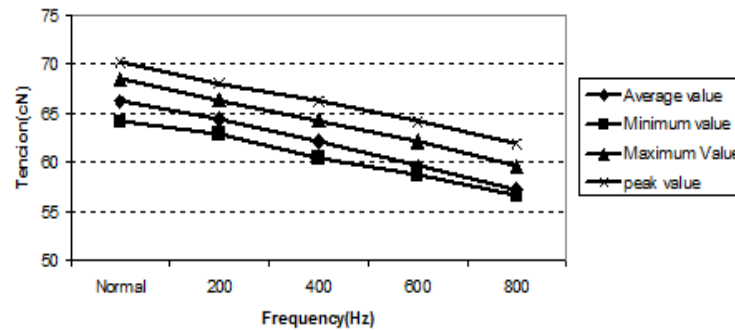
To identify the effect of frequency of vibration on ring; the amplitude of vibration is 0.5mm and frequency 200, 400, 600 and 800 Hz selected. Experiments are being done with the spindle speed of 8000, 10000 and 12000 r.p.m.



**Fig. 3.** Yarn Tension at different frequency of vibration at ring. (spindle speed 8000 r.p.m., amplitude 0.5mm)



**Fig. 4.** Yarn Tension at different frequency of vibration at ring. (spindle speed 10000 r.p.m., amplitude 0.5mm)



**Fig. 5.** Yarn Tension at different frequency of vibration at ring.(spindle speed 12000 r.p.m., amplitude 0.5mm)

The effects of frequency of vibration are displayed in Figures 3, 4 and 5. From the three figures it is seen that all the values of yarn tension (average, min, max, peak) decrease clearly with increasing the frequency of vibration. The tendency of tension decrease rate is almost linear for the three different spindle speeds. Frequency is an important parameter of vibration, which makes the repetition of oscillating motion per second of a vibratory body. Higher frequency ensures higher times of oscillation motion per second, which has strong effect on yarn tension. Yarn tension or friction between the ring and the traveller is inversely proportional to the frequency of vibration. It is very difficult to generate more than 800 Hz frequencies of vibration due to the system limitation. The system of vibration generation could not be more stable with too high frequency.

High frequency of vibration means more number of separations between vibration bodies and at the same time lower time for contacting surfaces, that is lower area of contact. This procedure reduces the resistance against the running of the traveller, causing the reduced tension. Therefore, the reduction of yarn tension for the increase of frequency of vibration is due to more separation of the contact surfaces. In fact the higher the separation, lower the time of contact between the frictional surfaces. As the frequency increases, keeping the amplitude of vibration constant, the acceleration of vibration will also increase that might cause momentary vertical load reduction, which causes the reduction of effective normal force resulting reduction of tension with the increase of frequency of vibration. The factors may be responsible for the momentary load reductions are:

- Superposition of static and dynamic force generated during vibration.
- Reversal of the friction vector
- Load transformation of vibration energy into heat energy
- Approaching excitation frequency to resonance frequency



Therefore it can be concluded that with the increase of frequency of vibration decreases the value of yarn tension as well as the friction.

#### 4.2 Effect of Amplitude of Vibration on Yarn Tension

To verify the effect of amplitude of vibration on the ring; the frequency of vibration is 400 Hz and amplitude 0.25, 0.5, 0.75, 1 and 1.25 mm selected. Experiments are being done with the spindle speed of 8000, 10000 and 12000 r.p.m and other parameters of spinning are taken the same as given in Table 1.1.

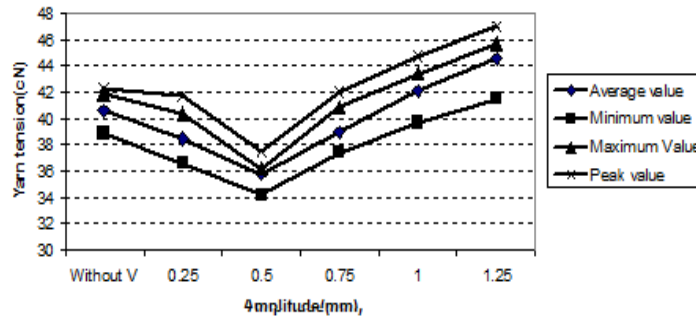


Fig. 6. Yarn Tension at different amplitude of vibration at ring. (spindle speed 8000 r.p.m., frequency 400 Hz)

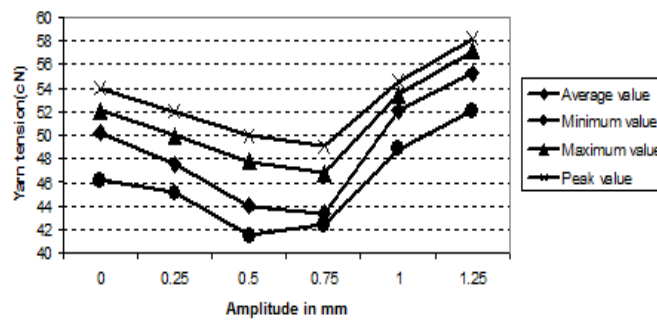


Fig. 7. Yarn Tension at different amplitude of vibration at ring. (spindle speed 10000 r.p.m., frequency 400 Hz)

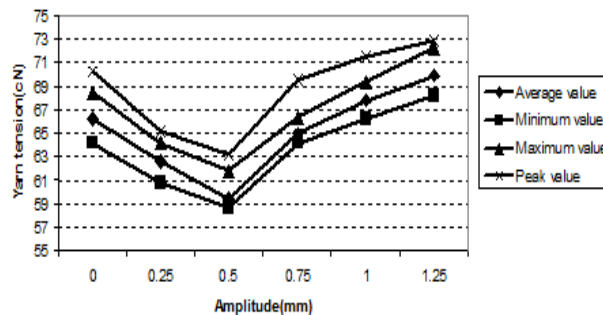


Fig. 8. Yarn Tension at different amplitude of vibration at ring. (spindle speed 12000 r.p.m., frequency 400 Hz)

Amplitude is also an important parameter for generation of effective vibration at the ring for the reduction of friction between ring and traveller. Figure 6, 7 and 8 show the effect of different amplitude of vibration on yarn tension. At first yarn tension is reduced up to 0.5 mm of amplitude but after 0.7 mm of amplitude, yarn tension is going to increase at upward direction. It may happen, high amount of amplitude creates some new problem to traveller, which makes large displacement from the surface of the ring and dropped again ring contact with additional load. When the traveller is going to drop at the surface of the ring at running condition from a long distance, suddenly a strong pressure arises between the ring and the traveller. This makes a serious problem to traveller and consequently deformed itself on ring surface and fly out.

Therefore it can be concluded that with the increase of amplitude of vibration, the value of yarn tension as well as the friction decreases. This may happen up to certain limit, for the increase of amplitude friction and consequently the yarn tension start to decrease. It can happen for the increase of mechanical interlocking that result increase of tension. The factors may be responsible for the momentary increase of load for the following reason:

- Addition of the friction vector
- Load transformation of vibrational energy into high heat energy, which deform the surface of comparative softer material (traveller) and increase frictional force.

Amplitude is an important factor for effective generation of vibration. Appropriate amplitude might help to reduce friction between the ring and the traveller of the ring spinning frame.

Vibration is one kind of oscillating motion and this oscillating motion of ring induces the traveller to maintain intermitted contact with ring. This reduction of contact time and area of contact has influence on the reduction of temperature of the meeting surface of ring and traveller and hence the rise of temperature is decreased. The same reason may be valid to the reduction of yarn tension.

Now it can be summarized that application of vibration is a new way, which can assist the traveller to run with intermittently contact on the ring. This process reduces yarn tension, temperature of meeting surface between ring and traveller and as well as its friction. To maintain the present running condition i.e the same friction, about 10% spindle speed can increased with the application of vibration. This will increase the production of a spinning machine.

## 5. Conclusion

Amplitude and frequency are two important parameters for generation of effective vibration at the ring for the reduction of friction between ring and traveller. Co-efficient of friction between ring and traveller decreases with increase of frequency of vibration but with the increase of amplitude of vibration, the value of yarn tension as well as the friction decreases, which happen up to certain limit and then it shows opposite character.

Selection of appropriate frequency and amplitude of vibration is very important for generation of effective vibration, which helps to reduce friction between ring and traveller of a ring spinning frame.

## 6. References

1. Barr, De and Catling, H, The Principles and Theory of Ring Spinning, Manual of Cotton Spinning, Volume 5 (1965), *The Textile Institute Butterworths Press, London, 1965.*
2. Klein, W, A Practical Guide to Ring Spinning, Manual of Textile Technology, Volume 4, (1995)*The Textile Institute, MFP Design and Print, Manchester, UK,*
3. Grosberg, P and Iype, C, Yarn Production ( Theoretical Aspects), (1999)*The Textile Institute International, Biddles, UK.*
4. Lord, P R, Yarn Production (Science Technology and economics), (2003) *The Textile Institute, Woodhead Publishing Limited, Cambridge England.*
5. Archard, J.F. (1980), "Wear theory and mechanism", in Peterson, M.B. and Winer, W.O.(Eds), *Wear Control Handbook, ASME, New York, NY, pp. 35-80.*
6. Arnov, V., D' Souza, A.F., Kalpakjian, S. and Shareef, I.(1984a), "Interactions among friction, wear, and system stiffness-Part 1 : "Effect of normal load and system stiffness", *ASME Journal of Tribology, Vol. 106, pp 54-58.*
7. Arnov, V., D' Souza, A.F., Kalpakjian, S. and Shareef, I.(1984b), "Interactions among friction, wear, and system stiffness-Part 2 : "Vibration induced by dry friction", *ASME Journal of Tribology, Vol. 106, pp 59-64.*
8. Bushan, B., 1999, Principle and Applications of Tribology, John Wiley & Sons, Inc., *New York, pp. 344-430, Chap. 6.*
9. Bushan, B. and Gupta, B.K. (1991), Handbook of Tribology Materials, Coatings, and Surface Treatment, *Mc-Graw-Hill, New-work,NY9reprint with corrections, Krieger, Malabar, FL(1997)*
10. Godfrey, D., 1967, "Vibration Reduces Metal to Metal Contact and Causes an Apparent Reduction in Friction," *ASME Transactions, 10, pp. 183-192.*
11. Skare, T. and Stahl, J. (1992), "Static and dynamic friction processes under the influence of external vibrations", *Wear, Vol. 154, pp. 177-92.*
12. Chowdhury, M. A. and Helali, M. M. September (2006), "The Effect of Frequency of Vibration and Humidity on the Co-efficient of Friction", *Tribology International, 39, pp. 958-962.*
13. Chowdhury, M. A. and Helali, M. M. (2007), "The Effect of Frequency of Vibration and Humidity on Wear Rate" *Wear, Vol. 262, pp. 198-203.*
14. Chowdhury, M. A. and Helali, M. M. (2008), "The Effect of Amplitude of Vibration on the Co-efficient of Friction", *Tribology International, Vol41, pp. 307-314.*
15. Lenkiewicz, W., 1969, "The sliding friction process- effect of external vibrations," *Wear, 13, pp. 99-108.*
16. Begum, Hosne Ara Ph. D Thesis, "Effects of Vibration on the Twisting Rate of Ring Spinning for Production of Yarn", *Bangladesh University of Engineering and Technology, February 2012.*

## Development of an Automatic Humidity Control System

M.E. Hoque, S.M. Rasid\*, Amit Roy, N. Paul, Ferdous Alam, Md. Raseluzzaman  
Department of Mechanical Engineering  
Rajshahi University of Engineering & Technology, Rajshahi-6204, Bangladesh  
E-mail: [emdadulhoque@gmail.com](mailto:emdadulhoque@gmail.com), [mamun06me\\_ruet@yahoo.com](mailto:mamun06me_ruet@yahoo.com)\*

### Abstract

*This paper presents an automatic humidity control system using microcontroller. The developed system actually consists of three parts. These are mechanical, electrical or electronic parts and software or logic parts. The mechanical part consists of a square shaped room, a cylindrical shaped chamber (humidification and dehumidification chamber) connected with the flexible pipes and two electric blowers. The electrical part consists of a ATmega-32 microcontroller, HSM-20G humidity sensor, LM-35 temperature sensor, LCD monitor, relays, transformer, diode, capacitor, transistor, etc. The logical part consists of an automatic humidity control system that is controlled by microcontroller. For automatic humidity control system, a humidity sensor is used that is attached in the room to measure the humidity. If the humidity of the room is greater than comfortable range (50%-70%R.H) then the humidity sensor (HSM-20G) senses this condition of air and sends this information to the microcontroller. The microcontroller executes this information and starts the blower, which is attached to the dehumidification chamber. In this way, the system acts as an automatic humidity controller using micro-controller. Finally the performance of the system is evaluated experimentally.*

**Keywords:** Automation, Microcontroller, Air conditioning.

### 1. Introduction

Control of humidity is the regulation of the degree of saturation (relative humidity) or quantity (absolute humidity) of water vapor in a mixture of air and water vapor [1-4]. Controlling the humidity is critical to staying comfortable and avoiding problems. Too much humidity during summer can cause allergies and promote the growth of mold, which can be a health risk and cause structural damage of different parts. Too little humidity during winter can cause colds and other infections as well as nosebleeds and dry skin [4], [5]. Control of humidity is most required condition of comfort or industrial conditioning systems. Humidity control can be highly critical in some areas such as hospitals operating rooms, electronic data processing equipment rooms, textile mills and many printing operations. [5]

Proper greenhouse humidity is important both in preventing plant diseases and promoting healthy plant growth. High humidity can promote the Botrytis and other fungal diseases. High humidity also restricts plant transpiration, which in turn limits evaporative leaf cooling and can lead to overheating of plant foliage. If high humidity persists for a long time, the restriction of transpiration can limit the transpiration stream of nutrients and can lead to nutrient deficiencies. Low humidity is best avoided because it may increase foliar transpiration to the extent that the root system cannot keep up. Humidity control system largely used in power plants requires protection against moisture. This system is used in defense, storage of fertilizer, cheese, sugar, coating and packaging etc. Humidity control system is used in air conditioning both in summer and winter seasons.[1-5]

Humidity can be controlled in two ways either manually or automatically. Hygrometer is used to measure the humidity in manual humidity control system and the blower is switched on-off the blower for humidification and dehumidification process manually. The automatic system has a great advantage than manual system because no labor needed to start the humidifying and dehumidifying blower. Therefore, labor cost is reduced in this system. Automatically humidity can be controlled in various ways such as using digital signal processor (DSP), programmable logic controller (PLC), microcontroller etc.[10] The DSP, PLC systems are very much expensive and large in size, therefore microcontroller is used as controller in the developed system because it is very cheap and small in size. In this work, a square shaped room is constructed, with a cylindrical chamber. With the help of ATmega32 microcontroller, HSM-20G humidity sensor, LM-35 temperature sensor, LCD monitor and other necessary components, the system is operated automatically.

## 2. Construction of the Automatic System

The automatically operated humidity controller consist of several parts such as cylindrical shaped chamber, square shaped room, flexible pipe, ATmega-32 microcontroller, HSM-20G humidity sensor, LM-35 temperature sensor, LCD monitors, blower, flexible pipe, sponge etc. which are described in the following.

### Cylindrical shaped chamber

This is a cylindrical shaped chamber and acts as a heart in this control system. The chamber is internally divided into two equal portions and both the portions has inlet and outlet ports The cylinder is required to hold the drawers that contain silica gel and sponge which wet with water. The cylinder is made of galvanized plain sheet.



(a) Front view of the chamber



(b) Side view of the chamber



(c) Inside view of the chamber

**Fig.1.** Photograph of the cylindrical shaped chamber

### Square shaped room

This room is another important part in this system. This room is considered as a testing room where the control of the humidity can be tested. This room has also inlet and outlet ports.



**Fig. 2.** Photograph of square shaped room

### ATmega-32 Microcontroller

The ATmega32 is a low-power CMOS 8-bit microcontroller based on the AVR enhanced RISC architecture. By executing powerful instructions in a single clock cycle, the ATmega32 achieves throughputs approaching 1 MIPS per MHz allowing the system designed to optimize power consumption verses processing speed.[8-9]



**Fig. 3.** ATmega-32 Microcontroller

### **HSM-20G Humidity Sensor**

Humidity sensor is used to sense the value of humidity in the square room whose humidity is to be controlled. It use voltage 7V DC, Storage temperature  $T_{sg}$ -40 to 85<sup>0</sup> C. Storage humidity range  $R_{hstg}$  0 to 100% RH. Operating temperature range  $T_a$  -30 to 80C.



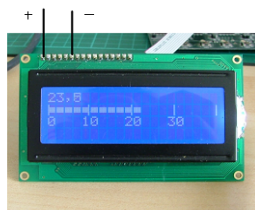
**Fig. 4.** HSM-20G Humidity Sensor

### **Blowers**

Two blowers are required to force the process air and reactivation air through the cylindrical shaped chamber from the square shaped room.

### **LCD Monitor**

A liquid crystal display (LCD) is a flat panel display, electronic visual display, or video display that uses the light modulating properties of liquid crystals.

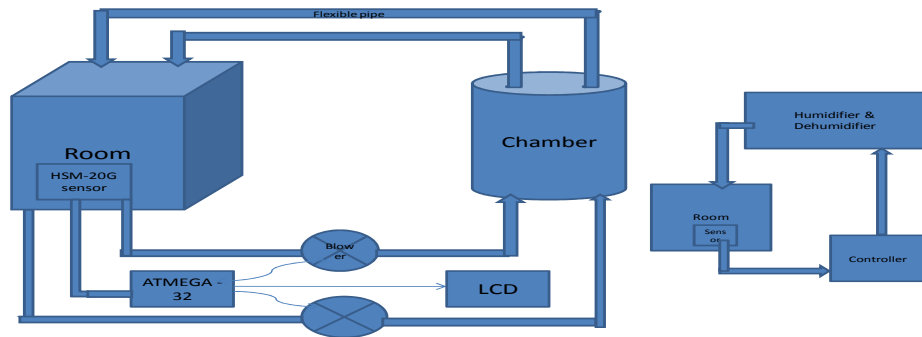


**Fig. 5.** LCD monitor

## **3. Experimental Set-up**

### **Description of the set up**

In this control system, two parts are essential. One is the room where the humidity is controlled and the other is a chamber by which the humidity can be controlled. Both room & chamber have inlet & outlet ports. The inlet ports of the chamber are connected with electric blowers and the outlet ports of the chamber are connected with the inlet ports of the room. On the other hand, the outlet ports of the room are connected with the blower. The chamber which is used to control the humidity is partitioned into two portions. Both the portions have inlet & outlet ports. Now at the middle of the chamber, there are two trays which are connected with the chamber. Trays are constructed with nets. The structure of one tray will be made of honey comb. In this tray silica gel is placed and in another tray a wet cloth is placed. In the portion where silica gel is placed, maintains the dehumidification process and in another portion humidification process.



**Fig. 7.** Schematic Diagram of humidity control system using microcontroller and feedback control



**Fig. 8.** Photograph of the complete assembly of humidity control system

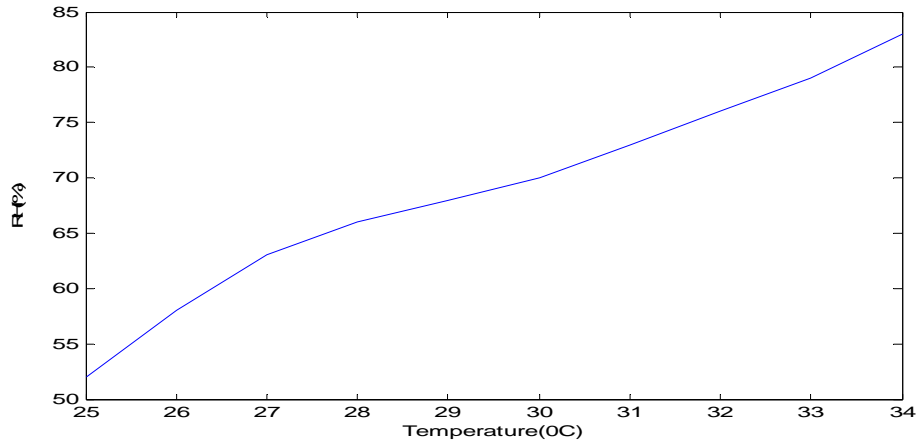
### Working principle

For the automatic control system, the main components are ATMEGA-32 micro-controller and a HSM-20G humidity sensor that is attached in the room which helps to measure the humidity. If the humidity of the room is greater than comfortable range (50%-70%R.H) then the humidity sensor (HSM-20G) senses this condition of air and sends this information to the microcontroller. The microcontroller executes this information and starts the blower which is attached with dehumidification chamber. After certain period the humidity falls down to comfortable range (50%-70% RH) after absorbing water particle by the silica gel. If the humidity of the room is less than the comfortable range similarly this condition of air is sensed by humidity sensor and is sent to the microcontroller. Similarly humidity is increased to the comfortable range. In this way the system acts as a automatic humidity controller.

## 4. Experimental Results

### Dehumidification

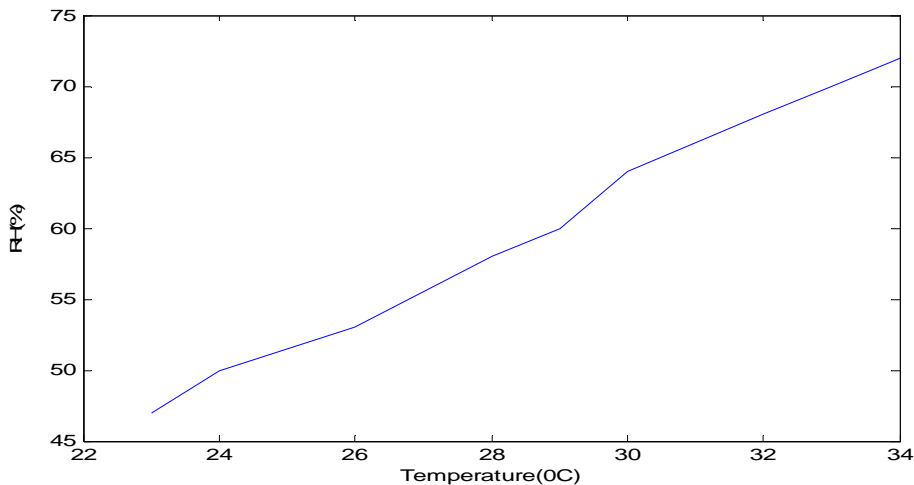
In this section, dehumidification is done by using Blue type silica gel and humidity is decreased from high range to low range within the comfortable range and the change of relative humidity with temperature is shown in the figure 9.



**Fig. 9.** Relative humidity Vs. Temperature diagram for dehumidification process

### Humidification

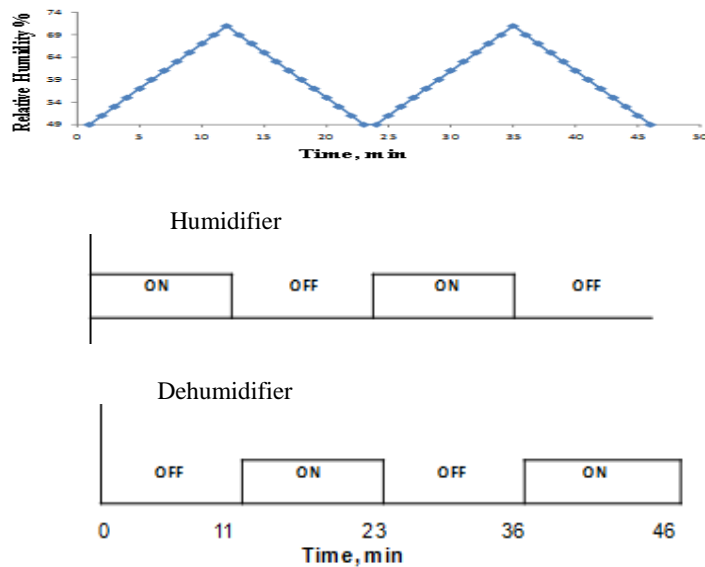
In this section, humidification is done automatically by using wet sponge and humidity is increased from low range to high range and the change of relative humidity with temperature is shown in the figure 9.



**Fig. 10.** Relative humidity Vs. Temperature diagram for humidification process

### Performance of the Controller

The Fig. 9 indicates the relative humidity vs time for humidification and dehumidification. The increasing and decreasing region of the figure represent the humidification and dehumidification, respectively. Since the comfortable range of humidity is 50-75%, when relative humidity decreases below the comfortable range humidity sensor sense the condition of room and send the signal in the microcontroller which turn on the humidifier and humidity gradually increases with time. It is also shown that after 11 min humidity reaches above the comfortable range, then microcontroller turn off the humidifier and turn on the dehumidifier. After 23 mins again humidifier turn on and dehumidifier turn off. In this way system control the humidity of a room.



**Fig.11.** Relative humidity vs. Time for humidification and dehumidification and automatic on-off of humidifier and dehumidifier

Since the comfortable range of humidity is 50-75%, when relative humidity decreases below 50% humidity sensor sense the condition of room and send the signal in the microcontroller which turn on the humidifier and humidity gradually increases with time which is shown in the figure 9. From the figure it is shown that after 11 min humidity reaches approximately 74% then microcontroller turn off the humidifier and turn on the dehumidifier. After 23 mins again humidifier turn on and dehumidifier turn off. In this way system control the humidity of a room.

## 7. Conclusion

An automatic humidity control system has been designed and fabricated. The humidification and dehumidification process of the system is done automatically. In case of dehumidification, humidity is reduced from 85 to 50% step by step. For this purpose, silica gel is used. On the other hand, humidity is increased from 50 to 85% by using wet sponge that contained water. It is seen from the result that developed humidity control system can provide the comfortable range of humidity automatically using microcontroller. Finally, this system is able to control the humidity of a room.

## 8. References

- [1] Stoecker. Wilbert F. and Jerold W. Jones, Refrigeration & Air Conditioning, 7<sup>th</sup> Edition, L. Heuber Publisher, 2010.
- [2] R.S. Khurmi & J. K. Gupta, Refrigeration & Air Conditioning, 6<sup>th</sup> Edition, S. Chad Publishing House (Pvt) Ltd., Ram Nagar, New Delhi-110055, 2009.
- [3] V. K. Jain, Refrigeration & Air Conditioning, 4<sup>th</sup> Edition, L. Heuber Publisher, 2010.
- [4] S.C Arora and S. Domkundwar (2009), Refrigeration & Air Conditioning, 8<sup>th</sup> Edition, Dhanpat Rai and Sons Publisher
- [5] Robert Chatenever, House & Home Heating, Ventilation & Air Conditioning, Arlington Publisher, 7<sup>th</sup> edition, 2010.
- [6] V.K.Metha (2009), Principles of Electronics, 9<sup>th</sup> Edition, S. Chand & Company Ltd.
- [7] R.P.Malvino (2010), Electronics Principles, 6<sup>th</sup> Edition, Tata McGraw-Hill, Arlington Publisher, 7<sup>th</sup> edition, 2010.
- [8] S. R.Ferguson & P. K. Devison, A Text Book of Mechatronics Engineering, 5<sup>th</sup> Edition, Washing D.C.: American Institute for Conversion.
- [9] T.S.William & V. K. Metha, Mechatronics Engineering, 8<sup>th</sup> Edition, Copyright © 2010.
- [10] William Godfride & R.G. Pique, A Text Book of Programming, C++, 4<sup>th</sup> Edition, 2009.
- [11] Grant McFarland, Microprocessor Design, McGraw-Hill Professional, 2010 ISBN 0071459510.
- [12] A.S. Sedra and K.C. Smith (2009), Microelectronic circuits, 5<sup>th</sup> Edition, New York: Oxford University Press. pp. 397 and Figure 5.17. ISBN 0-19-514251-9.
- [13] V.K.Metha (2009), Principles of Electronics, 9<sup>th</sup> Edition, S. Chand & Company Ltd.
- [14] R.P.Malvino (2010), Electronics Principles, 6<sup>th</sup> Edition, Tata McGraw-Hill, Arlington Publisher, 7<sup>th</sup> edition, 2010.



## **Design & Performance Analysis of a Smart Portable PV Charger**

Md. Abu Shahab Mollah<sup>1</sup>, M. A. Parvez Mahmud<sup>2</sup>, Md. Faysal Nayan<sup>1</sup>, Shahjadi Hisan Farjana<sup>3</sup>, Sharmin Sobhan<sup>1</sup>

<sup>1</sup>Ahsanullah University of Science & Technology, Dhaka, Bangladesh

<sup>2</sup>University of Science & Technology, Daejeon, South Korea

<sup>3</sup>Khulna University of Engineering & Technology, Khulna, Bangladesh

E-mail: piash117@gmail.com, shahabee\_06@yahoo.com, nayan102aust@gmail.com, sharmin\_sobhan@yahoo.com, shahjadisynty@yahoo.com

### **Abstract**

*In this paper a smart and simple PV charger for portable applications is presented. This proposed charger is low cost, low volume and light weight. Moreover this charger can realize three charging modes including the MPPT mode, the CV mode and the current limited mode. It can be integrated into an IC chip to reduce the size due to the simple structure. At last, a 60W prototype is built and tested to confirm the validity and applicability of the proposed system.*

**Keywords:** PV charger, Smart switch, Control circuit, Driver circuit.

### **1. Introduction**

The traditional charger is the component, which transfers the power from the grid to the battery. In normal condition, the grid can supply continuing and stable energy to the battery. Therefore, the battery can be charged according to its self-condition by the traditional charger. Normally, the charging process includes two stages: in the first stage, the battery is charged in the constant-current mode. When the voltage of the battery is up to the floating voltage, the charging mode is changed to the constant-voltage (CV) mode as the second stage. During the whole charging process, only the charging current and the voltage of the battery need to be controlled.

### **2. PV charger**

Photovoltaic or in short term PV is one of the renewable energy resources that recently has become broader in nowadays technology. PV has many benefits especially in environmental, economic and social. In general, a PV system consists of a PV array which converts sunlight to direct-current electricity, a control system which regulates battery charging and operation of the load, energy storage in the form of secondary batteries and loads or appliances. A charge controller is one of functional and reliable major components in PV systems.

### **3. Proposed Smart and simple PV charger**

To design an efficient photovoltaic charger we use some basic part to complete the design successfully. Main part of our design consists of PV array, smart switch, and control circuit, sample and hold circuit, driver circuit.

We can say our PV charger design is more smart system than other PV charger. In our design, PV array is used to reduce the system size. Step down buck converter is used as the charging circuit due to its simple structure and low cost. The overall block diagram consist of one PV array, three control loop, one smart switch, one insulation driver, one diode, one inductor, one capacitor and one lithium ion battery. So it can be smarter than other system.

The block diagram of proposed smart and simple charger circuit is given in **figure 1**:

### 3.1. PV array

Photovoltaic identifies the direct conversion of sunlight into energy by means of solar cells. The conversion process is based on the photoelectric effect. The photoelectric effect describes the release of positive and negative charge carriers in a solid state when light strikes its surface.

Here PV array is used to reduce the system size. Step down buck converter is used as the charging circuit due to its simple structure and low cost. The overall block diagram consist of one PV array, three control loop, one smart switch, one insulation driver, one diode, one inductor, one capacitor and one lithium ion battery.

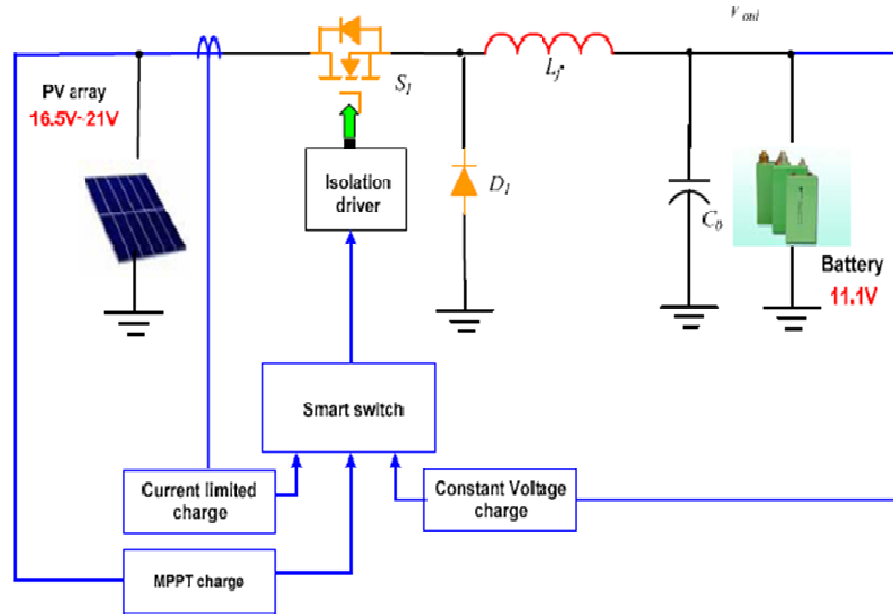


Fig. 1. Block diagram of proposed smart and simple PV charger

### 3.2. Smart switch

Here smart switch performs important role in case of selecting control loop for proper functions of PV charger. For three level of value of PV array it chooses three value of control loop.

### 3.3. Control circuit

The smart switch is achieved by two small diodes. At the beginning of the charging, the battery voltage is lower than the floating voltage, so the output of CV control loop is high. The diode D2 is reversed to block the CV control loop. And the Buck converter is controlled by the MPPT control loop. When the battery voltage reaches the floating voltage, the CV control loop takes effect to keep the output voltage steady instead of the MPPT control loop. The current limited control loop is realized by a control IC with current peak mode (CPM). The slope compensation is added to provide the circuit stability. So whichever control loop is chosen, the charge current will not be higher than the maximum charge current of the battery. The block diagram of driver circuit is given in **figure 2**.

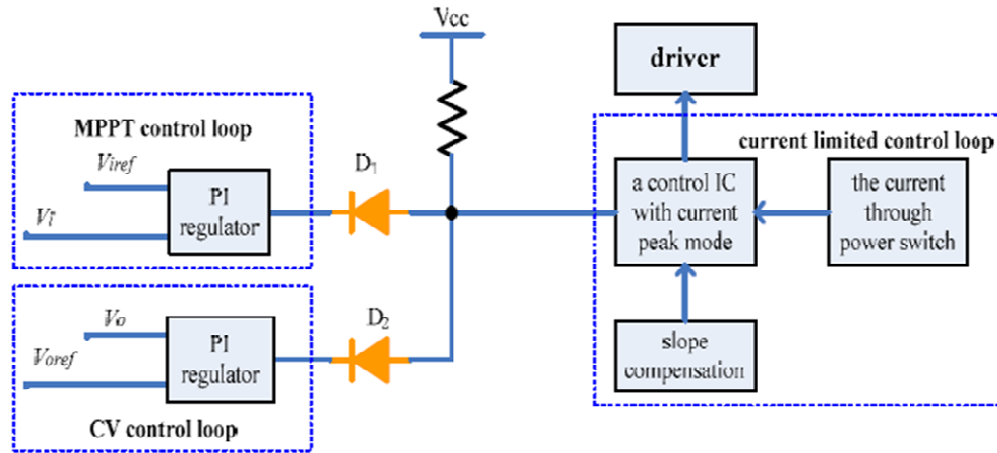


Fig. 2. Block diagram of driver circuit

### 3.4. Sample & hold circuit

The FOCV method is selected in this paper to realize MPPT. The block diagram of the sample & hold (S/H) circuit is shown in Fig.3. The open-circuit voltage is acquired by shutting down the power switch in Buck converter periodically. The 555 timer is used to generate the sampling pulse signal periodically. When its output is a high level, on one hand, it affects the control IC with CPM to shut down the power switch. On the other hand, the high level affects the S/H chip LF398 to make its output equal to the input voltage of Buck. At this time, as the power switch is shut down, the input voltage of Buck converter is just right the PV array open-circuit voltage. Thus the output voltage of LF398 is the sampling open-circuit voltage of the PV array. After the short sampling time, the output of 555 timer is a low level, the converter operates as normal Buck converter. Furthermore LF398 is in hold state to keep the output voltage invariable no matter how the input voltage of Buck changes. The voltage held by LF398 is still the sampling open-circuit voltage of the PV array. Then it is easily to obtain 80% of the sampling open-circuit voltage by applying divided resistors. This voltage is used as the reference voltage in MPPT control loop.

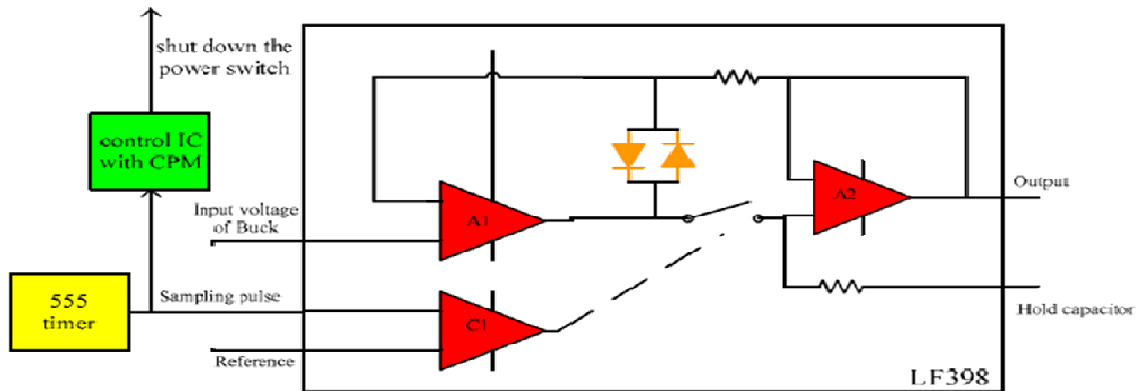
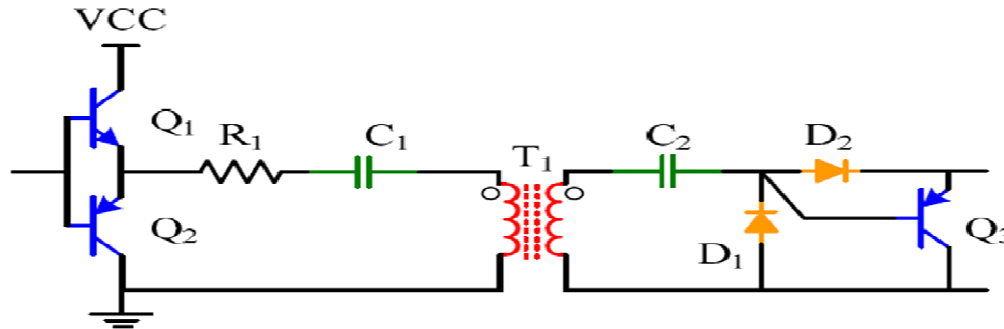


Fig. 3. Block diagram of sample and hold circuit

### 3.5. Driver circuit:

The MOSFET can't be driven as a normal one because its source is floated in the Buck converter. The gate driver methods can be divided as the isolation way and non-isolation way. In the non-isolation driver methods, the

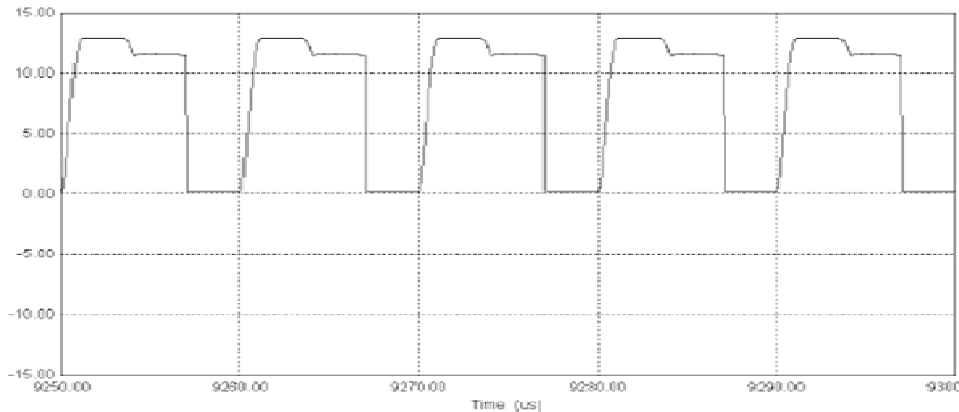
bootstrap is a good candidate. However, the load is the battery for PV charger. In this circumstance, before the converter starts, the voltage level of the source of the MOSFET is kept the same as the voltage of the battery. Therefore it is difficult to start the converter. The transformer driver circuit is shown in **Fig.6**. The transistors Q1 and Q2 are used to enhance the drive capability. The capacitors C1 and C2 are applied to strain away the dc component. D1 is the freewheeling diode. The transistor Q3 and the diode D2 are helpful to accelerate to turn-off speed of the MOSFET. The duty ratio can be changed in a wide scope in this transformer driver circuit shown in **figure 4**.



**Fig. 4.** Transformer driver circuit

#### 4. Simulation waveform of the driver circuit:

The simulation wave form of the driver circuit is shown in **Fig 5** below. From this simulation wave form we can see that the output power changes periodically with time .With the change in time 10 micro second the output power changes 0w to 13w and again 13w to 0w.So the period is 10 micro second.



**Fig. 5.** Simulations waveforms of driver circuit

#### 5. Wave forms of the driver circuit:

The experimental wave form of the drover circuit is shown in **Fig.6**. Here the gate to source voltage variation with time is shown. In this case the period is 8 micro second. i. e., after every 8 micro second the recurrence of voltage variation occurs. The maximum value of gate to source voltage is 14 V.

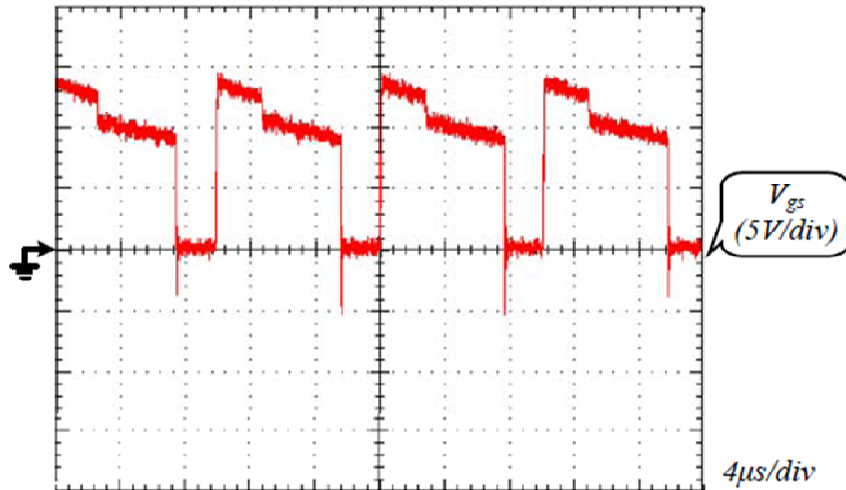


Fig. 6. Experimental waveforms of driver circuit

## 6. Simulation waveform of sampling open circuit voltage:

The simulation wave form of sampling open circuit voltage is shown in Fig.7. The sampling voltage  $V_{sample}$  can track the open-circuit voltage of the PV array  $V_{oc}$  when it changes.

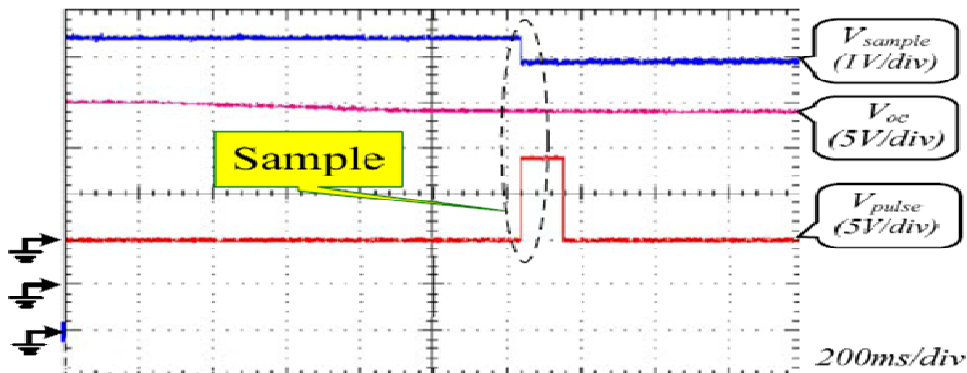


Fig. 7. Wave shape of sampling open circuit voltage

## 7. Simulation waveform when the charger works

The simulation wave form of PV charger when it works is shown in Fig 8 below. During the sampling time (the sampling pulse  $V_{pulse}$  is given), the MOSFET is shut down, and the input voltage of Buck converter  $V_{in}$  is equal to the PV array open-circuit voltage  $V_{oc}$ . During the holding time ( $V_{pulse}$  is low), the charger circuit works and  $V_{in}$  is equal to the operating voltage of PV array  $V_p$ . If the charger works in MPPT mode,  $V_p$  is equal to about 80% of  $V_{oc}$ .

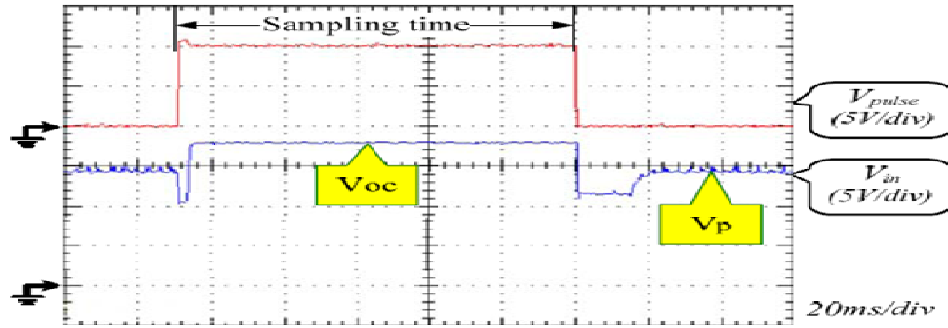


Fig. 8. Sampling waves when the charger works

### 8. Input and output voltages of buck converter:

The input voltage  $V_{in}$  and output voltage  $V_{out}$  of Buck converter are shown in Fig.9. Both of them demonstrate the proposed charger circuit works well.

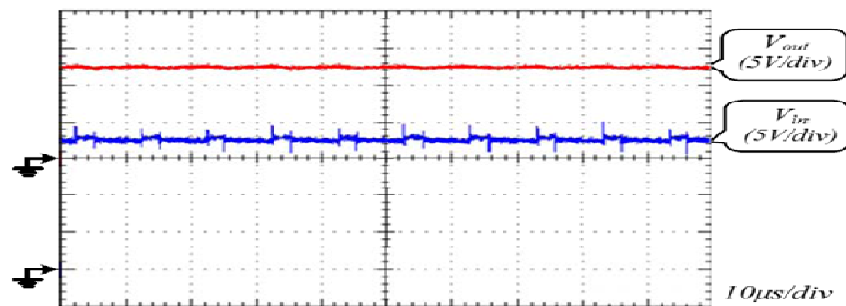


Fig. 9. Input and output voltages of Buck converter

### 9. Charging voltage and ratio of operational voltage to open circuit voltage

The experimental results of the ratio of the operation voltage  $V_{op}$  and the PV array open-circuit voltage  $V_{oc}$ . Charging voltage and  $V_{op}/V_{oc}$  is shown in Fig.14. At the beginning stage of the operation, the ratio is about 82%, which shows that the PV array works at the MPP. When the system changes to operate at CV charging mode, the ratio is bigger than 0.82, which shows that the PV does not work at the MPP any more to protect the battery.

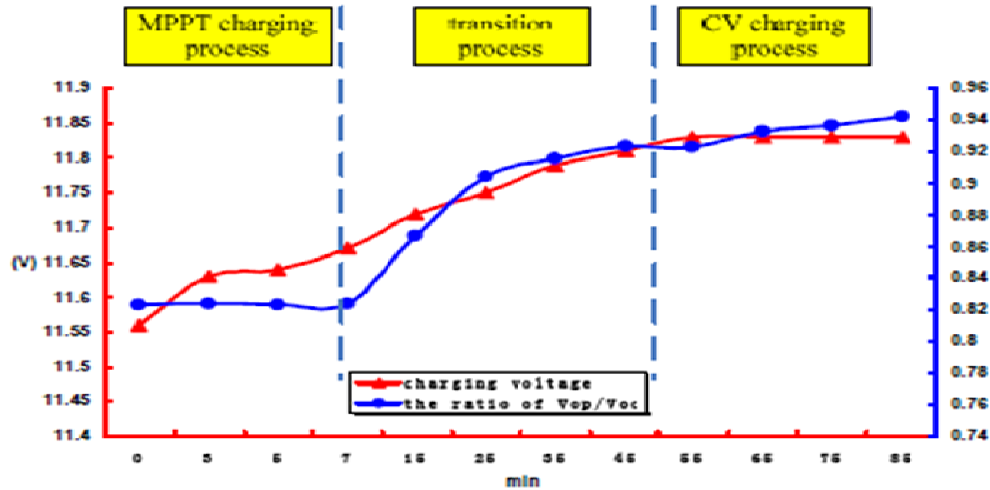


Fig. 10. Charging voltage and ratio of  $V_{oc}/V_{op}$

## 10. Conclusion:

With the increase of the energy demand and the concern of environmental pollution around the world, photovoltaic (PV) power system is becoming more and more popular. The off-grid PV power generation system is widely used in the portable applications to provide clear and long energy with a high power density. As a part of the off-grid PV power generation system, the PV charger is used to charge the battery from the solar energy. Nowadays, the portable equipment's relying on the solar energy as a power supply is widely used in the daily life. It is more suitable to make the PV charger cheaper, smaller and lighter in the portable applications. As a result, the PV charger should be simple and smart.

## 11. References

- [1] Min Chen, Gabriel A. Rincon-Mora, "Accurate, Compact, and Power-Efficient Li-Ion Battery Charger Circuit," IEEE Transactionson Circuits and Systems, Vol.53, NO.11, November 2006,pp.1180-1184.
- [2] J T. ESRAM, P. L. Chapman, "Comparison of Photovoltaic Array Maximum Power Point Tracking Techniques," IEEE Transactions on Energy Conversion, vol. 22, NO.2, June 2007, pp. 439-449.
- [3] Abu Tariq, M.S. Jamil Asghar, "Development of An Analog Maximum Power Point Tracker for Photovoltaic Panel," IEEE PEDS 2005, pp. 251-255.

## Development of Autonomous Line-Following Robots for Solving a Maze Problem

Md. Rokunuzzaman, Asif Ahmed Shishir, Md. Saeed Sharman, Amit Roy\*  
Department of Mechanical Engineering  
Rajshahi University of Engineering & Technology (RUET), Rajshahi-6204, Bangladesh  
E-mail: [royamit.me@gmail.com](mailto:royamit.me@gmail.com)

### Abstract

*This paper describes about the development of two autonomous robots (Bots) which cooperate each other to solve a maze. In this work, we have prepared two autonomous line-following robots which can communicate with each other so as to simultaneously solve two mazes via line following. We have been provided with turn indicators on 1 maze. A maze is formed by concentric circles connected to each other at some specific locations. There are two similar mazes with one maze having dimensions in a ratio greater than 1 radially. The maze is made up with white and black strips. In the maze solving process, First Bot has followed white strip to reach the center of the maze such that, if a black strip is encountered adjacent to line on left side, the bot will take the next left turn and If a black strip is encountered adjacent to line on the right side, the bot will take the next right turn. End of the maze is indicated by innermost black circle. This bot has communicated to the second bot and guide it to reach the end of respective maze. The second bot has received signals from the first bot and follow the line to reach the end of the maze.*

**Keywords:** Autonomous robots, Maze solving, Line-following method

### 1. Introduction

iARC: International Autonomous Robotics Competition is a great and entertaining way to enhance the learning process in the field of robotics. Students would gain first-hand experience in constructing and programming robots for competition, as well as allowing them to understand further the concept Mechatronics System Design [4]. Realizing this, iARC is organized by IIT Kanpur, one of the premier technical institute of India and Techkriti the annual technical and entrepreneurial festival of IIT Kanpur in conjunction with the Mechatronics System. This project-based course requires the students to build maze solving robot via line following and then to compete with each other. Its performances in this competition is measured and recorded as part of the evaluation scheme. In this competition, students are divided into groups of one, two, or three people maximum four and they are given freedom to design their own robots in terms of hardware and software used. For our group of two people, we developed maze solving robots with different kinds of drive trains. The requirements include that many equipment and sensors have to be synchronized, needing powerful real-time capabilities, under limited onboard batteries power [1].

### 2. Methodology



Fig.1 International Autonomous Robotics Competition (iARC) Arena



The rules of the International Autonomous Robotics Competition (iARC) are as below:

**Arena Specifications:**

- a. White strip width = 2.5 cm
- b. Black strip width = 2.5 cm
- c. Black strip length = 5 cm
- d. Separation between black and white strip = 2 cm
- e. Outermost diameter = 290 cm

**Robot size:**

- a. Maximum width: 200 mm
  - b. Maximum length: 200 mm
  - c. Maximum height: 200 mm
- The Robot must be stable and able to move on its own. A Bot not fulfilling these criteria will be disqualified.
  - Both the bots should be able to follow the line according to event specifications. In addition the bots should be able to communicate with each other. Communication can be wired or wireless
  - If communication is through wiring the team will be entirely responsible for problems due to entanglement of wires. Teams should bring sufficient length of wire for the same.
  - The wire should remain slack at all times.
  - Each team has to bring its own power supply for its robots.
  - The voltage difference between any two points on the bot must not exceed 24 volts.
  - Teams are advised to use an on-board power supply. In case they are using external power supply they will be responsible for any problem created by entanglement of wires.

### 3. Materials

#### 3.1 Mechanical construction

The development of our robot (see Fig. 2) utilizes plastic as its main body together with two 2 inch wheels with each wheel attached to one Bipolar stepper motor. One Ball castor (metal) is mounted further up front to provide stability for the robot. The differential drive method is implemented to enable the robot to rotate clockwise and counter clockwise. This means that one motor would rotate while another stops to let the robot turns towards the desired angle of rotation.

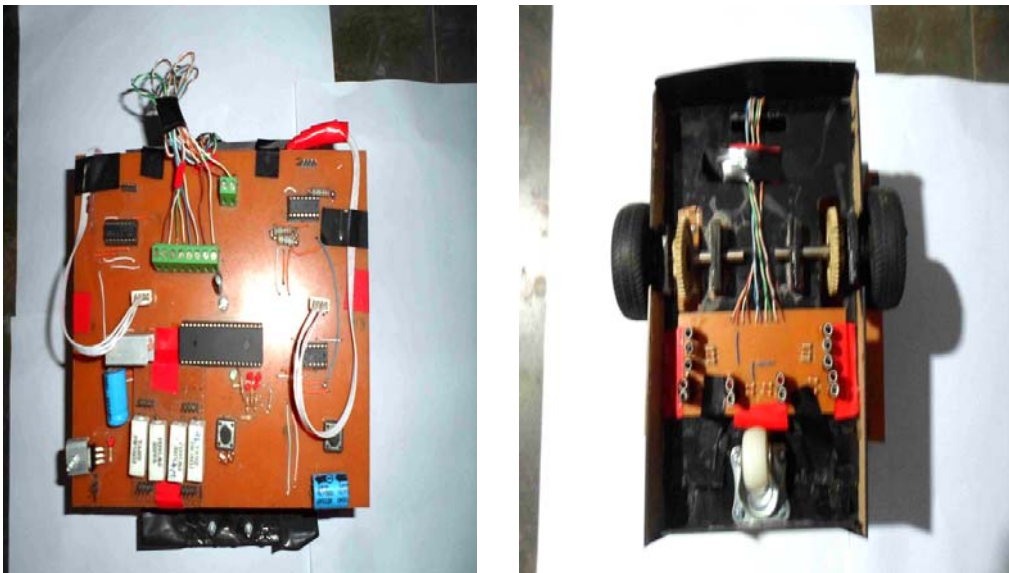


Fig. 2: Autonomous Robot with Bipolar Stepper motors as drive train

### 3.2 Circuitry interfacing

For the on-board microcontroller of the robot, the avr microcontroller and embedded system is implemented as the board set provides easy interfacing with sensors and actuators [5]. Furthermore, the ATmega32 microcontroller can be easily programmed using the C language .As for the line tracing sensors, three light dependent resistors (LDRs) are arranged in straight line and mounted below the motors and in parallel to their shafts. Three light emitting diodes are also mounted next to each of the LDR to provide uniform light source for the sensors.

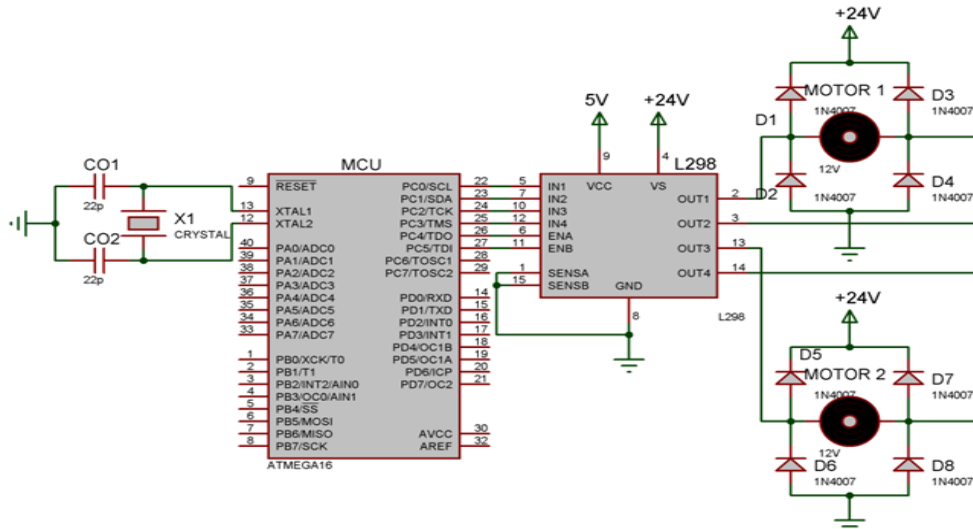


Fig.3: Circuit Diagram for motor control using L-29

### 3.2 Programming algorithm

The issue of control manifests itself in at least two aspects of the Robot Design project: in the development of the robots higher-level strategy from a conceptual standpoint, and in the actual programming of that strategy into the machine through the process of writing computer code. The analog signal received of each of the phototransistors is proportional to its coverage of the line, and lies between 0 and 2V. The signals of the sensors are weighted by 1, 2 and 3 for left, middle and right sensors respectively. The average of the weighted readings gives a value for deviation of the robot from the line. This average has the range between 1 and 3 when the line is at far left or far right of the robot respectively. This average is used to control the speed of the rear left and right wheels of the robot. Timer-0 and timer-2 in phase correct PWM mode are used for the left and right wheels. It is such that if the average of the weighted readings is 2, the robot is on the line and the OCR0, and OCR2 values are half the top, and correspondingly by an average value of 1 the right speed is highest and the left is 0, and by an average value of 3 the right speed is 0 and the left is highest. In between the speed (i.e. the values of OCR0 and OCR2) change linearly. It is assumed that the microcontroller frequency is to be 1 MHz, and the A/D clock to be lowest.

```

# Coding : Proteus
#include<avr/io.h>
#include<avr/interrupt.h>
#include<util/delay.h>
#define left 1
#define right 2
#define s 3
#define hleft 4
#define hright 5
#define hs 6
#define stop 7
int c[6],a[6],r1,r2,r3,r4,w1=0,w2=0,k;
int speed1=233,speed2=236;
int go(int n)
{
    switch(n)
    {
        case 1:
            PORTB&=~((1<<PB0)|(1<<PB2));
            PORTB|=(1<<PB0); //PB0 connect to the right motor on to turn left
            _delay_ms(10);
            break;
        case 2:
            PORTB&=~((1<<PB0)|(1<<PB2));
            PORTB|=(1<<PB2); // PB1 connect to the left motor on to turn right
            _delay_ms(10);
            break;
        case 3:
            PORTB|=(1<<PB0)|(1<<PB2); //PB0 and PB1 on for go straight
            _delay_ms(10);
            break;
    }
}

int adcr(int adcselect) //Function for get adc values
{
    //ADMUX &= 0b01000000; because AVCC as ref
    ADMUX &= 0b01000000;
    if(adcselect==0) ADMUX &= 0b01000000;
    if(adcselect==1) ADMUX |= (1<<MUX0); //adc2
    if(adcselect==2) ADMUX |= (1<<MUX1); //adc2
    if(adcselect==3) ADMUX |= (1<<MUX1)|(1<<MUX0); //adc3
    if(adcselect==4) ADMUX |= (1<<MUX2); //adc4
    if(adcselect==5) ADMUX |= (1<<MUX2)|(1<<MUX0); //adc5
    if(adcselect==6) ADMUX |= (1<<MUX1)|(1<<MUX2); //adc6
    if(adcselect==7) ADMUX |= (1<<MUX1)|(1<<MUX2)|(1<<MUX0); //adc7
    ADCSRA|=(1<<ADSC);
    while(ADCSRA &(1<<ADSC));
    return ADC;
}

```

## 4. Results

# Trial Video shots:



Fig 4.1



Fig 4.2



Fig 4.3



Fig 4.4

The results of our iARC robot competition are as follows:

Round	Result	Total teams
1 <sup>st</sup> round	9 <sup>th</sup> place	Out of 35 teams
Final Round	5 <sup>th</sup> place	Out of 9 teams

## 5. Discussion

During the preliminary round, it has performed nicely in following the lines, but the speed is rather too slow to reach the goal. Total 9 teams were selected out of 35 teams. And we have managed to reach second round. The use of LDRs provides a great low-cost line-tracing sensor. However, it is prone to the ambient light and is also not fast enough in scanning the white lines above on green color. Quite many times the robot has diverted from the white lines and junctions since the readings from the LDRs are not fast enough. For the final rounds, a small changed arena was supplied. So we had to change our code instantly in final round. That's why we were unable to manage to reach the full arena. The use of two Stepper motors had enabled the robot to move at a higher speed with 6 volt battery supply. But we lost 4 opponent teams which had great autonomous robots with great strategies. All is not lost actually, since our robot has actually brought a good fight for the opponent robot teams. And we took 5<sup>th</sup> place in this International Autonomous Robotics Competition.

## 6. Conclusion

From this autonomous robot competition, there are so much knowledge and experience obtained by just building a small-sized autonomous robot. Robotics competition is indeed a great platform for students to enhance their robotics skills in terms of mechanical construction, circuit interfacing and programming. Besides that, the implementation of good strategies is undeniably important in determining the success of the game played.

## 7. Recommendation

Further improvements can be made by using a better Micro-processor which has better processing power, bigger memory and built-in pulse-width-modulation (PWM) function. It should be made by using DC Gear motors or Parallax servos with sufficient speed and high torque plus so their drivers would enhance the mobility of the robot. It is also recommended that the Sharp image processing sensor is to be used with an analog-to-digital converter (ADC) chip in order to supply the micro-processor with a digital input. Different configurations for the line tracing sensors could also provide better results in terms of effective scanning of the lines. Instead of three sensors, perhaps the configuration of five sensors being aligned in a semicircle shape might provide better line sensing capability for the robot. For such a speed-critical competition, perhaps it is better to implement the infrared sensors image processing sensor.

## References

- [1] Jun'ichi Shibata, Gen'ichi Yasuda and Hiroyuki Takai, "A Microcontroller-Based Architecture for Locally Intelligent Robot Agents", Proceedings of the Sm World Congress on Intelligent Control and Automation, June 15-19, 2004, Hangzhou, P.R. China
- [2] Martin, F. "Ideal and Real Systems: A Study of Notions of Control in Undergraduates Who Design Robots", In Y. Kafai and M. Resnick (Eds.), Constructionism in Practice: Rethinking the Roles of Technology in Learning, MIT Press, MA, 1994.
- [3] McComb, G. (2000) "The Robot Builder's Bonanza", 2nd Ed. McGraw-Hill, New York, U.S.
- [4] Miglino, O., Lund, H. H., Cardaci, M. "Robotics as an Educational Tool", Journal of Interactive Learning Research, 1998.
- [5] <http://www.parallax.com>

## **Development of a Multipoint Digital Thermometer by Microcontroller**

Amit Roy\*, Md. M. Hasan, S. U. Ahmed and Md. Rokunuzzaman

Department of Mechanical Engineering, Rajshahi University of Engineering and Technology, Rajshahi-6204,  
Bangladesh

\*E-mail: [royamit.me@gmail.com](mailto:royamit.me@gmail.com)

### **Abstract**

*This paper describes about the title that the development of a multipoint digital thermometer by microcontroller. In this project, a digital thermometer is constructed with the temperature sensors connected to different points of a process. A microcontroller controls the switching action of the temperature sensors. There is a common display to show the temperature of different place or point, which is connected at different switch with temperature sensor. When one switch is pressed the temperature sensor detect the desired point and show the corresponding temperature in the display by means of microcontroller. For multi-temperature the number of switch is increased as necessary with the observation point. The device is used where the temperature in the range of  $(-20^{\circ}C \sim 150^{\circ}C)$ .*

**Keywords:** Digital Thermometer, Microcontroller, Sensor.

### **1. Introduction**

A thermometer is a device that measures temperature or temperature gradient using a variety of different principles. Digital thermometers are a quick, simple and effective way of obtaining temperature information. Most commonly-used electrical temperature sensors are difficult to apply. For example, thermocouples have low output levels and require cold junction compensation. Thermostats are nonlinear. In addition, the outputs of these sensors are not linearly proportional to any temperature scale. Early monolithic sensors, such as the LM3911, LM134 and LM135, overcame many of these difficulties, but their outputs are related to the Kelvin temperature scale rather than the more popular Celsius and Fahrenheit scales [1]. Fortunately, in 1983 two I.C.'s, the LM34 Precision Fahrenheit Temperature Sensor and the LM35 Precision Celsius Temperature Sensor, were introduced.

### **2. Experimental Setup**

Project Board, Atmega 32 chip, Temperature sensor LM35, LCD display (20\*4) / 7segment display, Burner, Resistance 10K $\Omega$ , Wire.

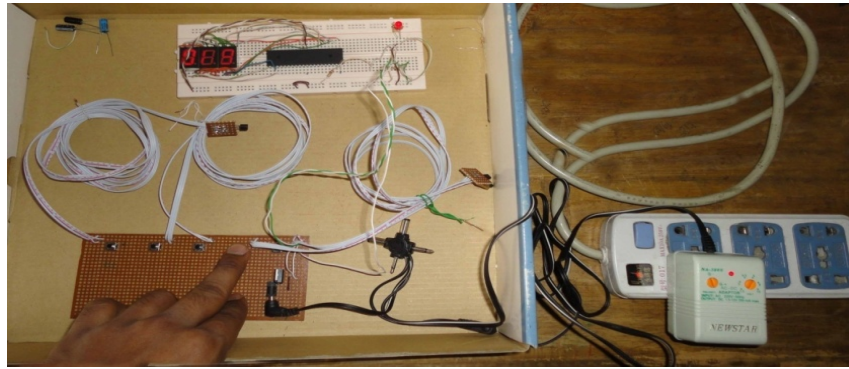


Figure 1: Multipoint Digital Temperature

## 2.1. Microcontroller

A microcontroller has a dedicated input device and often (but not always) has a small LED or LCD display for output. A microcontroller also takes input from the device it is controlling and controls the device by sending signals to different components in the device. A microcontroller is often small and low cost. The components are chosen to minimize size and to be as inexpensive as possible. Microcontrollers are used in automatically controlled products and devices, such as automobile engine control systems, implantable medical devices, remote controls, office machines, appliances, power tools, and toys. By reducing the size and cost compared to a design that uses a separate microprocessor, memory, and input/output devices, microcontrollers make it economical to control digital way even more devices and processes are available.

## 2.2 Segments display

7-Segments display is most widely used in displaying digits. There are mainly two types of 7-Segments display.

- Common anode
- Common cathode

We have used common anode 7-Segments display with our micro-controller. It has 10 legs and 8 of them are connected to MCU with resistors. By programming we can manipulate its digits.

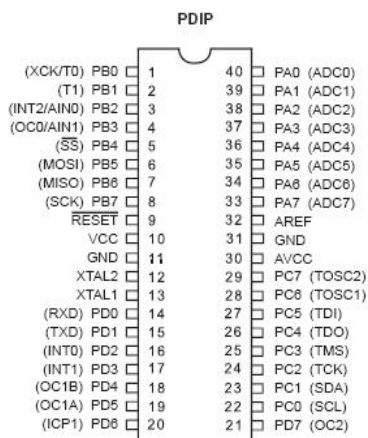


Figure 2.1: Pin Configuration



Figure 2.2: At mega 32

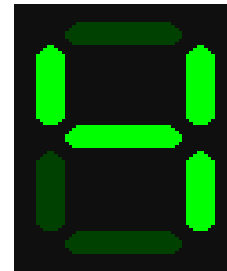


Figure 2.3: Segments

## 2.3 Temperature Sensors

There are two temperature sensors:

- **LM34** : calibrated in Fahrenheit
- **LM35** : calibrated in Celsius

These sensors have no moving parts, they are precise, never wear out, don't need calibration, work under many environmental conditions. They are very inexpensive and quite easy to use.

### 2.3.1 Temperature sensors (LM34)

The LM34 has an output of 10 mV/°F with a typical nonlinearity of only  $\pm 0.35^\circ\text{F}$  over a  $-50$  to  $+300^\circ\text{F}$  temperature range, and is accurate to within  $\pm 0.4^\circ\text{F}$  typically at room temperature ( $77^\circ\text{F}$ ) [2]. The LM34's low output impedance and linear output characteristic make interfacing with readout or control circuitry easy. For instance, many monolithic temperature sensors have an output of only  $1 \mu\text{A}/^\circ\text{K}$ . This leads to a  $1^\circ\text{K}$  error for only  $1 \mu\text{A}$  of leakage current. On the other hand, the LM34 may be operated as a current mode device providing  $20 \mu\text{A}/^\circ\text{F}$  of output current.



Figure 3: LM-34 Sensors

### Basic Fahrenheit Temperature Sensor ( $+5^\circ$ to $+300^\circ\text{F}$ )

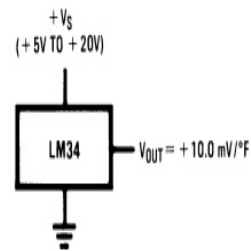


Figure 4: Fahrenheit temperature sensor

### 2.3.2 Fahrenheit temperature sensors

The LM34 is easy to use and may be operated with either single or dual supplies. Figure 4 shows a simple Fahrenheit temperature sensor using a single supply. The output in this configuration is limited to positive temperatures. The sensor can be used with a single supply over the full  $-50^\circ\text{F}$  to  $+300^\circ\text{F}$  temperature range, as seen in Figure 5, simply by adding a resistor from the output pin to ground, connecting two diodes in series between the GND pin and the circuit ground, and taking a differential reading [3]. This allows the LM34 to sink the necessary current required for negative temperatures. If dual supplies are available, the sensor may be used over the full temperature range by merely adding a pull-down resistor from the output to the negative supply as shown in Figure 6.

### Temperature Sensor, Single Supply, $-50^\circ$ to $+300^\circ\text{F}$

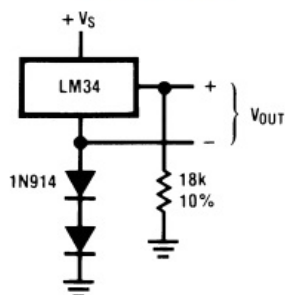


Figure 5: Temperature sensor single supply

### Full-Range Fahrenheit Temperature Sensor

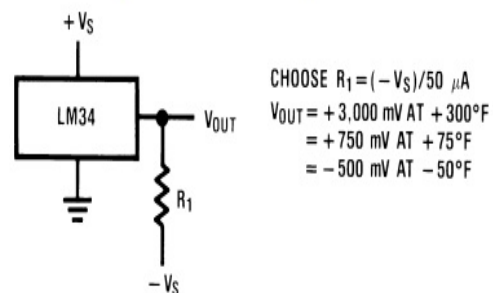


Figure 6: Temperature sensor full-range





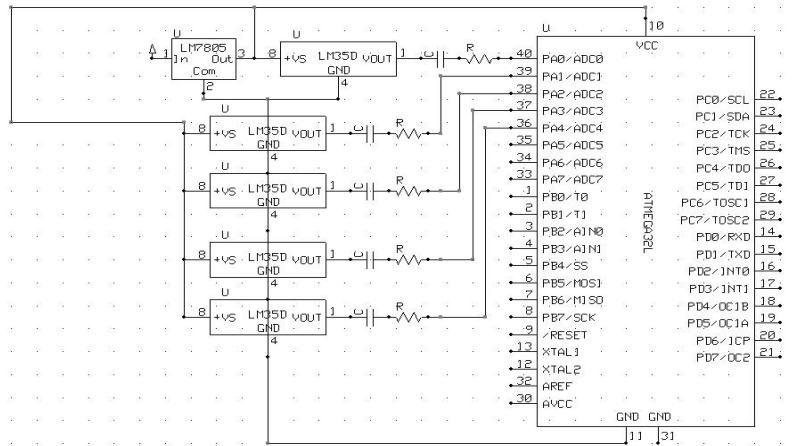


Figure 8: Circuit diagram

#### 4. Calibration Data

Table 1: Calibration data

Observation No.	Calibrated Digital thermometer ( $^{\circ}$ C)	Thermometer reading ( $^{\circ}$ C)
01	30	34
02	34	36
03	39	41
04	43	44
05	45	47
06	47	50
07	50	53
08	53	55
09	57	59
10	58	63
11	61	65
12	63	66
13	65	67
14	68	69
15	70	72

#### 5. Calibration Graph

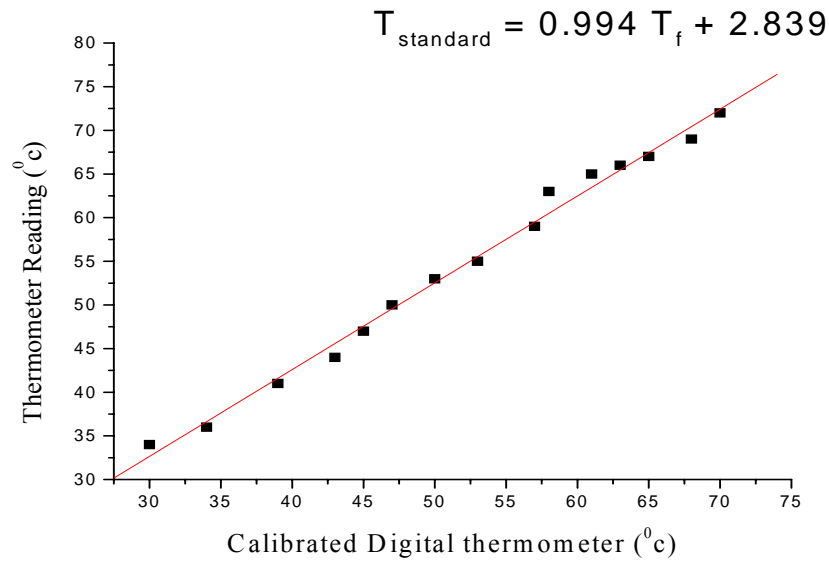


Figure 9: Calibration of Digital Thermometer against Standard Thermometer

## 6. Calibration Process

$$T_{\text{Standard}} = A \times T_{\text{Fabricate}} + B$$

$$T_{\text{Standard}} = 0.994 \times T_{\text{Fabricate}} + 2.839$$

The values of  $T_{\text{Standard}}$  and  $T_{\text{Fabricate}}$  which put in the program display at the above equation.

## 7. Conclusion

The device can measure temperature at five points at a time by five temperature sensor. In future development of our project can be done by the following ways- more than five temperature sensor can be used, instead of LM35, another sensor LM34 can be used, instead of project board, the PCB board can be used, instead of 7 segment display, the display monitor can be used. If more than five temperature sensor and the display monitor are used then the cost will be high. If PCB board is used instead of project board more precision accuracy will be obtained.

- ❖ Temperature range (-20°C ~ 150°C)
- ❖ Required Voltage (0 volt ~ 5 volt)
  
- ❖ Multipoint temperature and Small size & Cost comparative low.
- ❖ Surface contract & Point contract.
- ❖ Measuring temperature more accurately than a using a thermostat.
- ❖ The sensor circuitry is sealed and not subject to oxidation.
- ❖ The LM35 generates a higher output voltage than thermocouples and may not require that the output voltage be amplified.

Temperature measurement in-

- ❖ Duct system and any cold storage.
- ❖ Any kinds of Plate Temperature.
- ❖ Water Bath Temperature and Room Temperature.
- ❖ Solar Air and Water heater.

## **8. References**

- [1] R.A. Pease, "A Fahrenheit Temperature Sensor", pre-sented at the ISSCC Conference, February 24, 1984.
- [2] Robert Dobkin, "Monolithic Temperature Transducer", in Dig. Tech. Papers, Int. Solid State Circuits Conf., 1974, pp. 126, 127, 239, 240.
- [3] Michael P. Timko, "A Two-Terminal IC Temperature Transducer", IEEE Journal of Solid-State Circuits, December 1976, pp. 784–788.
- [4] R.P. Benedict (1984) *Fundamentals of Temperature, Pressure, and Flow Measurements*, 3rd ed, ISBN 0-471-89383-8, chapter 11 "Calibration of Temperature Sensors".
- [5] Gerard C.M. Meijer, "An IC Temperature Sensor with an Intrinsic Reference", IEEE Journal of Solid State Circuits, VOL SC-15, June 1980, pp. 370–373.

## Development of Automatic Smart Waste Sorter Machine

Mahmudul Hasan Russel<sup>1\*</sup>, Mehdi Hasan Chowdhury<sup>1</sup>, Md. Shekh Naim Uddin<sup>1</sup>, Ashif Newaz<sup>1</sup>, Md. Mehdi Masud Talukder<sup>2</sup>  
Department of Electrical and Electronics Engineering<sup>1</sup>, Department of Mechanical Engineering<sup>2</sup>  
Chittagong University of Engineering and Technology (CUET) Chittagong-4349, Bangladesh  
\*mahmudulrussel.eee.bd@gmail.com

### Abstract

*Modern world meets lots of challenges that includes Smart waste management system. It is become matter of big concern if proper disposal system is not managed. Managing waste effectively and recycling efficiently, a nation can ahead one step forward. In this work, an automatic sorter machine is developed which can sort out the wastes in various categories to make waste management easier and efficient. It can be possible to sort out metal, paper, plastics and glass by developing an electromechanical system using microcontroller and operational amplifier. For sorting metal and glass conventional sensors are used and for sorting paper and plastics a sensor using LASER and LDR is developed. A weight sensor and counter is used to find out the amount of sorted materials. By using the proper recycling system, the curse of waste will turn into blessings for the civilization. The sorting procedure will make recycling more efficient. By means of this waste sorter, the conventional waste management system will be transformed into SMART system. This SMART system will help to make our environment more suitable for living, reducing global warming and making the world healthier.*

**Keywords:** Automatic Sorter Machine; Smart waste management; Microcontroller; Operational amplifier, Microcontroller, Sensor implementation.

### 1. Introduction

From the beginning of the human civilization, people used various methods of waste disposal to get rid of unwanted material. Sometimes it was buried in the land, thrown in the sea, fed to the animal or burnt. Getting rid of unwanted material is always a major concern for the modern society. Trash has played a tremendous role in history. The Bubonic Plague, cholera and typhoid fever, to mention a few, were diseases that altered the populations of Europe and influenced monarchies. They were perpetuated by filth that harboured rats, and contaminated water supply [1]. When wastes are not properly managed then it may cause serious hazard, as seen in 1350. "Black plague" erupted and more than 25 million people from all over Europe fall victim to it in just five years [2]. There is an increasing rate of waste generation in Bangladesh and it is projected to reach 47,064 tonnes per day by 2025. The Waste Generation Rate (kg/cap/day) is expected to increase to 0.6 in 2025. A significant percentage of the population has zero access to proper waste disposal services, which will in effect lead to the problem of waste mismanagement [3]. The total waste collection rate in major cities of Bangladesh such as Dhaka is only 37%. When waste is not properly collected, it will be illegally disposed of and this will pose serious environmental and health hazards to the people of Bangladesh [4]. This is not the only problem of Dhaka city but also for other big cities around the world [5]. With so much concern recently about being greener and economically friendly, waste management has become a very important topic. People and companies are starting to realize that the things they use and the way they dispose of them can make a big impact on our world. Proper management of waste plays a vital role in global environment. That is why a waste sorting system is designed which can be used in houses, offices, industries as a part of smart waste management system.

### 2. Present Status of Solid Waste Generation

Present condition of the solid waste generation can be described in different point of views. The generation and management of solid wastes are described in World and Bangladesh perspective.

**7.1 World Scenario**

Confederation of European Waste to Energy Plants (CEWEP) [6] and European Environment Agency (EEA) [7] provides sound, independent information on the environment.

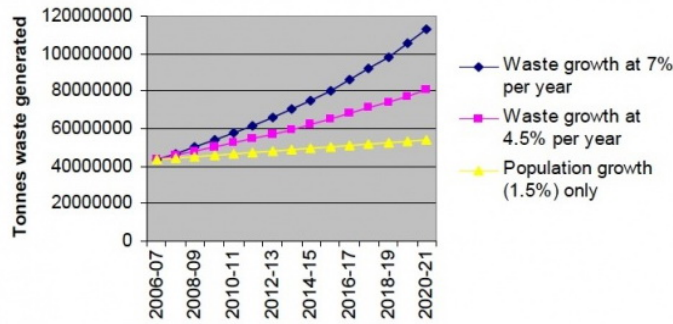


Fig. 1 Comparative waste generation 2006-07 to 2020-21.

Fig. 1 has been generated from the corresponding data from CEWEP and EEA [6], [7]. Considering present condition, waste growth at 7% per year is plotted. Considering future waste reduction, waste growth at 4.5% per year is plotted. Fig. 1 illustrates the fact about the total generation of wastes around the world. The total amount is increasing day by day and hence the waste management is becoming a challenge for both the developed and developing countries. Hence, recycling is becoming very important [5]. Recycling is a resource recovery practice that refers to the collection and reuse of waste materials such as empty beverage containers. The materials from which the items are made can be reprocessed into new products. For recycling the waste is required to separate into various different bins. As it enables us to convert waste into a valuable resource, gradually this practise is gaining popularity.

**7.2 Bangladesh Scenario**

The waste generation amount by Zone at Dhaka metropolitan city, Bangladesh is shown in Fig. 2 [8].

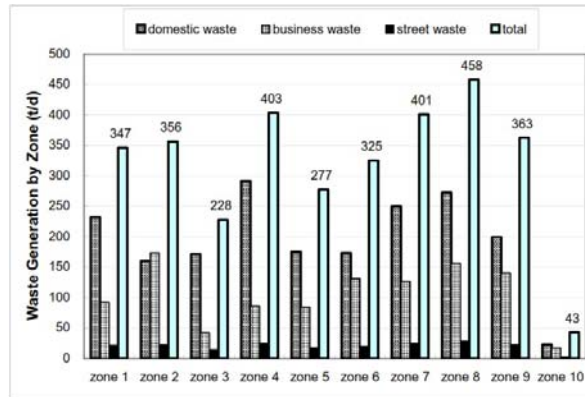


Fig. 2 Waste generation amount by zone at Dhaka metropolitan city, Bangladesh

The zonal average of waste generation is estimated at 320 t/d (tonnes per day) with the maximum at approximately 460 t/d in Zone 8 and the minimum at 43 t/d in Zone 10. The zonal waste generation reflects the population size and business activities in each zone [8]. Estimated Volume of paper, glass, metal and plastic waste generation in Dhaka City is shown in Table 1 [8].

TABLE I

ESTIMATED GENERATION OF PAPER, GLASS, METAL AND PLASTIC WASTES IN DHAKA CITY

Materials	Estimated Generation (t/d)
Plastic	124
Paper	260
Glass	46
Metal	27
<b>Total</b>	<b>457</b>

### 3. Methodology

The system activates when the IR detects some sorts of material is being put on the system tray. Then at first the weight sensor activates and find out the weight of the trash, then the metal sensor and glass sensor starts their actions. If metal sensor detects the material as metal, then a servo motor will put that trash in the bin 3 (which is dedicated for metals). If the glass sensor detects glass then it will perform same action and put the trash in bin 4. If both sensors fail to detect then the LASER and LDR activates. If the LASER passes through the trash then it is decided as a transparent and moves to bin 2. If the LASER fails to pass then the material is decided as Paper and move to bin 1.

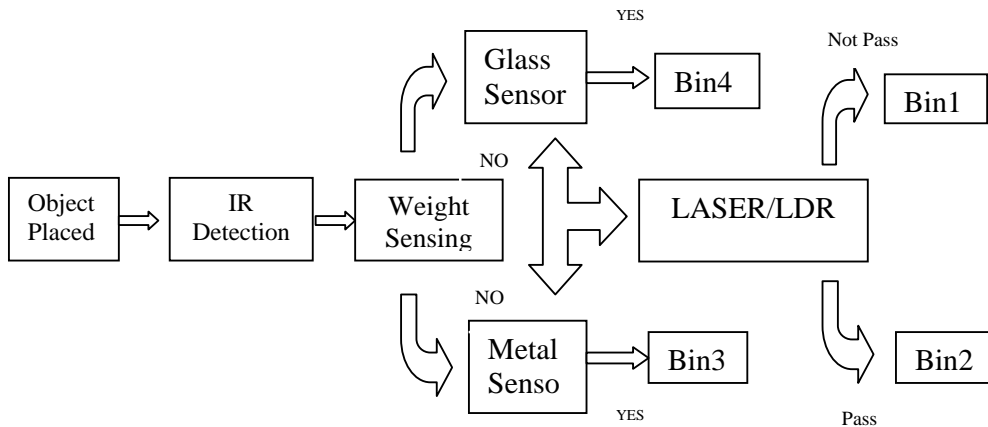


Fig. 3 Sequential Logic Flow Chart.

### 4. Sorting System Details

The sorting system consists of Light Dependent Resistor (LDR), LASER, Infrared (IR) transmitter and receiver, Metal Sensor (Capacitive proximity sensor *E2K-C*) [9], glass sensor (Omron *E3SCR67C*), Weight Sensor (MLC900 micro weight sensor) [10] and a Liquid Crystal Display (Alpha-numeric 16\*4 LCD). The whole program is run by a microcontroller (PIC 16f877A) [11].

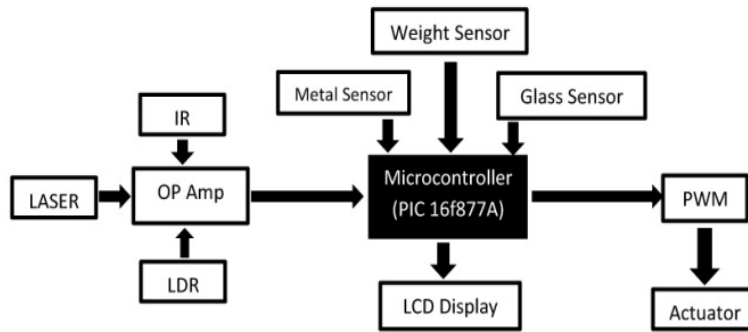


Fig. 4 Block diagram of the sorting system.

A servomotor (HS-65MG, Mighty Metal Gear Feather Servo) [12] based electro-mechanical system works as an actuator which puts trash in the desired bin. The microcontroller will count the trash sequence number and also the total weight of definite type of wastes.

## 5. Electromechanical Setup

An Automatic Sorter Machine setup consists four Bins. Each Bin is used to contain unlike materials. Bin 1 is for Paper, Bin 2 is for Metallic elements, Bin 3 is for Plastic elements and Bin 4 is for Glass particles. At first, the object is placed at the **Detection zone**. The sensor applies its sensing activity to detect the material. Sensing signal is moved to microcontroller and final output signal comes out from microcontroller [11] that run the servo motor to a definite direction depending on the material that is being sensed.

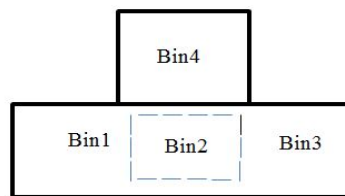


Fig.5 Top view of the Sorter

A servo motor is a motor which forms part of a servomechanism. The servo motor is paired with some type of encoder to provide position/speed feedback. This feedback loop is used to provide precise control of the mechanical degree of freedom driven by the motor. A servomechanism may or may not use a servomotor. For example, a household furnace controlled by a thermostat is a servomechanism, because of the feedback and resulting error signal, yet there is no motor being controlled directly by the servomechanism. Servo motors have a range of 0°-180° [13].

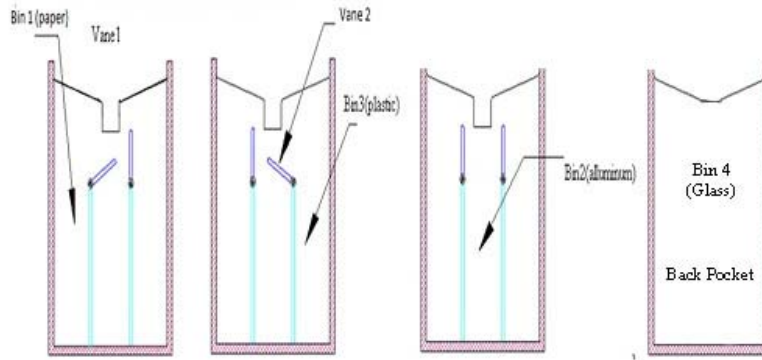


Fig.6 Sorting mechanism

The Servo motor is controlled by sending a pulse of variable width by the microcontroller. The control wire is used to send this pulse. The parameters for this pulse are that it has a minimum pulse, a maximum pulse, and a repetition rate. Given the rotation constraints of the servo, neutral is defined to be the position where the servo has exactly the same amount of potential rotation in the clockwise direction as it does in the counter clockwise direction. It is important to note that different servos will have different constraints on their rotation but they all have a neutral position, and that position is always around 1.5 milliseconds (ms). The angle is determined by the duration of a pulse that is applied to the control wire. This is called Pulse width Modulation [13]. The servo expects to see a pulse every 20 ms. The length of the pulse will determine how far the motor turns. For example, a 1.5 ms pulse will make the motor turn to the 90 degree position (neutral position). When these servos are commanded to move they will move to the position and hold that position. If an external force pushes against the servo while the servo is holding a position, the servo will resist from moving out of that position. The maximum amount of force the servo can exert is the torque rating of the servo. Servos will not hold their position forever though; the position pulse must be repeated to instruct the servo to stay in position [14].

## 6. Comparative Studies

Comparison between the existing waste sorting bin and Automatic Sorter Machine for Smart Waste Management System is discussed below.

### 2.1 Automation

Most of the waste sorters available presently are manual, which are less user friendly. Automatic Sorter Machine for Smart Waste Management System is fully automated, which have made the whole sorting procedure very easy and effective.



Fig. 7 Manual Waste Sorting Bin

### 2.2 Cost Comparison

Many local and international companies manufacture trash can. Among them Carron Phoenix Disposal Products are worldwide famous. But at present the price of the trash cans, by Carron Phoenix, ranges from \$120 to \$250 [15]. The Automatic Sorter Machine for Smart Waste Management System will cost around \$90. It is cheaper



than other because a unique algorithm to sort paper and plastic is developed and the mechanical structure is very simple.

### **2.3 Bin Number**

Presently available trash bins can sort out only two or three types of trash materials [16]. But Automatic Sorter Machine for Smart Waste Management System can automatically sort out minimum four types of trash materials very easily and efficiently.

### **2.4 Unique Sensor Designing**

Special type of sensor by using LDR and LASER is used in Automatic Sorter Machine for Smart Waste Management System. These have replaced the conventional sensors available in the market for sorting out paper and plastic.

### **2.5 Power Consumption**

The power supply of Automatic Sorter Machine for Smart Waste Management System is driven by 9 V (DC). It can be driven by 220 V (AC) like the other available automatic trash bins.

## **7. Future Scope**

Automatic Sorter Machine for Smart Waste Management System can be deployed to solve our existing problem as well as can bring about a change in our daily life meeting our own demand.

### **7.1 Sorting More Types of Materials**

The developed Automatic Sorter Machine for Smart Waste Management System can sort only four types of waste materials. If more sensors are used then it will be possible to sort more types of materials (Such as: Transparent and nontransparent plastics, Thick and thin papers, Semi-conductor and Conductors, Rubber materials, Organic etc.).

### **7.2 Reduction of Cost**

Companies those are manufacturing and distributing trash bin throughout the world, currently producing manual trash bins. If a large scale production of Automatic Sorter Machine for Smart Waste Management System is possible then the price of this product will be cheaper than present manufacturing cost. It will be cheaper because the mechanical structure is very simple and the sensors will be industrial grade.

### **7.3 Increasing Response Time**

The response time of electromechanical system is relatively fast. But it can be made faster by using industrial grade servo motor. The microcontroller and servo motor used in presently developed Automatic Sorter Machine for Smart Waste Management System are properly synchronized. When the industrial grade servo motor will be used, then the system should be synchronized to perform smoothly and more faster.

### **7.4 Health Service**

Special type of sensor could be used to sort out the organic parts of the wastes. When the organic parts of the wastes are sorted out then they may be tested automatically to find out the food habit of the user and analyze it for the improvement of the user's diet. Another application of sorting out the organic parts of the wastes is, the organic parts may help to diagnosis several disease of the user. Thus the health issues of the user of Automatic Sorter Machine for Smart Waste Management System will be insured at some extent.

### **7.5 Primary Recycling and Reusing Unit**

A primary recycling and reusing plant may be installed with the automatic sorter machine. This will ensure that a home user will practice recycling and reusing. The primary plant may consist of only paper or plastic recycling unit. This will ensure a healthier life style and guarantee cost minimization for the home or industrial users.

## 8. Conclusions

In communities where appropriate sites are available, sanitary landfills usually provide the most economical option for disposal of solid waste. However, it is becoming increasingly difficult to find sites that offer adequate capacity, accessibility and environmental conditions. The amount of waste, which is been recycled or reused, stands for the reduction of waste to be managed by the authority. Proper management of waste plays a vital role to control global warming [1]. Automatic Sorter Machine for Smart Waste Management System is an excellent example of proper waste management. It will also ensure effective recycling system. Hence, the improvement of waste sorter will ensure economic and ecological development.

## 10. Acknowledgement

The first generation of the sorter was partially automatic. The ability of total sorted waste type was three. That was plastics, metal (Aluminum) and paper (non transparent) items. This time we have upgraded our sorter is full autonomous system. Also increase the number of bins. We add the glass sensor for sorting of glasses which is one of the burning burden around the world. Our previous work was published among the two international conference named International Conference on Mechanical Engineering and Renewable Energy 2011 (ICMERE2011) 22- 24 December 2011, Chittagong, Bangladesh, ICMERE2011-PI-128 [18] and 1<sup>st</sup> International Conference on Advances in Civil Engineering 2012 (ICACE 2012) 12 –14 December 2012 CUET, Chittagong, Bangladesh, ID: AEE 069.[17]

## 11. References

- [1] Rathje William and Cullen Murphy, Rubbish! The Archaeology of Garbage, Harper Collins Publishers. 1992.
- [2] Jo N. Hays, Epidemics and pandemics: their impacts on human history . p.23. ABC-CLIO Publishers. 2005
- [3] Alamgir M. and Ahsan A, Municipal Solid Waste and Recovery Potential: Bangladesh Perspective. Iran. J. Environ. Health. Sci. Eng., 2007, Vol. 4, No. 2, pp 67 – 76. 2007.
- [4] I. Enayetullah, S. S. A. Khan and A. H. Md. M. Sinha, Urban Solid Waste Management. Scenario of Bangladesh: Problems and Prospects, Waste Concern Technical Documentation. 2005.
- [5] US Environmental Protection Agency, Decision-Maker's Guide to Solid Waste Management, Volume II, Solid Waste and Emergency Response (5305W), August, 1995.
- [6] (2012) Confederation of European Waste to Energy Plants. [Online] Available: [www.cewep.eu](http://www.cewep.eu)
- [7] (2012) European Environment Agency. [Online] Available: <http://www.cewep.eu/information/data/index.html>
- [8] Dhaka City Corporation, The Study on The Solid Waste Management in Dhaka City, Final Report, Volume 2, March 2005, Pacific Consultants International, Yachiyo Engineering Co., Ltd.
- [9](2012) OMRON Industrial Automation. [Online]. Available:[http://www.ia.omron.com/product/family/470/index\\_fea.html](http://www.ia.omron.com/product/family/470/index_fea.html)
- [10] (2012) Manyear Technology Co., Ltd. [Online]. Available: <http://manyear.en.hisupplier.com/product-542764-MLC900-weighing-scale-load-cell.html>
- [11] (2012) Microchip Technology Inc. [Online]. Available: [www.microchip.com/stellent/pic16f877a](http://www.microchip.com/stellent/pic16f877a)
- [12] (2012) HITEC RCD USA. [Online]. Available: <http://www.hitecred.com/products/analog/micro-mini/hs-65mg.html>
- [14] Yasuhiko Dote, Servo Motor and Motion Control: Using Digital Signal Processors, Prentice Hall and Texas Instruments Digital Signal Processing Series. 2008.
- [15] (2012) Carron Phoenix. [Online]. Available: [http://www.carron.com/products/waste\\_disposal/waste\\_sorter\\_bins](http://www.carron.com/products/waste_disposal/waste_sorter_bins)
- [16] (2012) Busch Systems [Online]. Available: <http://www.buschsystems.com/product/super-sorter-series-recycling-bins.php>
- [17] 1<sup>st</sup> International Conference on Advances in Civil Engineering 2012 (ICACE 2012) 12 –14 December 2012 CUET, Chittagong, Bangladesh, ID: AEE 069

[18] International Conference on Mechanical Engineering and Renewable Energy 2011 (ICMERE2011) 22- 24 December 2011, Chittagong, Bangladesh, ICMERE2011-PI-128

## Improvement of Vibration Isolation Characteristics using Acceleration Feedback Based on Kalman Filter Estimation

M. M. Zaglul Shahadat<sup>1</sup>, T. Mizuno<sup>2</sup>, Y. Ishino<sup>2</sup>, and M. Takasaki<sup>2</sup>

<sup>1</sup> Graduate School of Science & Engineering, Saitama University

<sup>2</sup> Department of Mechanical Engineering, Saitama University

E-mail: shahadat230@yahoo.com

### Abstract

A horizontal vibration isolation system utilizing displacement cancellation technique is studied both analytically and experimentally. The isolation and middle tables of the investigated vibration isolation system, involving displacement cancellation technique, are controlled by an infinite stiffness control and positive stiffness control, respectively. In this study, the dynamic characteristics of the vibration isolation system are improved by adding acceleration feedback to the original controllers. MEMS (Micro Electrical Mechanical System) accelerometers are used to measure acceleration for the feedback. Since the acceleration measured by a MEMS accelerometer usually contains undesired noise, the estimated acceleration by Kalman Filter (KF) is used instead of the measured value in the acceleration feedback. The dynamic responses of the system are investigated with the acceleration feedback based on the KF estimation and the measured signal individually. The experimental results show that the KF-estimated acceleration feedback improves the vibration isolation characteristics significantly.

Keywords: Active control, Vibration isolation, Infinite stiffness, Zero compliance, Acceleration feedback.

### 1. Introduction

Nowadays, the position accuracy in Hi-tech manufacturing process has progressed to nanometer range. A small scale disturbance in high precision production site may hamper the system to acquire the desired accuracy. In most silicon wafer and semiconductor industries, the accuracy is a key performance objective. Thus, the demand for high performance vibration isolation system is increasing recently in various industrial sectors such as semiconductor industries, silicon wafer industries and so on. There are two main sources of vibration: (1) vibration transmitted from ground (ground vibration) through suspension and (2) vibration caused by disturbances acting on vibration isolation table directly (direct disturbance). A vibration isolation system should be able to suppress simultaneously both disturbances.

Low-stiffness systems are better for attenuating ground vibration, whereas high-stiffness systems are suitable for direct disturbance [1]. In addition, a trade-off regarding high stiffness and low stiffness is inevitable in conventional passive type vibration isolation systems. In contrast, active vibration isolation systems, in principle, are not vulnerable with respect to this difficulty [2]. Consequently, the active micro-vibration isolation technology has recently received satisfactory emphasis in the Hi-tech industries [2-4].

To acquire high stiffness and low stiffness simultaneously by a single active vibration isolation unit, the mechanism, involving two series connected isolators, was proposed [5-6]. Mizuno *et al.* have applied negative stiffness technique to isolate vibration using two isolators connected in series [5-6], where one isolator is controlled to have negative stiffness and the other has positive stiffness of same amplitude. First, a zero-power control magnetic suspension system was connected with a normal spring in series [5]. Zero-power control magnetic suspension systems have itself unique characteristic that they behave as if they have negative stiffness. Mizuno *et al.* acquired a vertical vibration isolation system by a linear actuator connected with a normal spring in series, where the linear actuator was controlled with proper negative stiffness controller [6], and the characteristics of this system was further improved by using positive stiffness actuator instead of the normal spring [7]. However, in practice, it is often difficult to maintain equal absolute stiffness of both isolators, and unequal stiffness of the isolators in negative stiffness technique hampers the vibration isolation system to obtain zero compliance. The vibration isolation system using a displacement cancellation technique can overcome this problem [8] because the displacement cancellation control focuses on the displacement rather than the stiffness of the isolator.

Mizuno *et al.* developed a horizontal vibration isolation system using displacement cancellation control [8], where an integral-controlled linear actuator is connected with a normal spring in series. The authors have

developed a three-axis horizontal vibration isolation system using this technique, where voice coil motors (VCMs) are used as actuators. Nevertheless, the transient response is still a problem of the aforementioned system and should to be improved. A feedforward control can reduce the transient displacement. To realize a feedforward control, however, the prediction of the disturbances is necessary although in most cases the disturbances are unpredicted.

In this paper, an acceleration feedback is added to the controllers to improve such vibration isolation characteristics for unknown disturbances. In the experiment, MEMS accelerometers are used instead of servo-accelerometer to measure acceleration. An advantage of MEMS is low in cost. However, the output signal of MEMS accelerometers includes undesirable noise. To reduce such noise from the measured signal, various filter techniques are available, and one of them is Kalman Filter (KF). The KF performs suitably to improve the accuracy of the rotor position in active magnetic bearings [9]. In this study, the acceleration feedback based on KF-estimation instead of direct measured acceleration is used to avoid the noise in the measured acceleration.

## 2. Displacement cancellation technique to isolate vibration and developed system

The zero-compliance against direct disturbance and the soft suspension against ground vibration are two required criteria for a vibration isolation system. In this study, a displacement cancellation technique is applied to realize these two criteria simultaneously in a horizontal vibration isolation system. In the following, the concept of the displacement cancellation technique is presented.

The displacement cancellation technique comprises from two series connected isolators, one of which is a soft spring and the other is controlled to cancel displacement of the spring as shown in Fig. 1. Because stiffness  $k_1$  is positive, the displacement of the isolation table  $\bar{y}$  against a direct disturbance is cancelled by the upper isolator (Fig. 1) with the I-PD (integral-proportional derivative) control; the upper portion behaves as itself has negative stiffness. The displacement  $\bar{y}$  can be expressed as

$$\bar{y} = (y_1 + y_2) - (y_1 - \Delta y_1 + y_2 - \Delta y_2), \quad (1)$$

where  $\Delta y_1$  and  $\Delta y_2$  respectively indicate the displacements of the lower and upper portions, respectively. The resultant displacement of the upper mass would be zero when following condition is satisfied:

$$0 = (y_1 + y_2) - (y_1 - \Delta y_1 + y_2 - \Delta y_2), \Rightarrow \Delta y_1 = -\Delta y_2 = \Delta y. \quad (2)$$

Equation (2) indicates that zero-compliance against direct disturbance takes place in the series combination of two isolators (Fig. 1) when contraction in one isolator is absolutely equal to the extraction in the other isolator.

For ground vibration, meanwhile, the combination of the middle mass and spring works as a mechanical filter that attenuates the transmission of vibration to the isolation table. In addition, an electric filter should be inserted into the feedback loop from the displacement of the middle mass to the actuator for improving the vibration isolation performance. A simple structural diagram of a horizontal vibration isolation system using this concept is shown in Fig. 2. For the developed system, the middle mass is suspended from the base through actuators (VCM) with PD (proportional derivative) control and the isolation table is mounted on the middle table through actuators (VCM) with I-PD control. A photograph of the developed horizontal vibration isolation system is shown in Fig. 3.

Moreover, to improve the dynamic responses of the system against unpredicted disturbances, two MEMS accelerometers are individually attached with two moving table of the developed system. MEMS accelerometers which are usually small in size can be placed in any part of the system. In addition, the acceleration signals measured by MEMS are estimated by the Kalman filter (KF) for improving the signal quality before being used in the acceleration feedback.

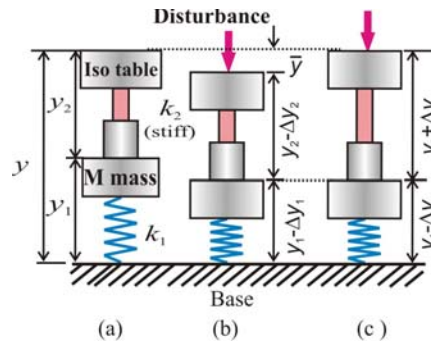


Fig. 1 Concept of displacement cancellation technique

### 3. Control system design

#### Basic equation

A basic model of a single-degree-of-freedom horizontal vibration isolation system is shown in Fig. 4, and the controllers will be designed based on this model. The basic motion equation of the table can be written as follows:

$$m\ddot{x} = f_a, \quad (3)$$

where

- $m$ : mass of the table,
- $x$ : displacement of the table along  $x$ -axis,
- $f_a$ : actuator's thrust force.

The thrust force  $f_a$  is proportional to coil current  $i$  as expressed by

$$f_a = k_i i, \quad (4)$$

where  $k_i$  is the thrust force coefficient of the actuator. The Laplace transforms of Eqs. (3) and (4) yield the transfer function representation written as

$$X(s) = \frac{k_i}{ms^2} I(s), \quad (5)$$

where each Laplace-transform variable is denoted by its capital.

#### Design of infinite stiffness controller including acceleration feedback

The isolation table is guided with I-PD control and is presented by block diagram shown in Fig. 5. The I-PD control operates to cancel the relative displacement of the table using a command signal  $r$ ; hence, the control current for the I-PD control can be expressed as follows:

$$i = -P_z \int (x-r) dt - P_d x - P_v \dot{x} - P_a \ddot{x}, \quad (6)$$

where  $P_d$ ,  $P_v$ ,  $P_z$  and  $P_a$  denote proportional, derivative, integral and acceleration feedback gains of the controller, respectively. The Laplace-transform of Eq. (6) becomes

$$I(s) = \frac{P_z}{s} r(s) - \frac{P_z}{s} X(s) - P_d X(s) - P_v s X(s) - P_a s^2 X(s). \quad (7)$$

Substituting of Eq. (7) into Eq. (5) leads to the transfer function representation of the I-PD controlled system represented as

$$\frac{X(s)}{R(s)} = \frac{\hat{t}_n(s)}{\hat{t}_c(s)}, \quad (8)$$

where the numerator part is given by  $\hat{t}_n(s) = \frac{k_i P_z}{(m + k_i P_a)}$ . In Eq. (8),  $\hat{t}_c(s)$  indicates the characteristic equation of the system (Fig. 4) with an acceleration feedback, which is given by

$$t_c(s) = s^3 + \frac{k_i P_v}{m + k_i P_a} s^2 + \frac{k_i P_d}{m + k_i P_a} s + \frac{k_i P_z}{m + k_i P_a}. \quad (9)$$

Equation (9) indicates that this system is a 3rd-order system. The characteristic equation of a 3rd-order ideal system is supposed to be represented as

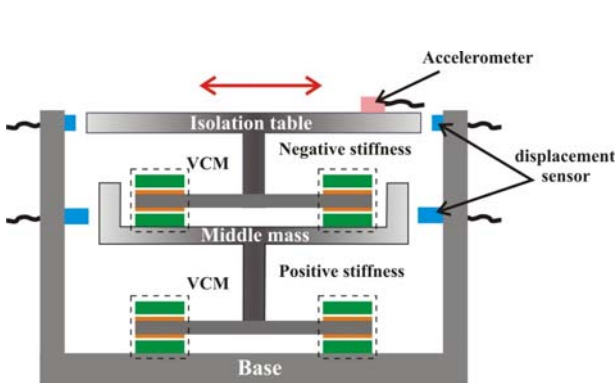


Fig. 2 Structure of horizontal vibration isolation system

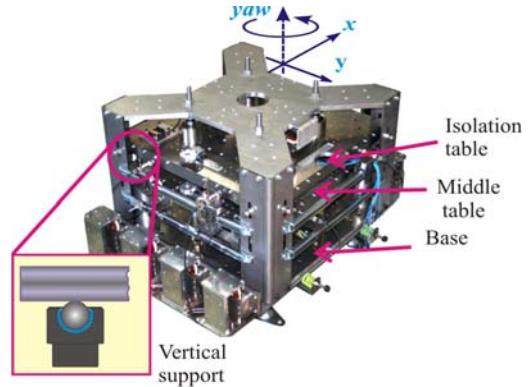


Fig. 3 Photograph of the developed system

$$t_d(s) = (s^2 + 2\zeta_1\omega_1s + \omega_1^2)(s + \omega_2) = s^3 + \alpha_2s^2 + \alpha_1s + \alpha_0. \quad (10)$$

According to the pole assignment method, the controller gains ( $P_d, P_v, P_z$ ) are determined uniquely by matching of the coefficients of Eqs. (9) and (10) as

$$P_z = \frac{\alpha_0}{k_i}(m + k_iP_a), \quad P_d = \frac{\alpha_1}{k_i}(m + k_iP_a), \quad P_v = \frac{\alpha_2}{k_i}(m + k_iP_a),$$

where  $\alpha_2 = 2\zeta_1\omega_1 + \omega_2$ ,  $\alpha_1 = 2\zeta_1\omega_1\omega_2 + \omega_1^2$ ,  $\alpha_0 = \omega_1^2\omega_2$ . The theoretical analysis outlined above shows that the addition of an acceleration feedback increases the mass of the system virtually, and a heavy system has smaller displacement than to a light system for the same disturbance. Hence, the acceleration feedback can improve the dynamic responses of a vibration isolation system. However, in practice, the system would be unstable if the value of  $P_a$  is too large beyond a certain range. In experiment, the value of  $P_a$  is selected so that the system maintains stability.

#### 4. Optimum acceleration estimation using Kalman filter

The acceleration signal measured by a MEMS accelerometer usually contains undesirable high frequency noise. There are several methods to reduce the noise level from a signal. In this study, the KF is used to deduct noise from the measured acceleration signal and this KF-estimated acceleration is for utilized realizing the acceleration feedback in the controlled system. The KF used in this study is an observer based filter, which estimates the signals by minimizing mean-square estimation errors and shown in Fig. 6. The KF algorithm comprises two steps; (i) prediction of states, and (ii) updating of the predicted states.

The state space theoretical model of the system (Fig. 4) including process noise ( $w$ ) and measurement error ( $v$ ) can be represented as follows:

$$\dot{X} = AX + BF_d + w, \quad (11)$$

$$y = CX + v, \quad (12)$$

The discrete formats of Eqs. (11) and (12) are given in below which are used in the KF algorithm with sampling time  $\Delta t$ .

$$\bar{X}_T = \phi\hat{X}_{T-1} + B\Delta tF_d + \Delta t.w, \quad (13)$$

$$y = C\bar{X}_T + v, \quad (14)$$

where  $\phi = A\Delta t + I$ ,  $\bar{X}$  and  $\hat{X}$  define predicted and estimated value of  $X$ , respectively. The subscript  $T$  denotes the time step. The discrete KF algorithm is given as follows:

*Predicted step*

$$\bar{X}_{T-1} = \phi\hat{X}_{T-1} + Bu, \quad (15)$$

$$\bar{P}_{T-1} = \phi\hat{P}_{T-1}\phi' + Q. \quad (16)$$

*Updated state*

$$\hat{X}_T = \bar{X}_{T-1} + K_T(y_T - C\bar{X}_{T-1}), \quad (17)$$

$$K_T = (\bar{P}_{T-1}C')/(C\bar{P}_{T-1}C' + R), \quad (18)$$

$$\hat{P}_T = (I - K_T C)\hat{P}_{T-1}. \quad (19)$$

where  $A$ : state transition matrix,  $B$ : control input matrix,  $C$ : measurement matrix,  $Q$ : process noise covariance

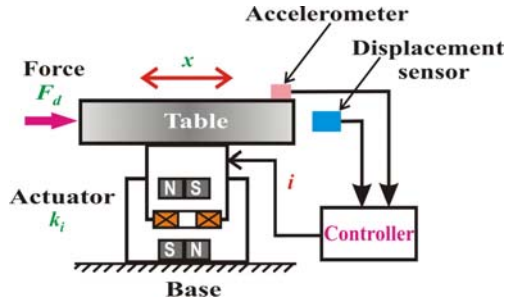


Fig. 4 Basic model of single axis control system

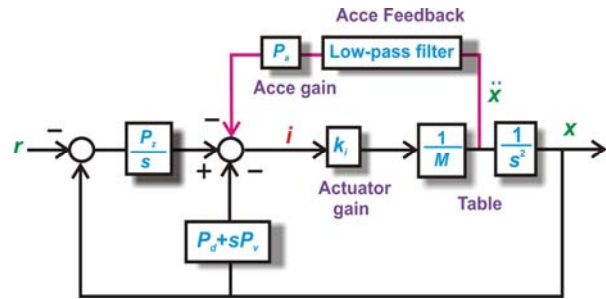


Fig. 5 I-PD controller with acceleration feedback

matrix,  $R$ : measurement covariance matrix,  $K$ : Kalman gain matrix,  $X$ : states matrix,  $P$ : covariance matrix of error in estimation. The influences of the KF on the control system are studied by numerical simulations. It is assumed that the control system is subject to a white Gaussian noise. Figure 7 shows the simulation results. The simulations are conducted for (i) control based on the KF estimation and (ii) control based on direct measured signal. It is observed that the KF can appropriately estimate the measured signal with low levels of noise as shown in the upper chart. Moreover, the control based on the measured displacement signal makes the object being deviated highly. On the other hand, the control based on KF-estimated displacement signal decreases the control deviation significantly.

### 5. Experimental results and discussions

In the experiments, the frequency responses to direct disturbance of the developed system are measured. To generate direct disturbances on the isolation table, two VCMs are mounted on the isolation table and fixed respect to the base. Moreover, to compare the dynamic responses, the responses of the developed system with and without acceleration feedback are drawn in the same graph. At the same time, the effect of the KF-estimated acceleration feedback on the behaviors of the developed system is investigated.

The displacement gains and phase angles of the isolation table with respect to the frequency of applied direct disturbance are shown in Fig. 8. The responses are measured for both with and without the acceleration feedback to the controller. The individual and combined effects of the acceleration feedback of the isolation table and middle table on the behaviors of the developed system are investigated. It is found that the addition of acceleration feedback with the original controller improves the vibration isolation behaviors. The controller gains are kept constant through the experiments, where the value of  $P_a$  is chosen 0.2 ( $As^2/m$ ) for both tables.

In theoretical analysis, it was observed that the larger acceleration feedback gain ( $P_a$ ) causes the improvement of vibration isolation characteristics (Eq. (8)). This theoretical finding is confirmed by experimental results shown in Fig. 9. In Fig. 9, the frequency responses of the isolation table with varying  $P_a$  (0.2 to 0.4  $As^2/m$ ) are shown. Because the poles of the controlled system depend on the value of  $P_a$ , the gains of the controller are reselected to keep the same poles in these experiments.

The effect of acceleration feedback based on KF estimation on the frequency responses to direct disturbance of the isolation table is shown in Fig. 10. It is observed that the acceleration feedback based on the KF estimation can reduce the gain by 6% at a resonance frequency respect to no acceleration feedback. The KF algorithm produces an estimated output that depends on the average value of previous successive outputs. Therefore, it has less possibility to have two successive signals which are very different in magnitude in the KF-estimated signals. This may one of the reasons for improvement in vibration isolation characteristics using KF.

### 6. Conclusion

The horizontal vibration isolation system with displacement cancellation technique was studied. The acceleration feedback added to the original controllers improved the dynamic characteristics of the vibration isolation system. In this investigation, the MEMS accelerometers were used to measure acceleration. The KF was used to decrease the levels of noise in the acceleration signal measured by MEMS accelerometer. From the experimental results, it was observed that the acceleration feedback based on the KF estimation decreased the peak gain by 6% compared to that without acceleration feedback.

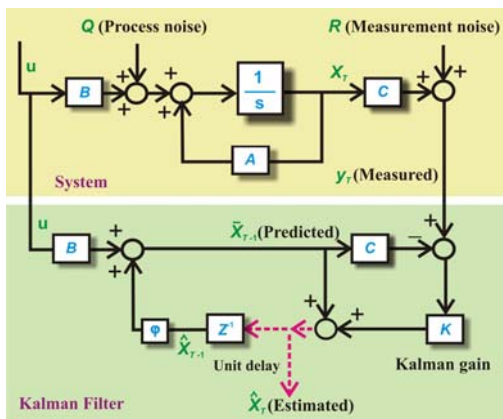


Fig. 6 KF algorithm by block diagram

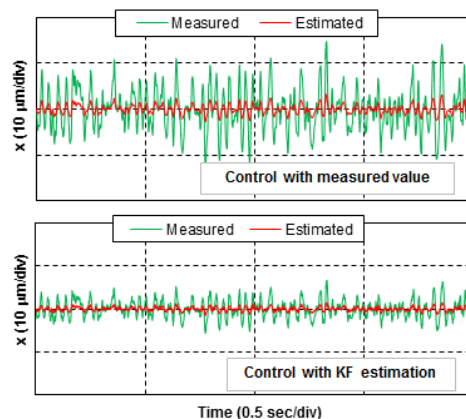
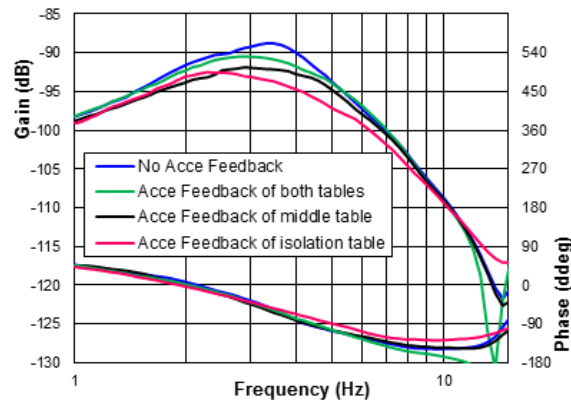


Fig. 7 Noise reduction and system behavior with KF (simulated)

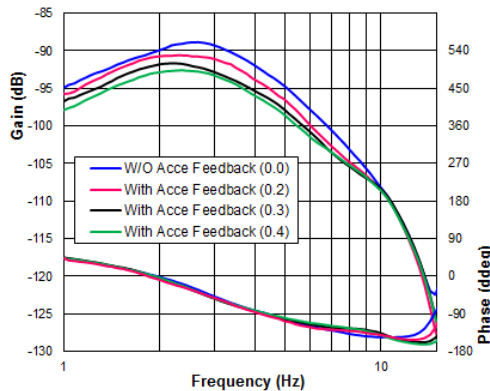


## 6. References

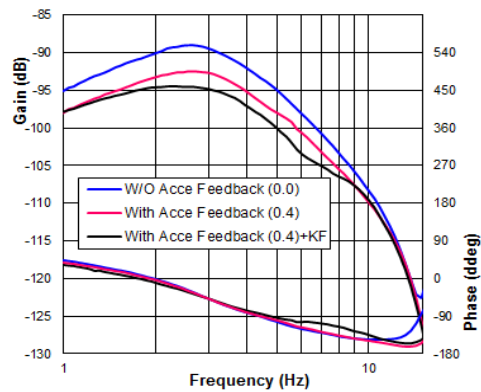
- [1] M. Yasuda, and M. Ikeda, "Double-Active Control of Micro vibration Isolation Systems to Improve Performances (Application of Two-Degree-of-Freedom Control)". *Transaction of Japan Society of Mechanical Engineers*, C, 59,562, pp.1694-1701, 1993.
- [2] E. I. Rivin, "Vibration Isolation of Precision Equipment," *Precision Engineering*, vol. 17, pp. 41-56.
- [3] C. R. Fuller, S. J. Elliott, and P. A. Nelson, "Active Control of Vibration", *Academic Press*, , 1996, pp. 213-220,1995.
- [4] D. L. Trumper, and T. Sato, "A Vibration Isolation Platform," *Mechatronics*, vol. 12, pp. 281-294, 2002.
- [5] T. Mizuno, M. Takasaki, D. Kishita, and K. Hirakawa, "Vibration Isolation System Combining Zero-Power Magnetic Suspension with Springs", *Control Engineering Practice*, Vol.15, No.2, pp 187-196, 2007.
- [6] T. Mizuno, T. Toumiya, and M. Takasaki, "Vibration Isolation Using Negative Stiffness", *JSME International Journal*, Series C, vol. 46, (3), pp. 807-812, (2003).
- [7] Md. E. Hoque, M. Takasaki, Y. Ishino, and T. Mizuno, "Development of a Three-Axis Active Vibration Isolator Using Zero-Power Control", *IEEE/ASME Transactions on Mechatronics*, vol. 11, no. 4, pp.462-470, 2006.
- [8] T. Mizuno, T. Furushima, Y. Ishino, and M. Takasaki, "Realization of Zero-Compliance System by Using Displacement Cancellation Control", *Journal of Vibration and Control*, vol. 16(4), pp. 585-599, 2010.
- [9] T. Schuhmann, W. Hofmann, and R. Werner, "Improving Operational Performance of Active Magnetic Bearing Using Kalman Filter and State Feedback Control", *IEEE Transactions on Industrial Electronic*, vol. 59, no. 2, pp. 821-829, 2012.



**Fig. 8** Effect of Acceleration feedback on frequency response (isolation table) to direct disturbance



**Fig. 9** Frequency responses for different acceleration feedback gain



**Fig. 10** Effect of KF estimated acceleration feedback

## **Design and Fabrication of a Model Remote Control Gun Fire**

Dr. Md. Tazul Islam<sup>1</sup>, Syed Al-Mamun<sup>2</sup> and M Raisul Islam<sup>2</sup>  
<sup>1,2</sup> CUET,  
<sup>3</sup> AIUB, Bangladesh  
E-mail: tazul2003@yahoo.com

### **Abstract**

*Now a day's one of the most talked problem is lack of security in national and international level. Terrorisms and unwanted aggressions through borders has increased to high level. The border security forces are sometimes proving themselves helpless in front of sudden entry. For that purpose when some unwanted entry occurs the distance controlled gun firing system can easily locate it and starts firing to make them flee away or injured. This project is aimed at making the gun firing system which is consisting of a structural support with a gun mounted on it which rotate almost 180 degree along X-X axis and 120 degree along Y-Y direction , computer controlled electronics, and software to teach and control the arm. The mouser gun and a camera along with a remote controlled robot which will shoot object by tracking it via image processing software. Camera will track the object and move on its axis in the direction of robot and shoot it after a particular condition or a particular time as required.*

**Keywords:** Security, terrorisms, tracking, robot and computer controlled

### **1. Introduction**

An automatic firearm is any firearm that will continue to fire so long as the trigger is pressed and held and there is ammunition in the magazine/chamber. While both "semi automatic" and "fully automatic" weapons are "automatic" in technical sense that the firearm automatically cycles between rounds with each trigger pull, under conventional usage a merely semi-automatic firearm is not correctly referred to an "automatic weapon" or an "automatic firearm". The terms "automatic weapon" and "automatic firearm" are conventionally reserved to describe fully automatic firearms. Confusion can be avoided by this convention. A semi-automatic firearm fires one round with each individual trigger pull, while a fully automatic continuously fires rounds whilst the trigger is pressed and held.[1]

A fire-control system is a number of components working together, usually a gun data computer, a director, and radar, which is designed to assist a weapon system in hitting its target. It performs the same task as a human gunner firing a weapon, but attempts to do so faster and more accurately.[2]

"A story on NPR reports that the Tracking Point rifle went on sale today, and can enable a 'novice' to hit a target 500 yards away on the first try. The rifle's scope features a sophisticated color graphics display (video). The shooter locks a laser on the target by pushing a small button by the trigger... But here's where it's different: You pull the trigger but the gun decides when to shoot. It fires only when the weapon has been pointed in exactly the right place, taking into account dozens of variables, including wind, shake and distance to the target. The rifle has a built-in laser range finder, a ballistics computer and a Wi-Fi transmitter to stream live video and audio to a nearby iPad.[3]

This project is about making a gun fire without direct handling of a person rather making the control possible from distance. During this project some new terms and ideas are included by me like different terms of a firearm, its trigger mechanism, its diversities at trigger pulls, firearms auto-loading system for cartridges, required trigger pull of a typical firearm which can be implemented identically for many of the existing lightweight firearms, superior microcontrollers and interfacing via serial ports and object locating which have lead the project to success. The scope of the project includes the designing and building of the hardware and software for a compatible structure. The project is consisting of a structural support with a gun mounted on it, computer controlled electronics, and software to teach and control the arm. This project is aimed at making

mouser gun and a camera along with a remote controlled manual support which will shoot object by tracking it via image processing software. Camera will track the object and move on its axis in the direction of manual robot and shoot it after a particular condition or a particular time as required.

The project is aiming to ensuring border security and to stopping unwanted aggression at national level. Moreover, it can be fruitfully used in security system and in making a location free from unwanted mischievous. In brief, while working on the ideas of this project the enthusiasm in me leads to a very innovative applications which can be used in making a worldwide popular security enhancer.

### **Application**

- a) The machine can be applied at places where it becomes tough to have a person to ensure safety all the time. The place will be thoroughly monitored under the technical implementation of this machine with all the features it has and the processing system embedded in it.
- b) In low density area where animals can freely roam there this system can be used to make them senseless using required anesthetic fluid injected into them by pushing.
- c) It can also be applied at the the warfield at defending own transport like ballistic tank from any damaging through fast attack or any suicidal attack by quick response of the system featured with faster handling and shooting.

## **2. Design Technology**

This System to be act as to be complementary to a firearm a model has improved which would move as it is directed from a PC interfaced via a USB cable. A compatible program is to be made to compile microcontroller and other devices such as stepper motor synchronized with driver IC. Power to be supplied from AC Power Supply which is stepped down by a Center-tapped 12V transformer and then filtered with rectifier to convert into DC current for driving 3-12V stepper motor which would drive the whole device as directed as up-down, right-left, and making proper trigger pull.

### **Devices and instrumentation:**

- a) Microcontroller ( PIC 18F2550)2
- b) Motor driver IC (ULN2003A)
- c) 3-12v Stepper motor
- d) Transformer
- e) Rectifier
- f) TouchSwitch
- g) USB connection
- h) Some gear arrangement to make proper movement and sufficient trigger pull.

### **Rotation and movement by the gun**

The system is designed such that it can have a rotation of about 300 degree from its center so as to cover the total front area. It is done to impede the support from causing certain breakage of the structure behind it. Also to make the gun being stopped automatically after required movement before damaging the structure behind two touch switch has been introduced. The gun also can make 180 degree up-down movement with the rotation of worm wheel mounted with the shaft attached to gun.

### **Required rpm of trigger pull motor**

Pulling the trigger with sufficient force *i.e*, proper rpm is a momentous operation in executing the gun at faster handling action. As this system is built complementary with lightweight military rifles and semi-automatic firearms it's trigger pull has to maintain the same as those of existing. Getting N rpm from motor we get,

Range of typical trigger pull:  $\omega = 2 * \pi * N / 60$

Centripetal force at a distance r from center of a mass m is:  $F = m\omega^2 r$

Distance from center to mass of the arm which pull the trigger *i.e*,  $r = 1$  inch. or,  $r = 0.0254$  m

Trigger pull required,  $m = F/g$

As rpm of 250 is arranged here, calculating from above we get the pull of 3.9lb which is good enough for making smooth fire of the existing firearms.

### Execution of touch plate and switch:

Touch Switch moves with arm. The arm which pulls the trigger rotates clockwise, a spring is attached with it which works as a switch moves with arm between the two touch plates. The switch made there, is a spring so that when it stuck with those plate, does not damage because of its flexibility. While touches with upper plate motor will execute a reverse operation just after the trigger been pulled and thus moves backward till it touches the lower plate.

### 3. Circuit diagram

This circuit is a combination of different electronics and chips to make an arrangement to drive those motors. A brief description is given below:

- A microcontroller(PIC18F2550)
- 2 motor drive IC (ULN2003A)
- 2 Diode
- A 12d Down transformer
- Several resistors
- Several Capacitors
- Transistors
- A Relay
- AC power connection from transformer
- USB connection
- Necessary Wires & wire Connections.

The circuit diagram and complete circuit are shown in the Fig. 1

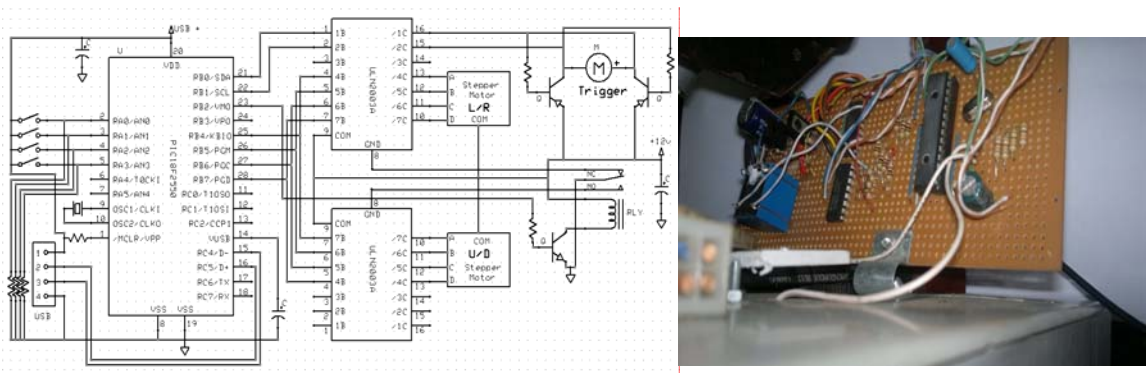


Fig. 1. Circuit diagram and circuit board of the remote control gun fire system

### 4. Working principle

This project is aimed at making a mouse gun and a camera along with a remote controlled manual support which will shoot objects by tracking it via image processing software. The photograph of the remote control gun fire system is shown in the Fig. 2

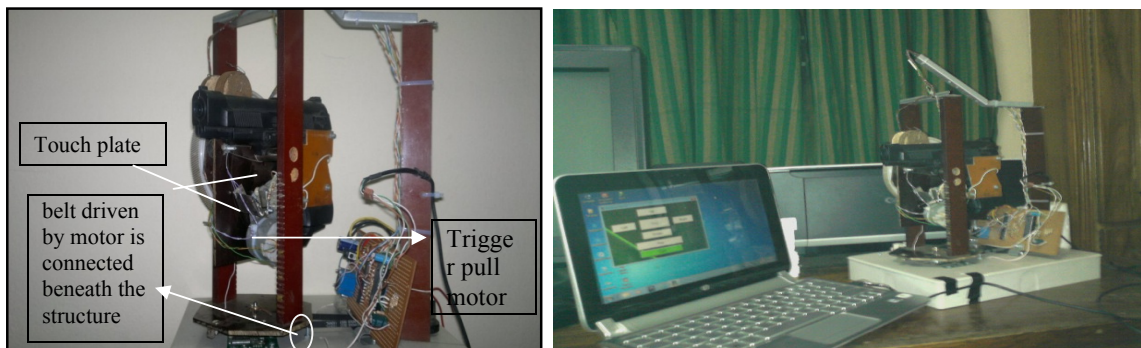


Fig.2 Fire gun controlled by USB compatible programmed application software via PC.

For a movement right-left, a motor has been mounted right behind the circuit and is connected with a drum situated beneath the structure of firearm. Motor and drum is connected by a belt. This drum is a combination of shaft which rigidly locked with the support structure and inside of drum is attached with two ball-bearing. And for an up-down movement, an worm drive and wheel arrangement is attached at the right side of the gun. The worm drive is driven by a 12V stepper motor as it is being commanded. Another motor is placed at the bottom of trigger. The rpm of this motor has been reduced by some reduction gear arrangement but proper for a good trigger pull for any typical gun with a trigger pull at 7-8 lb.

There has been an arrangement of two touch switch, one is metal support shaft mounted through the middle of structure and another is a tin plate. A spring attached with trigger pull arm which while touches the metal shaft, it gets a command to rotate the motor reverse. This has been built such that firearm just get onto trigger and pull it and then getting a command from touch switch to make reverse action. After that when it again touches another tin plate switch it gives a command to stop the motor right there. And the motor gets ready for another firing action when it gets any command.

The gun firing system is consisting of a structural support with a mouser gun mounted on it which rotate almost 180 degree along X-X axis and 120 degree along Y-Y direction , computer controlled electronics, and software to teach and control the arm. The mouser gun and a camera along with a remote controlled robot which will shoot object by tracking it via image processing software. When a command is given through computer at first camera will track the object and move on its axis in the direction of the robot and shoot it after a particular condition or a particular time as required

## 5. Discussion

During this project some new terms and ideas are studied like different terms of a firearm, its trigger mechanism, its diversities at trigger pulls, firearms auto-loading system for cartridges, required trigger pull of a typical firearm which can be implemented identically for many of the existing light weight firearms, superior microcontrollers and interfacing via serial ports and object locating which have lead the project to success.

Such system can enervate the defense of enemy by efficacious controlling at remote as less or no casualties of human life would occur. To be an assist of such attack into the region where it is impervious by direct persons appearing because of risk, be dominated.

This project has been fabricated as it can be executed at practical field as well as studying about firearms history, latest technologies and developments, related terms parts and techniques of sophisticated mechanism enriching knowledge in the field of ballistic science by overcoming the following draw backs

A rigid structure need to be made to support heavy load of riffles and firearms. For progressive trigger action it should be programmed such that the pull of arm on trigger would remain for the time it is needed. In that case the upper touch switch of metal shaft is to be removed and command should be given such that the arm attached with motor will pull the trigger and remain at that pulling action till another command is given to release it. Moreover, a huge improvement needed at imaging object. A night vision camera can also be recommended to make the system capable of shooting 24 hours.

## 6. Conclusion

This project is aimed at making the gun firing system which is consisting of a structural support with a gun mounted on it which rotate almost 180 degree along X-X axis and 120 degree along Y-Y direction , computer controlled electronics, and software to teach and control the arm. The mouser gun and a camera along with a remote controlled robot which will shoot object by tracking it via image processing software. Camera will track the object and move on its axis in the direction of robot and shoot it after a particular condition or a particular time as required.

## 7. References

- [1] [en.wikipedia.org/wiki/Automatic\\_firearm](https://en.wikipedia.org/wiki/Automatic_firearm).
- [2] [en.wikipedia.org/wiki/Fire-control\\_system](https://en.wikipedia.org/wiki/Fire-control_system)
- [3] [tech.slashdot.org/story/13/05/16/016209/a-computer-based-smart-rifle-with-incredible-accuracy-now-on-sale](https://tech.slashdot.org/story/13/05/16/016209/a-computer-based-smart-rifle-with-incredible-accuracy-now-on-sale)

## **Development of an Obstacle Avoidance System for Mobile Robot to Avoid Accident by Using Microcontroller**

Md. Rokunuzzaman, \*Amit Roy, S. M. Rasid, Md. Sumon Reza and Md. Anik Islam  
Department of Mechanical Engineering  
Rajshahi University of Engineering & Technology (RUET), Rajshahi-6204, Bangladesh  
\*E-mail: [royamit.me@gmail.com](mailto:royamit.me@gmail.com)

### **Abstract**

This paper describes a control car to avoid accident by microcontroller interfacing with a motor control circuit. For the development of the obstacle avoidance system, the control circuit of a toy car was modified. An algorithm was also developed to command the control circuit. The control circuit consists of infrared sensor, motor driver circuit with power supply, transmitter circuit, receiver circuit and infrared LED (IR-LED). DC motor was used as an actuator to control the designed car. Infrared sensors were used to generate high and low frequency in the transmission circuit. High frequency was generated when the response of the capacitor was low and low frequency was generated when the response of the capacitor was high. According to the signal from receiver circuit, the microcontroller sends signal to the program that controls the DC motor to drive the car. The results show that the designed car can satisfactorily avoid most of the common obstacles.

Keywords: obstacle avoidance; mobile robot; microcontroller; infrared sensor.

### **1. Introduction**

An obstacle avoidance system is a mobile robot that follows markers or wires in the floor, or uses vision or lasers or sensors. They are most often used in industrial applications to move materials around a manufacturing facility or a warehouse. Application of the automatic guided vehicle has broadened during the late 20th century and they are no longer restricted to industrial environments. Automatic guided vehicle is a field of application automation, which is a modern technology in automobile sector. Automated guided vehicles (AGVs) increase efficiency and reduce costs by helping to automate a manufacturing facility or warehouse. The first AGV was invented by Berrett Electronics in 1953. The AGV can tow objects behind them in trailers to which they can autonomously attach. The trailers can be used to move raw materials or finished product. The AGV can also store objects on a bed. The objects can be placed on a set of motorized rollers (conveyor) and then pushed off by reversing them. Some AGVs use forklifts to lift objects for storage. AGVs are employed in nearly every industry, including, pulp, paper, metals, newspaper, and general manufacturing. Transporting materials such as food, linen or medicine in hospitals is also done. An AGV can also be called self-guided vehicle (SGV). In Germany the technology is also called Fahrerlose Transport system (FTS) and in Sweden forecloses trucker. Lower cost versions of AGVs are often called Automated Guided Carts (AGCs) and are usually guided by magnetic tape. AGCs are available in a variety of models and can be used to move products on an assembly line, transport goods throughout a plant or warehouse, and deliver loads to and from stretch wrappers and roller conveyors [1].

There are many systems available for the development of this type obstacle avoidance system following: - Laser Target Navigation, Steering control, Vision-Guidance, Forward sensing control system, Path select mode.

In this paper we work with forward sensing control system. Forward sensing control uses collision avoidance sensors to avoid collisions with other AGV in the area. Most AGVs are equipped with a bumper sensor of some sort as a failsafe. The optical uses an infrared transmitter/receiver and sends an infrared signal which then gets reflected back is familiar concept. The problems with these are they can only protect the AGV from so many sides. They are relatively hard to install and work with as well.

## 2.1 System Overview

This project is about automatic guided vehicle to avoid accident. For this infrared LED is used to radiate continuously infrared ray and detect any reflection of these beams on any obstacle in front of the vehicle. At first vehicle drives at constant speed, if any obstacle in front of the vehicle comes, the vehicle would automatically stops and search for alternative way to pass out. The main components of the circuit are DC motor, transistor, resistor, diodes and 8V DC supply.

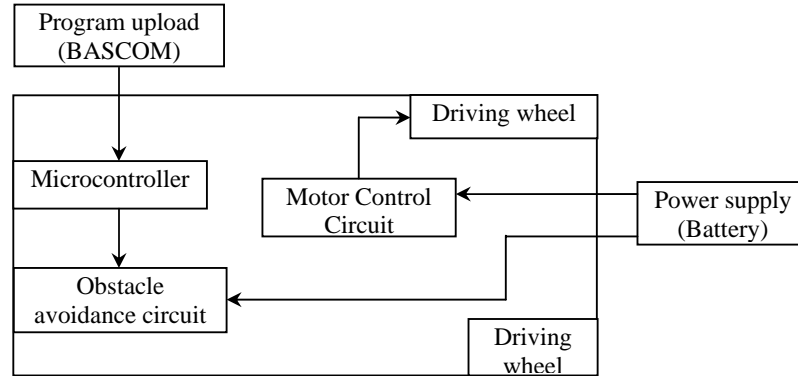


Fig: 1: System overview

Here infrared sensor is used to generate high and low frequency in the transmission circuit. High frequency is generated when capacitor's capacity is low and low frequency is generated when capacitor's capacity is high. Another circuit which is called receiver circuit, which receives the high and low frequency and analyze whether it is high or low frequency and sends signal to the program that controls the DC motor according to the analysis result. Variable resistor and capacitor is used for adjusting high and low frequency.

## 2.2 Methods And Tools Used

Table 1: Specification of a System

Item	Specification
Language Used	C++(BASCOM)
For circuit animation	Protious_7.6
Microcontroller	AT mega32

## 3. DC Motor Controller Driver Circuit

DC motor driver circuits connected with microcontroller at pin 20 and 21 namely T1 and T2 through resistor. When T1 is closed, DC motor rotates clockwise and vehicle moves forward. When T2 is closed, DC motor rotates anticlockwise and vehicle moves backward.

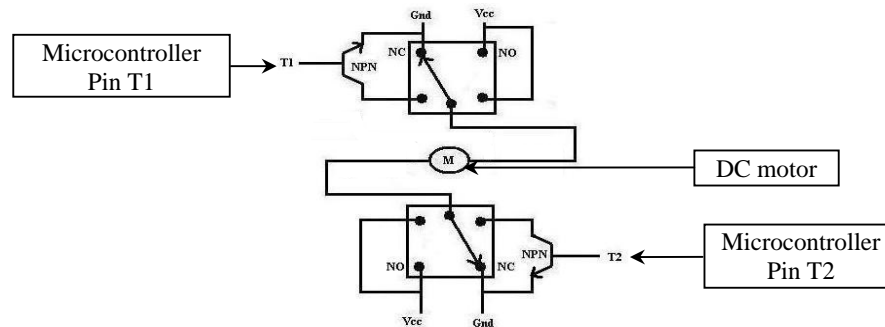




Fig: 2: DC motor driver circuit

#### 4. Experimental Setup

In this paper infrared sensor and infrared LED is used as sensor. Infrared (IR) sensors contain an emitting diode as well as a detector. Both the emitter and detector face in the same direction. If the sensor is pointed at nothing it returns a high value. If there is something nearby, that will reflect the IR light then the value decreases. These sensors have an active range of approximately 2 cm. The actual range depends on the reflectance and size of the object being detected. [5]

Controlling system of the vehicle is completed by controlling the speed of DC motor. The speed of a DC motor is directly proportional to the supply voltage, so if we reduce the supply voltage the speed of the motor will reduce gradually. The speed controller works by varying the average voltage sent to the motor. It could do this by simply adjusting the voltage sent to the motor, but this is quite inefficient to do. A better way is to switch the motor's supply on and off very quickly. If the switching is fast enough, the motor doesn't notice it, it only notices the average effect. [5]

The experimental setup of obstacle avoidance system for mobile robot to avoid accident is following-

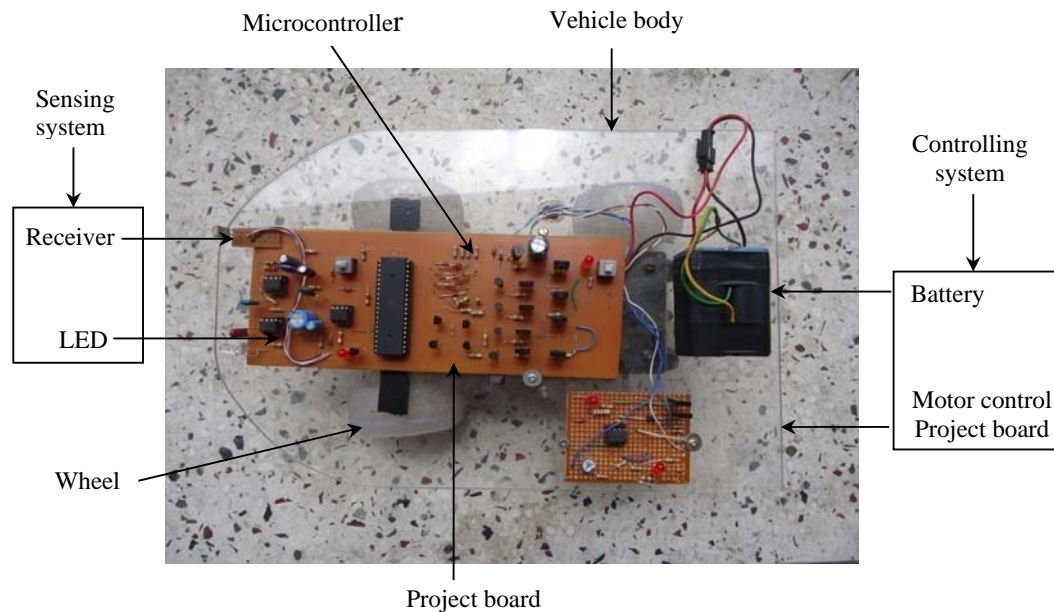


Fig: 3: Experimental setup of the obstacle avoidance system

#### 4. Sensor Selection

A sensor is a device which receives and responds to a signal or stimulus. Here, the term "stimulus" means a property or a quantity that needs to be converted into electrical form. Hence, sensor can be defined as a device which receives a signal and converts it into electrical form which can be further used for electronic devices. A sensor differs from a transducer in the way that a transducer converts one form of energy into other form whereas a sensor converts the received signal into electrical form only.

In selecting a sensor for a particular application three number of factors that need to be considered:

1. The nature of the measurement required e.g. the variable to be measured, its nominal values, the range of values, the accuracy required. The required speed of measurement, the reliability required the environmental conditions under which the measurement is to be made.
2. The nature of the output required from the sensor, thus determining the signal conditioning requirements in order to give suitable output signals from the measurement.
3. Then possible sensors can be identified, taking into account such factors as their range, accuracy, linearity, speed of response, reliability, maintainability, life power supply requirements, ruggedness, availability and cost.

## 5. Block Diagram of the System

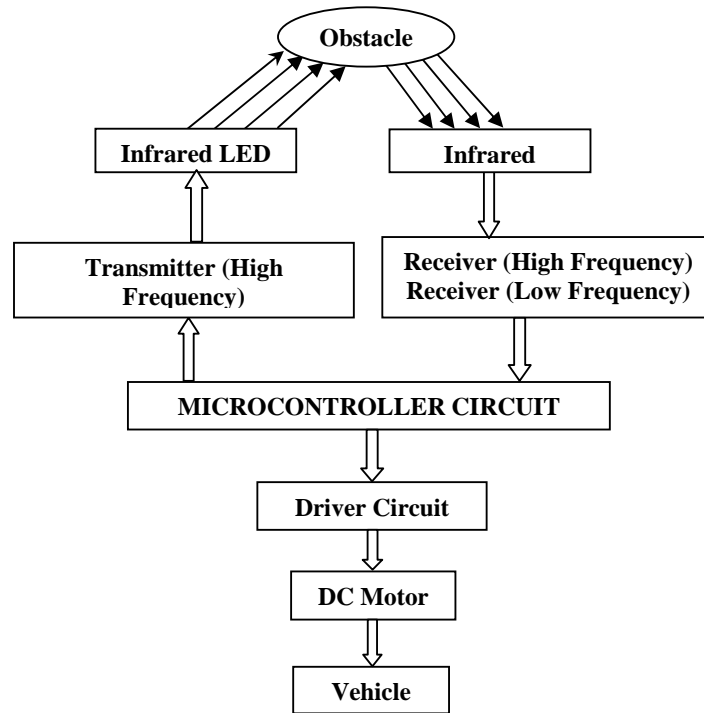


Fig: 4: Block diagram of the system.

## 6. Algorithms of the System

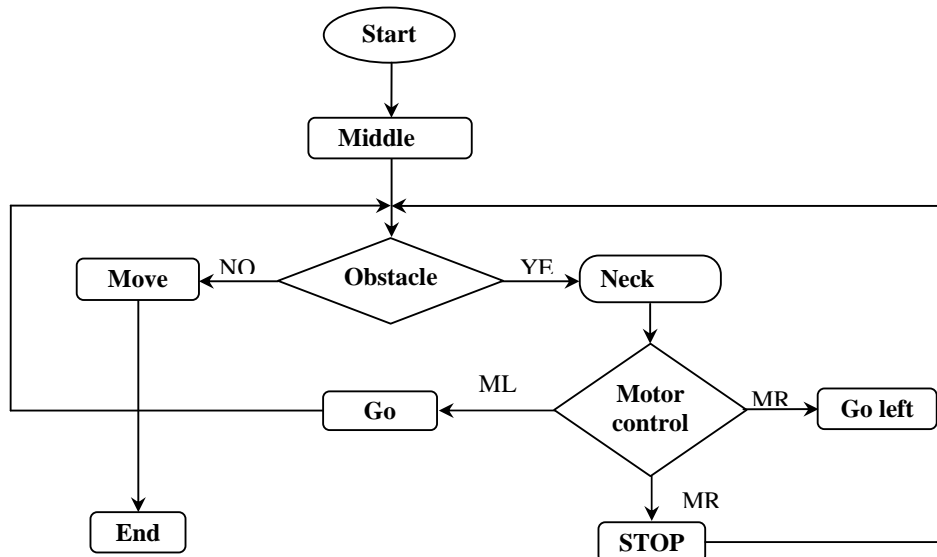


Fig: 5: Flowchart of the system

**Legend**  
 M= Middle  
 L=Left R=Right

## 7. Working Principle of Controlling System

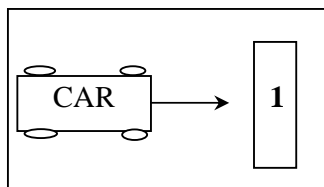
There are many types of motors that are in used these days. The common ones are DC types, AC types, stepper motors and brushless DC motors. The speed of a DC motor is directly proportional to the supply voltage, so if we reduce the supply voltage from 12 Volts to 6 Volts, the motor will run at half the speed. How can this be achieved when the battery is fixed at 12 Volts? The speed controller works by varying the average voltage sent to the motor. It could do this by simply adjusting the voltage sent to the motor, but this is quite inefficient to do. A better way is to switch the motor's supply on and off very quickly. If the switching is fast enough, the motor doesn't notice it, it only notices the average effect.

When you watch a film in the cinema, or the television, what you are actually seeing is a series of fixed pictures, which change rapidly enough that your eyes just see the average effect - movement. Your brain fills in the gaps to give an average effect. Now imagine a light bulb with a switch. When you close the switch, the bulb goes on and is at full brightness, say 100 Watts. When you open the switch it goes off (0 Watts). Now if you close the switch for a fraction of a second, and then open it for the same amount of time, the filament won't have time to cool down and heat up, and you will just get an average glow of 50 Watts. This is how lamp dimmers work, and the same principle is used by speed controllers to drive a motor. When the switch is closed, the motor sees 12 Volts, and when it is open it sees 0 Volts. If the switch is open for the same amount of time as it is closed, the motor will see an average of 6 Volts, and will run more slowly. As the amount of time that the voltage is increases compared with the amount of time that it is off, the average speed of the motor increases. We can see that the average speed is around 150, although it varies quite a bit. If the supply voltage is switched fast enough, it won't have time to change speed much, and the speed will be quite steady. This is the principle of switch mode speed control. Thus the speed is set by PWM – Pulse Width Modulation [10].

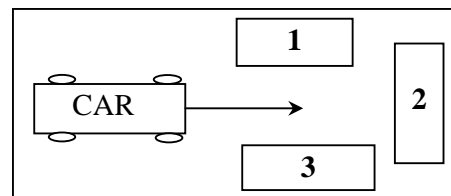
## 8. Experimental Scenario

The constructed obstacle avoidance vehicle is able to avoid different types of shape of objects. In this system the LED transmitted ray which is reflected by the objects presents in front of the vehicle and receive by the receiver circuit. Then microcontroller circuit controls the DC motor by regulating the voltage. Then the vehicle search for alternative ways to move. Here some configuration in which the constructed vehicle is performed.

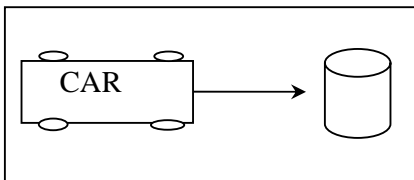
**Configuration 1:**



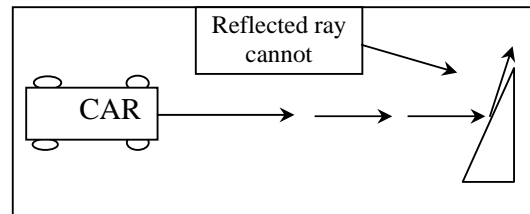
**Configuration 2:**



**Configuration 3:**



**Configuration 4:**



## 9. Experimental data

Table 2: Experimental data

Configuration	Obstacle No	Observation	Obstacle Avoidance
1	1	1	Yes
		2	Yes
		3	Yes
2	3	1	No
		2	Yes
		3	Yes
3	1 (circular)	1	No
		2	No
4	1(Inclined)	1	No
		2	No

## 10. Performance

Table 3: Performance accuracy

Configuration	Accuracy
1	100%
2	66.67%
3(circular)	0%
4(Inclined)	0%

The performance of obstacle avoidance system is good. The vehicle can avoid obstacle very carefully and the successful operation percentage is 100% for the configuration 1. For the configuration 2 there is failure for 1 observation. Hence the performance of the vehicle for configuration 2 is 66.67%. The vehicle is unable to sense circular obstacle in the configuration 3. For configuration 4, as the reflected ray cannot receive by the sensor so the car cannot avoid accident for inclined surface. The car can sense an obstacle more than 3 inch high. It cannot sense an obstacle less than 3 inch high; this is disadvantages of the constructed car.

## 11. Discussion

It is the time for automation. In automatic guided vehicle, the vehicle automatically senses the presence of obstacle in front of the vehicle and stops. Then the vehicle search for alternative way to pass out. Some improvements in the performance can be achieved by changing the components used (e.g. high range sensor for receiver circuit). Automatic guided vehicle will not be able to obey oral instructions from policeman, so a digital system will have to be developed. Toy car is used for the design and construction of the vehicle is made as required to fulfill the objectives. In automobile sector computer controlled software is used to control the vehicle. But we select this topic to use microcontroller because of- Low cost, Simplicity in design, Greater flexibility, Low weight, Required less space.

If high range (ultrasonic sensor) sensor is used, it can easy to detect the long distance object. For control the vehicle efficiently, program also be updated requirement. If receiver and transmitter circuit can develop, high accuracy may be achieved. Image processing software may be used for identifying the obstacle. However the automatic guided vehicle developed is performed satisfactorily as required. The car cannot sense inclined and round surface.

## 12. Conclusion

For the development of system, a vehicle has been designed by designing various elements. Then system circuit diagram and project have been designed. The performance of the vehicle tested and the vehicle can carry load of about 2 kg. In this project infrared sensor is used to detect obstacle nearer the vehicle about 6 inches. But when this concept developed in large vehicle then high range sensor or high-resolution camera can be used. Image processing software may be used to identify the obstacle. For detecting low and high distance obstacle receiver module will be developed and send data quickly in the control unit to control the vehicle. So it will be most beneficial technology now a day. If high range sensor is used, it can easy to detect the long distance object. For control the vehicle efficiently, program also be updated requirement. If receiver and transmitter circuit can develop, high accuracy may be achieved. Image processing software may be used for identify the obstacle.

## 13. References

- [1] [Online] Available: <http://www.Wikipedia.com>
- [2] Virgil Moring Faires (1965), "*Design of Machine Elements*", 4th Edition, The Macmillan Company.
- [3] Mehta V.K. (2000), "*Principles of electronics*", 9th Edition, S. Chand and Company Ltd
- [4] Boylestad R. L. and Nashelsky L. (2002), "*Electronics Devices and Circuit Theory*", 8th Edition, Prentice Hall
- [5] Malvino R.P. (2002), "*Electronics Principles*", 6th Edition, Tata McGraw-Hill
- [6] F.R. Coughlin and F.F. Driscoll, "*Operational Amplifiers and Linear Integrated Circuits*", 5th Edition
- [7] Apostolopoulos, D., Wagner, M. and Whittaker, W. (1999), "*Technology and field demonstration results in the robotic search for Antarctic meteorites*", Proceedings of the International Conference on Field and Service Robotics, pp. 185 -190
- [8] Broggi, A. (1995), "*Vision-based road detection in automotive systems: A real-time expectation-driven approach*", Journal of Artificial Intelligence Research 3 pp. 325-348
- [9] Lilienfeld, Julius Edgar, "*Method and apparatus for controlling electric current*", U.S. Patent 1,745,175 1930-01-28 (filed in Canada 1925-10-22, in US 1926-10-08).
- [10] Heil, Oskar, "*Improvements in or relating to electrical amplifiers and other control arrangements and devices*", Patent No. GB439457, European Patent Office, filed in Great Britain 1934-03-02, published 1935-12-06 (originally filed in Germany 1934-03-02).
- [11] David Bodanis (2005), "*Electric Universe*", Crown Publishers, New York. ISBN 0-7394-5670-9.

## An Analytical Study of Passive Anti-Roll Tanks

Gazi Md. Khalil<sup>1</sup>, Syed Marzan-ul Hasan<sup>1</sup>, Md. Ehsan Khaled<sup>2</sup>

<sup>1</sup>Dept. of Naval Architecture & Marine Engineering, BUET, Dhaka-1000

<sup>2</sup>Yokohama National University, Japan

E-mail: hasan\_name06@yahoo.com

### Abstract

*This paper presents a detailed theoretical analysis using the principle of conservation of energy and spring-mass system analogy for the oscillation of water in two identical tanks connected by pipe. An expression is derived for the frequency of oscillation of water as a function of the affecting parameters in anti-roll tanks. It is mathematically demonstrated that the circular and rectangular tanks produce the same frequency of oscillation of water if their cross-sectional areas remain same. Furthermore, this paper takes into account the additional damping forces which arise from friction between the moving fluid and the surrounding tank wall. This makes the theoretical model more realistic. The computational results are plotted graphically and then physically interpreted in order to demonstrate the effect of the depth of water and the area of cross-section of each vertical tank; the effect of the length, diameter and number of connecting pipes; and the effect of damping on the oscillation of water in the tanks. The results of this analytical study are expected to be useful in the design of anti-rolling tanks which will effectively reduce the rolling motion of ships.*

Keywords: Natural frequency of oscillation, rolling motion, anti-roll tank, passive control, damping effect

### 1. Introduction

The understanding and control of rolling motion i.e. the rotational motion about the longitudinal axis of a ship is essential for efficient ship manoeuvring, ensuring crew comfort and proper functioning of onboard equipment. Till date, a variety of roll control mechanisms like bilge keels, fin stabilizers, gyro stabilizers, anti-roll tanks, etc. have been subjected to comprehensive theoretical study and detailed practical experimentation.

Anti-roll tanks (ART) generate anti-rolling moments using differences in water heights at the two limbs of U-tank whose oscillation is exactly out of phase to the incoming wave excitations. The use of ART has an added advantage of controlling the rolling motion even if the vessel is not underway. An Active ART uses pumps or any mechanical means to generate the moments from fluid flow and often become impractical in case of large vessels. Passive anti-roll tank (PART), on the other hand, with no active means to generate counter moments relies solely on accurate tuning techniques to ambient conditions, and therefore, require a greater study across the linear and non-linear range.

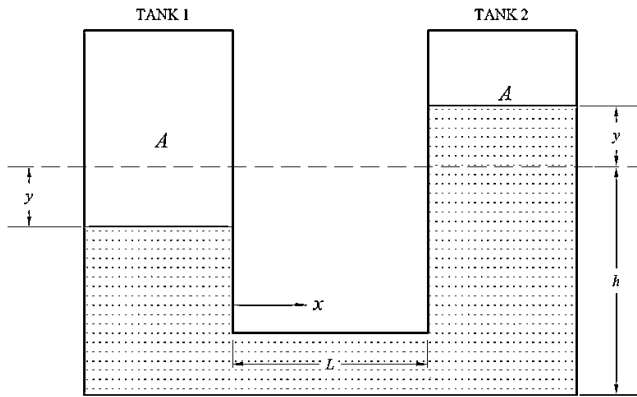
Froude [11] was the first to use anti-roll tanks to reduce roll motion. He installed water chambers in the upper part of the ship. The free-surface effect of the water tank lengthened the period of the rolling motion but reduced the ship's stability; consequently, the system was abandoned. Frahm[4], a German naval engineer revived the method, and was the first to understand the importance of placing the horizontal leg or cross-duct in the U-tube. An active counterpart of Frahm's passive tank was conceived by Minorsky[8]. A restoring moment was developed by transferring the water directly with a proper phase from one leg of the U-tube tank to the other at a high rate. Chadwick [6] derived the governing equations for rolling motion in calm water and found that the axis of roll does not necessarily pass through the centre of gravity of the ship. The hydrodynamic effects are considered linear and hence superimposable. Crockett [9] in his report illustrated a step-by-step preliminary design procedure for designing, installing, and tuning of passive anti-roll tanks based on some empirical formulae and practical experiences. Bell and Walker[5] found that the positioning of the tanks is a critical issue and the typical designs and characteristics of vessels must be taken into account while designing an effective ART. Gawad *et al.* [1] paid attention to the fluid motion inside the tank itself. They mentioned that proper tuning of the anti-roll tank to the ship's natural frequency is very important in reducing the roll motion. Dallinga [10] noticed that for a given wing-tank area (which determines the restoring term in the natural period) the height of the connecting duct is the remaining design parameter for the tuning effect. Samoilescu *et al.* [3] mentioned

that tank stabilizers are virtually independent of the forward speed of the vessel: they generate anti rolling forces by phased flow of appropriate masses of fluid (water or reserve fuel, etc.) in transverse tanks installed at suitable heights and distances from the ship's centre line. Tanizawa *et al.* [7] used a numerical wave tank (NWT) which was applied to the simulation of coupled motions of ship and ART in beam seas. Holden *et al.* [2] presented two novel nonlinear models of U-shaped ART for ships, and their linearization. The models were derived using Lagrangian mechanics.

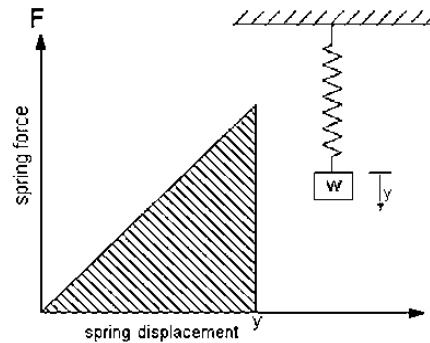
Water in the reservoirs of an ART is expected to oscillate with the same period but exactly out of phase to the vessel's oscillation. For the greatest effect, ARTs are often placed where they would induce the highest counter-rolling moment (often, high up on the vessel). The motivating force for the anti-roll tanks is predominantly the action of gravity on the mass of the fluid. Since the fluid can only flow downhill and has inertia, it cannot start to move until the ship has rolled a few degrees. The natural restoring forces limit the maximum roll angle and initiate a roll in the opposite sense. In the meantime, the fluid continues to flow downhill, accumulating on the still low side and provides a moment opposing the ship motion. As the ship returns and passes its upright position, fluid again flows downhill to repeat the process. The transverse acceleration of the fluid generates an inertia force and thereby a moment, about the roll centre, which reduces the gravity moment when the tanks are below the roll centre and increases it when they are above. Maximum moment is experienced at the vertical position of the ship. The kinetic and potential energies of the fluid in the tanks are originated from the energy generated during rolling. Part of the energy is dissipated by vortex shedding and fluid viscous effects related to skin friction on the walls of the tank. Thus, the phase lag may be increased, within limits, by placing obstructions e. g. orifice plates, grilles, etc. in the fluid flow path to increase the damping. In contrast to the other papers available on this topic, the present paper takes a new theoretical approach to determine the period of oscillation of water in tanks that can be used to counterfeit anti-rolling motion in ships.

## 2. Theoretical Analysis

Let us consider two identical tanks each of cross-sectional area  $A$ . The tanks are connected at their bottom by a horizontal pipe of length  $L$  and cross-sectional area  $a$ , as shown in (Figure 1). The tanks are filled with water up to a depth of  $h$ .



**Fig. 1.** Natural oscillations of water in two identical tanks connected by a pipe.



**Fig. 2.** Simple spring-mass system

Suppose that oscillation occurs in the tanks due to some external disturbance. In such a case, the water level will fall in one tank, with a corresponding rise in the other. The head of water, causing flow in the pipe, will be the difference between the two water levels. Let the water level in Tank 1 fall down by  $y$ . Then the water level in Tank 2 will rise up by  $y$ . Let  $x$  be the horizontal displacement of water in the pipe. The volume of water that has passed from Tank 1 is  $Ay$ . From constancy of volume of water, we can write

$$Ay = ax \quad (1)$$

$$\therefore x = \frac{Ay}{a} \quad (2)$$

Using the principle of conservation of energy, the natural frequency of an oscillating system can be easily determined, and in this case, it can be done using an analogy with the spring-mass system. For a vibrating system, the energy is partly kinetic and partly potential. The kinetic energy  $K$  is associated with the velocity of the mass and the potential energy  $P$  is due to the strain energy stored in the spring. Thus,

$$K + P = \text{Total Energy} = \text{constant} \quad (3)$$

Therefore, the rate of change of energy is zero,

$$\frac{d}{dt} (K + P) = 0 \quad (4)$$

The equation of motion of the spring mass system can be derived from energy considerations. The kinetic energy of the mass is given by

$$K = \frac{1}{2}mv^2 = \frac{1}{2}m\dot{y}^2 \quad (5)$$

The potential energy of the system is due to strain energy stored in the spring (Figure 2) and is given by

$$P = \int_0^x ky \, dx = \frac{1}{2}ky^2 \quad (6)$$

Therefore, one can now easily write down the expressions for the potential energy of the water oscillating in the tanks. In this case, the restoring force is

$$F = 2Ay\rho g \quad (7)$$

$$\therefore k = \frac{2Ay\rho g}{y} = 2A\rho g \quad (8)$$

Combining Eqn (6) and Eqn (8), we get

$$P = A\rho gy^2 \quad (9)$$

$$\therefore \frac{dP}{dt} = 2A\rho gy\dot{y} \quad (10)$$

The kinetic energy of the oscillating column of water is given by

$$K = \frac{1}{2}Ah\rho\left(\frac{dy}{dt}\right)^2 + \frac{1}{2}Ah\rho\left(\frac{dy}{dt}\right)^2 + \frac{1}{2}aL\rho\left(\frac{dx}{dt}\right)^2$$

It can be easily shown from the above that

$$\frac{dT}{dt} = \rho \left[ 2Ah + aL\left(\frac{A}{a}\right)^2 \right] \dot{y}\dot{y} \quad (11)$$

From Eqn (4),Eqn(10) and Eqn(11), we obtain

$$\rho \left[ 2Ah + aL\left(\frac{A}{a}\right)^2 \right] \dot{y}\ddot{y} + 2A\rho gy\dot{y} = 0$$

Dividing the above expression by  $p\dot{y}$  throughout, we get

$$\left[ 2Ah + aL\left(\frac{A}{a}\right)^2 \right] \ddot{y} + 2Agy = 0 \quad (12)$$

$$\text{or, } \ddot{y} + \left[ \frac{2Ag}{2Ah + aL(A/a)^2} \right] y = 0$$

which is similar to

$$\ddot{y} + p^2y = 0 \quad (13)$$

where  $p$  is the natural frequency of oscillation in radian/second. Therefore,

$$p^2 = \frac{2Ag}{2Ah + aL(A/a)^2} \quad (14)$$

$$\text{or, } p = \left[ \frac{g}{h + \frac{L}{2}\left(\frac{A}{a}\right)} \right]^{1/2} \quad (15)$$

It can be easily shown that for multiple pipes,

$$p = \left[ \frac{g}{h + \frac{L}{2}\left(\frac{A}{na}\right)} \right]^{1/2} \quad (16)$$

where  $n$  is the number of connecting pipes. For rectangular tank connected by rectangular pipe, we get

$$p = \left[ \frac{g}{h + \frac{L}{2}\left(\frac{bl}{h'l'}\right)} \right]^{1/2} \quad (17)$$

where  $b$  and  $l$  are the breadth and longitudinal extent of the vertical arm of the tanks and  $h'$  and  $l'$  are the height and longitudinal extent of the horizontal pipe respectively. When the longitudinal extent of the rectangular vertical arm and that of the horizontal pipe are same, Eqn (17) reduces to



$$p = \left[ \frac{g}{h + \frac{L}{2} \left( \frac{b}{h'} \right)} \right]^{1/2} \quad (18)$$

For two identical square tanks connected by a duct of square cross-section, Eqn (17) gives

$$p = \left[ \frac{g}{h + \frac{L}{2} \left( \frac{b}{h'} \right)^2} \right]^{1/2} \quad (19)$$

Similarly for two circular tanks connected by a circular pipe,

$$p = \left[ \frac{g}{h + \frac{L}{2} \left( \frac{D}{d} \right)^2} \right]^{1/2} \quad (20)$$

For two identical square tanks connected by a circular pipe,

$$p = \left[ \frac{g}{h + \frac{2L}{\pi} \left( \frac{b}{d} \right)^2} \right]^{1/2} \quad (21)$$

The above derivation takes into account an ideal fluid flow condition. Taking the effect of damping into consideration, and  $D_e$  as the loss of energy due to damping, Eqn (4) gives

$$\frac{d}{dt}(K + P) = -D_e \quad (22)$$

The energy lost due to damping can be considered as the product of the damping force and the reduction in height of the water column due to damping. Since the damping force is proportional to the velocity, we get

$$D_e = C\dot{y}h_d \quad (23)$$

Where  $C$  is the damping constant and  $h_d$  is the reduction in height of the water column due to damping. If  $U_d$  is the change in potential energy and  $T_d$  is the change in kinetic energy due to damping,

$$D_e = P_d + K_d \quad (24)$$

Let  $U_1$  and  $U_2$  be the potential energy of the water column in ideal fluid and viscous fluid respectively. Therefore, Eqn (9) gives

$$P_1 = A\rho gy^2 \quad (25)$$

therefore,

$$P_2 = A\rho g(y - h_d)^2 \quad (26)$$

Neglecting the second order terms and using the Newton's equation of motion,

$$P_d = P_1 - P_2 = 2A\rho gyh_d \quad (27)$$

$$y = \frac{\dot{y}^2}{2g} \quad (28)$$

$$P_d = A\rho \dot{y}^2 h_d \quad (29)$$

Similarly, the corresponding expressions for the kinetic energy can be written as

$$K_1 = \frac{1}{2}\rho \left[ 2Ah + aL \left( \frac{A}{a} \right)^2 \right] \dot{y}^2 \quad (30)$$

$$K_2 = \frac{1}{2}\rho \left[ 2A(h - h_d) + aL \left( \frac{A}{a} \right)^2 \right] \dot{y}^2 \quad (31)$$

Thus we get

$$K_D = K_1 - K_2 = A\rho h_d \dot{y}^2 \quad (32)$$

Therefore Eqn(24) becomes

$$D_e = 2A\rho \dot{y}^2 h_d \quad (33)$$

So from Eqn (22),

$$\rho \left[ 2Ah + aL \left( \frac{A}{a} \right)^2 \right] \dot{y}\ddot{y} + 2A\rho gy\dot{y} = -2A\rho \dot{y}^2 h_d \quad (34)$$

which gives

$$\ddot{y} + \left[ \frac{2Ag}{2Ah + aL(A/a)^2} \right] y + \left[ \frac{2h_d A}{2Ah + aL(A/a)^2} \right] \dot{y} = 0 \quad (35)$$

Let

$$p^2 = \frac{2Ag}{2Ah + aL(A/a)^2} \quad (36)$$

and

$$2n = \frac{2Ah_d}{2Ah + aL(A/a)^2} \quad (37)$$

Then Eqn (35) becomes

$$\ddot{y} + 2n\dot{y} + p^2 y = 0 \quad (38)$$

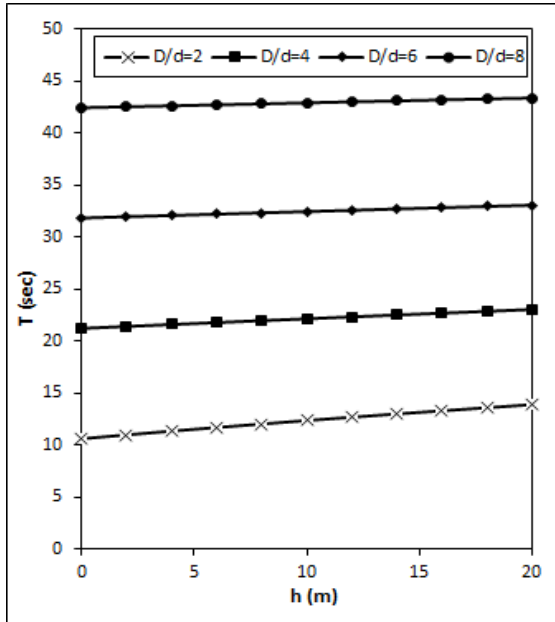
which is a second order linear homogeneous differential equation. Considering the roots of the characteristic equation real and distinct, and the solution of the equation

$$y = e^{rt} \tag{39}$$

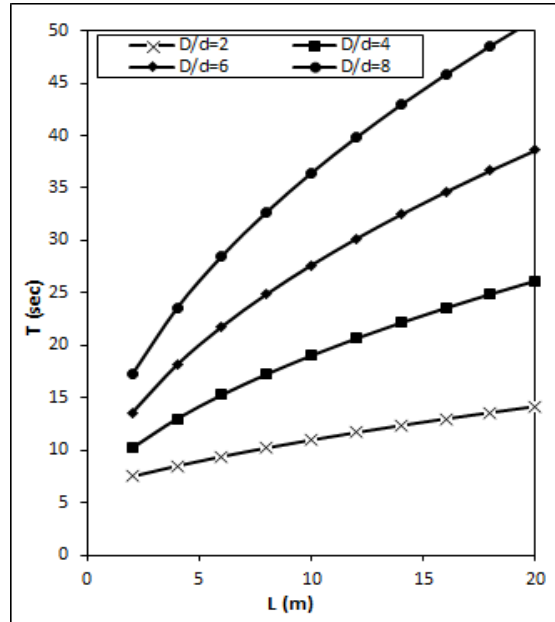
It can be easily shown that  $r = -n \pm \sqrt{(n^2 - p^2)}$  (40)

So the damped frequency can be expressed as  $p_d = \sqrt{(p^2 - n^2)}$  (41)

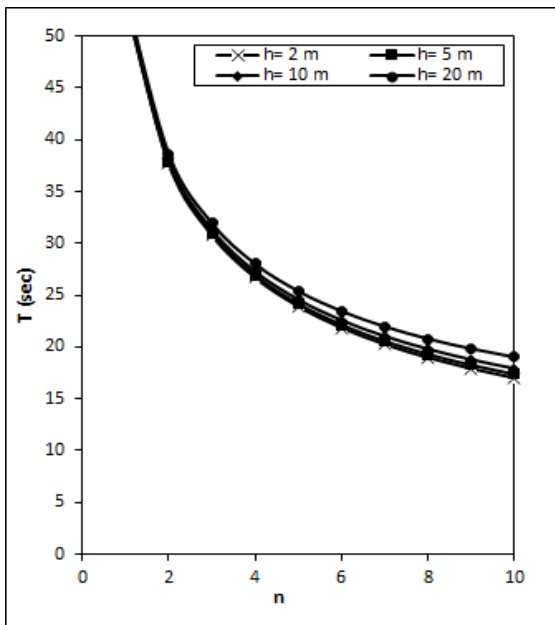
### 3. Results and Discussion



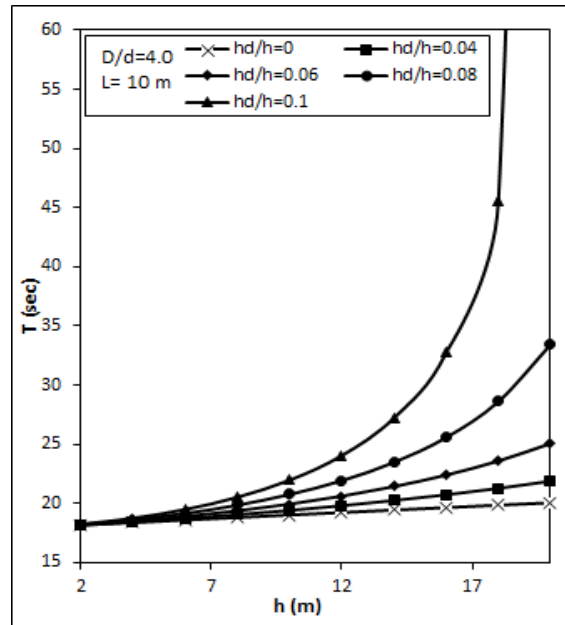
**Fig. 3.** Variation of the period of oscillation ( $T$ ) with the height ( $h$ ) of the column of water in circular tanks connected by a circular pipe for different values of  $D/d$ .



**Fig. 4.** Variation of the period of oscillation ( $T$ ) with the length ( $L$ ) of the connecting pipe for circular tanks connected by a circular pipe for different values of  $D/d$ .



**Fig. 5.** Variation of the period of oscillation ( $T$ ) with the number of connecting pipes ( $n$ ) for different water heights ( $h$ ) in the upright tanks.



**Fig. 6.** Variation of the time period ( $T$ ) with the vertical rise of water in upright tanks ( $h$ ) for different damping ratios ( $hd/h$ ).

Based on the theoretical analysis, a number of computer programs have been developed in Fortran 2003 and executed on the Core-2-Quad based processor. The computational results are plotted graphically. It may be noted that the expression for the frequency of oscillation (which has been derived in the preceding section) has been used for finding the period of oscillation ( $T$ ) using the well-known relationship  $T=2\pi/p$ . Furthermore, it is to be noted that the period of oscillation has been used as a key parameter for the analysis of results. It is clearly seen from Eqn (15) that the tank parameters (i.e. breadth, diameter and length of the tanks) do not affect the period of oscillation as long as the cross-sectional areas of the tanks are the same. So the results obtained are generalized using only circular tank connected by a circular pipe. The ratios of the diameter of the tank to the connecting pipe have been used to visualize the particular changes associated with the change in areas. Fig. 3 shows that as the height of the water column in the vertical tanks increase the time period increases but the rate of increase is very low. It is also observed that the period of oscillation increases rapidly with the increase of the ratio ( $D/d$ ) where  $D$  is the diameter of the vertical tanks and  $d$  the diameter of the circular pipe. Fig. 4 shows that the period of oscillation increases remarkably as the length of the connecting pipe increases but the variation is not linear. Furthermore, the period of oscillation increases rapidly with the increase of the ratio ( $D/d$ ). It is seen from Fig. 5 that the period of oscillation can be reduced significantly by increasing the number of connecting pipes. However, no remarkable change in the period of oscillation is observed with the change in the depth of water in the tanks. It is already mentioned in the previous section that additional damping forces arise from the friction between the moving fluid and the surrounding tank wall. This damping effect is clearly observed from Fig. 6 that the period of oscillation is found to increase significantly with the increase of the ratio  $h_d/h$  where  $h_d$  is the loss of height due to damping and  $h$  is the depth of water.

#### 4. Conclusions

The following conclusions can be drawn from the present study:

- (a) Firstly, an expression for the frequency of oscillation of water in two identical tanks has been derived assuming ideal fluid flow theory. Subsequently, the expression for the frequency of oscillation has been modified taking into consideration the additional damping forces which arise from friction between the moving fluid and the surrounding tank wall. Obviously, this theoretical model is more realistic than the one derived on the assumption of ideal fluid.
- (b) Both the circular and the rectangular tanks produce the same period of oscillation provided their cross-sectional areas are equal.
- (c) Once the tanks are installed on a ship, the dimensions of the tanks (length, breadth and diameter) cannot be changed. However, the depth of water in the tanks is the only parameter which can be varied to match with the ambient condition.
- (d) The period of oscillation is found to decrease sharply as the number of connecting pipes increases.
- (e) Finally, the period of oscillation is found to increase with the increase of the depth of water in the tanks. However, the rate of increase is quite low in case of ideal fluid flow assumption. On the other hand, the period of oscillation increases at a rapid rate with the depth of water when the effect of damping is taken into account.

#### 5. References

- [1] A. F. Gawad, A. S. Ragab, H. A. Nayfeh, and T. Mook, "Roll Stabilization by Anti-Roll Passive Tanks", *Ocean Engineering*, Vol. 28, pp. 457-469, 2001.
- [2] C. Holden, T. Perez, and T. I. Fossen, "A Lagrangian Approach to Non-Linear Modeling of Anti-Roll Tanks", *Ocean Engineering*, Vol. 38, pp. 341-359, 2011.
- [3] G. Samoilescu, and S. Radu, "Stabilizers and Stabilizing Systems on Ships", *Naval Academy Mircea Cel Batran, 8<sup>th</sup> International Conference, 2002*.
- [4] H. Frahm, "Results of Trials of the Anti-Rolling Tanks at Sea", *Journal of the American Society for Naval Engineers*, Vol. 23, Issue 2, pp. 571-597, 1911.
- [5] J. Bell, and W. P. Walker, "Activated and Passive Controlled Fluid Tank System for Ship Stabilization", *SNAME Transactions*, Vol. 74, pp. 150-193, 1966.
- [6] J. H. Chadwick, "On the Stabilization of Roll", *Proceedings of SNAME*, Vol. 63, pp. 237-280, 1955.
- [7] K. Tanizawa, T. Harukuni, and H. Sawada, "Application of NWT to the Design of ART", *Proceedings of the 13<sup>th</sup> International Offshore and Polar Engineering Conference*, pp. 307-314, 2003.
- [8] N. Minorsky, "Problems of Anti-Rolling Stabilization of Ships by the Activated Tank Method", *American Society of Naval Engineers*, Vol. 47, pp. 87-119, 1935.
- [9] R. C. Crockett, "Passive Anti-Roll Tanks", *Design Data Sheet, US Navy, Bureau of Ships*, 1962.
- [10] R. P. Dallinga, "Roll Stabilization at Anchor: Hydrodynamic Aspects of the Comparison of Anti-Roll Tanks and Fins", *MARIN*, 2002.
- [11] W. Froude, "Considerations Respecting the Rolling of Ships at Sea", *INA Transactions*, Vol.14, pp. 96-116, 1874.

## Implementation of Drive by Wire Technology Replacing the Conventional Vehicle Control System

Ahmad Jarjis Hasan<sup>1\*</sup>, Md. Zonayed Hossain<sup>1</sup>, G.M Sultan Mahmud Rana<sup>2</sup>, Niamat Ullah Ibne Hossain<sup>3</sup>

<sup>1\*,1,2,3</sup> Department of Mechanical Engineering, Khulna University of Engineering & Technology, Khulna-9203, Bangladesh

E-mail: [jarjishasan@gmail.com](mailto:jarjishasan@gmail.com), [niamat.hossain@gmail.com](mailto:niamat.hossain@gmail.com)

### Abstract

*Drive by Wire technology is one important step of taking the car's mechanical control to a computerized one. This technology will take driving to the next level where driving will be a very less complicated task. This paper will concentrate on cars with automatic transmission only. Here we will discuss about converting the mechanical controlled car to a car with Drive by Wire technology. This will include micro-controllers, actuators, sensors etc. Nowadays the combustion engines are totally microcomputer controlled. This paper will focus on controlling steering, acceleration, deceleration and brake. Gear shifting and Hand brake are considered as secondary control and are out of the concern of this paper. The total driving system is operated by a simple 4\*4 matrix keypad. The complete functionality is also explained. A Steer by Wire system has been constructed, which is without mechanical backup while acceleration and brake system is mechanically backed up.*

**Keywords:** Drive-by-wire, Steering control, Break and acceleration control

### 1. Introduction

Drive-by-wire is a catch-all term that can refer to a number of electronic systems that take the place of old mechanical controls. Instead of using cables, hydraulic pressure, and other things that provide the driver with direct, physical control over the speed or direction of a vehicle, drive-by-wire technology uses electronic controls to activate the brakes, control the steering, and operate other systems [1]. There are many people who can't drive correctly, find it hard and thus doesn't get a driving license either. Drive by Wire is a possible and simple solution for them as, this makes driving a lot easier. It is like, holding a keypad and pushing up, down, right, left and the car responds. It's like playing a game where you need to drive. This technology can give the car very good maneuverability, much easier control and confidence. Multi-button presses give the ability of driving the car almost as you wish. Accelerate or decelerate the car along with turning, even drifting all is possible. Hydraulic pressure is needed in the power steering system nowadays which is responsible for more power consumption. But here a Steer by Wire technology is enabled which doesn't require hydraulic power.

A good free control response refers to a well damped return-to-center of steering wheel from an off-center release, or due to an impulsive (jerk& release) excitation from on-center [2]. Here, IR sensors are used to determine the center of the wheel which maintains free control.

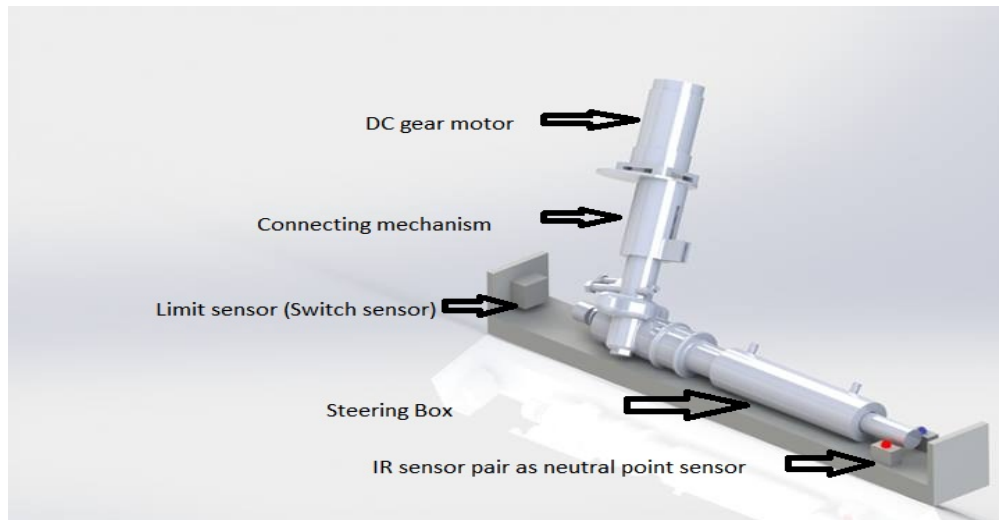
### 2. Steering Control

Steer-by-wire (SBW) systems allow the amount of steering wheel operation to be transmitted in the form of electric signals to the vehicle wheels. These systems help improve control performance for vehicle safety while increasing vehicle design freedom. Thus, this type of system seems to have promise as a next generation automotive steering system [3]. Here a DC gear motor is mounted on a steering box (rack and pinion type). The DC motor is controlled by a microcontroller.

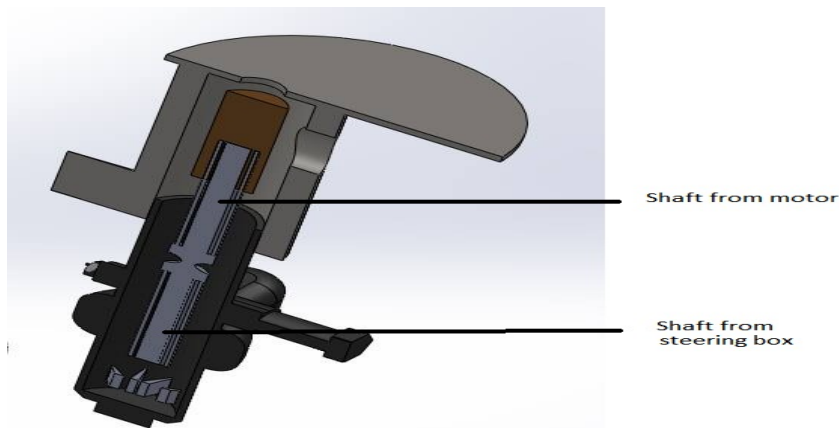
This Steer by Wire system eliminates the need of hydraulic power for the steering system and replaces this with a rotary actuator. This is how the power consumption is greatly reduced. There are two limit sensors at the end points of the rack to send feedback to the control unit that the end point has reached and the motor will not turn further. The response from the keypad will lead the car. This is explained in the following tabular form.

**Table 01:** Car Direction according to the response from Keypad

Keypad Button	Motor Direction	Rack Direction	Car Direction
4	Clockwise	Left	Left
6	Counter-clockwise	Right	Right



**Fig. 2.1:** Construction of the Steering Control system in order to imply Steer-by-wire (Rendered from Solidworks 2013 premium)



**Fig. 2.2:** Cross section of the connecting mechanism (Rendered from Solidworks 2013 premium)

**Free Control:**

For free control of the vehicle (which was previously described), one IR sensing system has been implemented. The rack can go 11.5 cm left from the last limit to the right. An IR transmitter and a receiver is set in across the rack to sense the center point (at 5.75cm from the last limit to the left). The button number 5 in the keypad is used to activate the free control. At full speed of the motor (2A, 12V and defined speed 255 in microcontroller), the rack moves 2.5 cm (average) per click. Holding the buttons pressed is also possible and the rack will move continuously. The performance of the steering can be tuned by changing the input of the microcontroller program. The defined motor speed can vary from 0 to 255.

**Performance tuning of the Steer by wire system:**

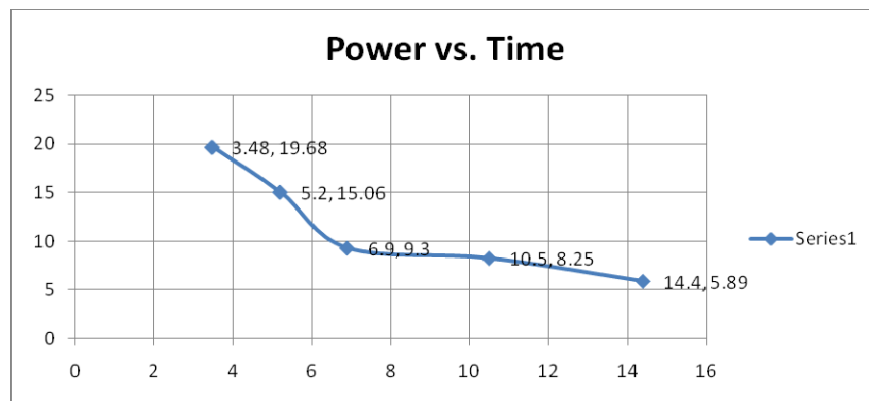
After implying variable power source to the steering control system (while the acceleration and break controls are ineffective), the time required to rotate the steering fully from left to right has been measured along with the variable power.

As stated earlier, the rack can go 11.5 cm left from the last limit to the right. But it is to be noted that the rack takes different amount of time, to reach the sensor placed at right side, due to the variation of power supply. The observation to measure the time variation is presented below.

**Table 02:** Measurement of required time with variable power source

Observation No.	Current (in mA)	Voltage applied (in volts)	Power (in miliwatts)	Time needed to overcome 11.5 cm (in seconds)
01	78	2	0.156	The Rack does not move
02	870	4	3.48	19.68
03	1010	5	5.2	15.06
04	1150	6	6.9	9.30
05	1500	7	10.5	8.25
06	1800	8	14.4	5.89

After plotting the obtained values (Table 02) of Power along the abscissa and time needed vertically, the following graphical form appears.



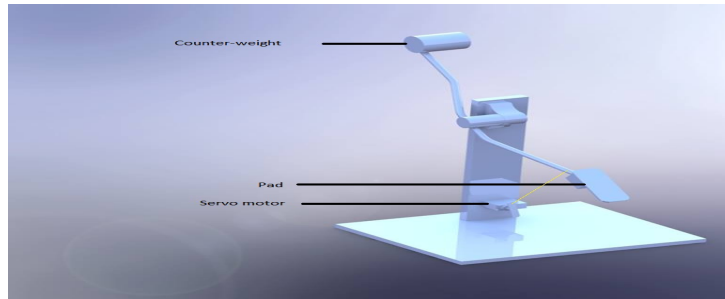
**Fig. 2.3:** Variation of Time necessary in accordance with Power supply variation

This graph shows us that, without minimum power the motor will not start. Then with the increase in power the required time to reach the end point decreases. That also means the rotation of the motor shaft and speed of rack increases with increasing power input.

**3. Acceleration and Deceleration control**

The acceleration and deceleration control is mechanically backed up and the control is directly applied to the acceleration pad. A servo motor is connected to the acceleration pad. The servo motor is controlled by the

micro-controller. Button 2 and 3 controls acceleration and deceleration simultaneously. Holding these buttons will continuously rotate the servo but if buttons are clicked only, 5 degrees rotation will occur per click.



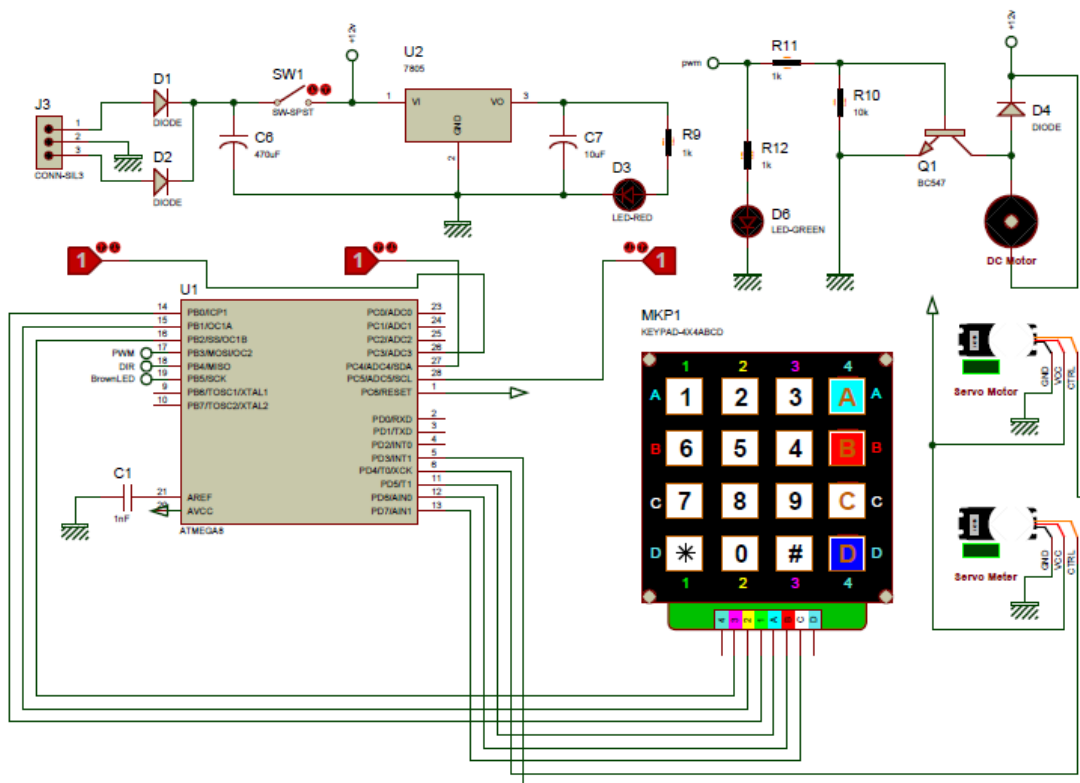
**Fig.3.1:** Acceleration pad (Rendered from Solidworks 2013 premium)

#### 4. Brake control

The braking system is mechanically backed up and the control is directly applied to the brake pad. This system is same as the Acceleration-deceleration control. Just this is applied on the brake pad. Button 7 and 9 controls brake on and release simultaneously.

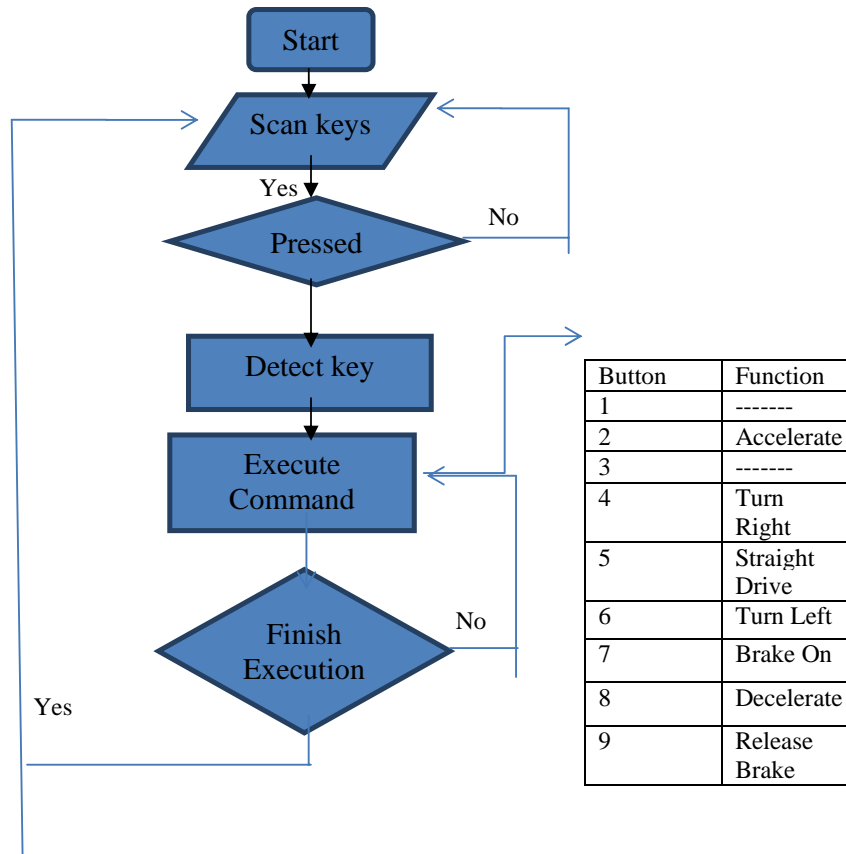
#### 5. Control System

The circuit diagram of the control system is illustrated below:



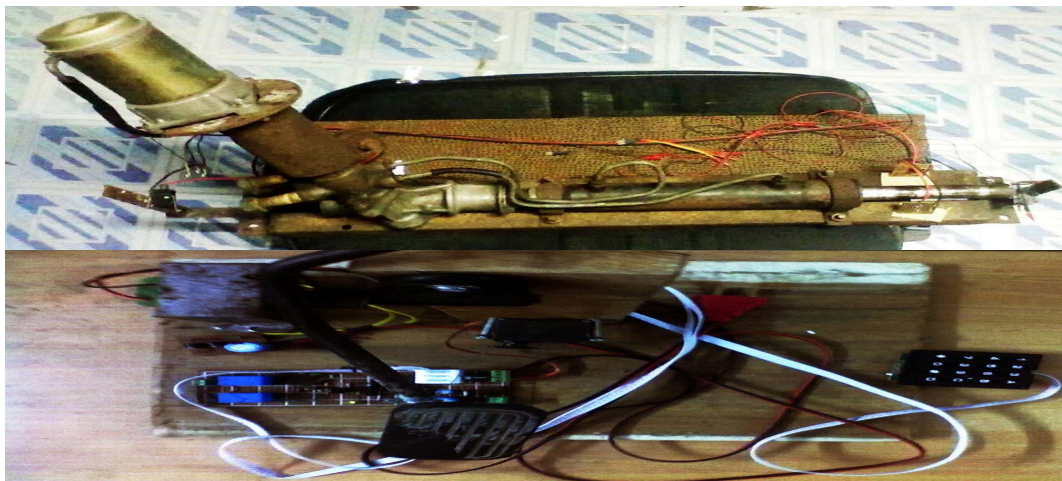
**Fig. 5.1:** Circuit diagram of the control system

Here the DC gear motor has been used to control the steering box. The servo motors are for acceleration and brake control. The keypad is used as the input. This sends signals to the microcontroller and the controller performs the action. The microcontroller sends the necessary signals to the motors and they perform the pre-programmed task.



The flow diagram of the algorithm is as shown above.

### 7. The Final Construction:





## 8. Conclusion

Drive by wire technology has been developed here but hydraulics still plays a vital part in acceleration and brake control. Hopefully it will be taken care of in near future. The steer by wire system works perfectly as was expected. Light, horn and other indicative systems will be controlled by the same keypad in the future. A nice thing is, a car does not have to be made with this technology. Any car with automatic transmission can be converted to have this marvelous technology.

## 9. References:

- [1] Laukkonen, J. (n.d.). What is Drive-by-Wire Technology? Retrieved from <http://cartech.about.com/od/Safety/a/What-Is-Drive-By-Wire-Technology.htm>
- [2] Amberkar,S., Bolourchi,F., Demerly,J.,Millsap, S., “A Control System Methodology for Steer by Wire Systems”,*SAE Technical Paper Series*, 2004
- [3] Mogi, K., Sugai, T.,Sakurai, R., Suzuki, N., “Development of a New Steer-by-wire System”,*NTN Technical Review No.79*, 2011

## PLC Based Automatic Railway Gate Control & Remote Monitoring System Khandaker Marsus , Md. Selim Habib, Mohammad Ezaz Hossain , Md. Reaz Uddin, Md. I.H.

Bhuiyan

Department of Electrical & Electronic Engineering,  
Rajshahi University of Engineering & Technology

E-mail: [kmarsus@gmail.com](mailto:kmarsus@gmail.com), [selim041073@yahoo.com](mailto:selim041073@yahoo.com), [ezaz.hossain@banglacad.com](mailto:ezaz.hossain@banglacad.com),  
[reaz.uddin@banglacad.com](mailto:reaz.uddin@banglacad.com), [imam.hossain@banglacad.com](mailto:imam.hossain@banglacad.com)

### Abstract

*The objective of this paper is to provide an automatic railway gate at a level crossing replacing the gates operated by the gatekeeper. It deals with two things. Firstly, it deals with the reduction of time for which the gate is being kept closed and secondly, to provide safety to the road users by reducing the accidents. By the presently existing system once the train leaves the station, the stationmaster informs the gatekeeper about the arrival of the train through the telephone. Once the gatekeeper receives the information, he closes the gate depending on the timing at which the train arrives. Hence, if the train is late due to certain reasons, then gate remain closed for a long time causing traffic near the gates. By employing the automatic railway gate control at the level crossing the arrival of the train is detected by the pressure switch placed near to the gate. Hence, the time for which it is closed is less compared to the manually operated gates and also reduces the human labor. This type of gates can be employed in an unmanned level crossing where the chances of accidents are higher and reliable operation is required. Since, the operation is automatic; error due to manual operation is prevented. And finally a computer based monitoring system is applied to the crossing area. This could be monitored through internet from anywhere. That's why any unusual problem could be easily solved remotely. Automatic railway gate control is highly economical with PLC based arrangements that could be designed for using in almost all the unmanned level crossings in the country.*

**Keywords:** Railway gate control, railway remote controlling system.

### 1. INTRODUCTION

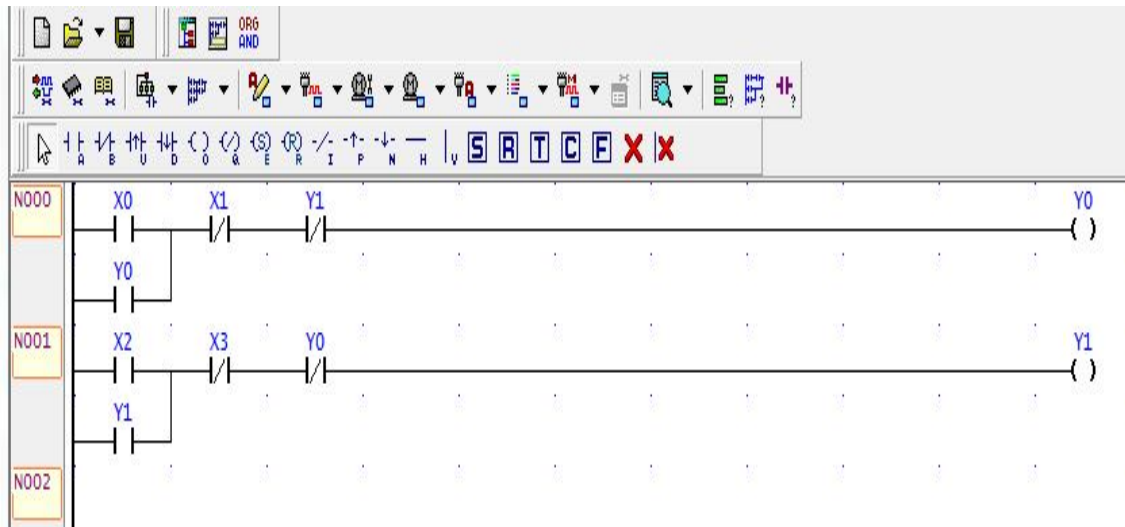
In this paper I am concerned of providing an automatic railway gate control at unmanned level crossings replacing the gates operated by gate keepers and also the semi automatically operated gates. It deals with two things. Firstly, it deals with the reduction of time for which the gate is being kept closed. And secondly, to provide safety to the road users by reducing the accidents that usually occur due to carelessness of road users and at times errors made by the gatekeepers. By employing the automatic railway gate control at the level crossing the arrival of train is detected by the pressure switch placed on either side of the gate at about 5km from the level crossing. Once the arrival is sensed, the sensed signal is sent to the PLC. Subsequently, buzzer indication and light signals on either side are provided to the road users indicating the closure of gates. The departure of the train is detected by pressure switch placed at about 1km from the gate. The signal about the departure is sent to the PLC, which in turn operates the motor and opens the gate. Thus, the time for which the gate is closed is less compared to the manually operated gates since the gate is closed depending upon the telephone call from the previous station. Also reliability is high as it is not subjected to manual errors.

### 2. CIRCUIT DIAGRAM & DESCRIPTION

Programming software WPL has been utilized in this project. WPL-Programmer is a PLC programming tool for the creation, testing and maintenance of programs. It provides facilities for the support of PLC devices and address information and for communications their supported network types.

### 3. LADDER DIAGRAM

In this paper, we define an event is the occurrence of pressure pulse created by train wheel. Here is the plc ladder diagram for whole logic.



### 3.1 PLC CONNECTION DIAGRAM

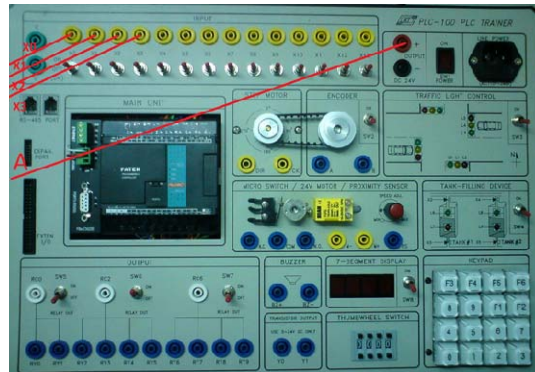


Fig. 1 Experimental setup

### 3.2 BUZZER & RELAY CONNECTION

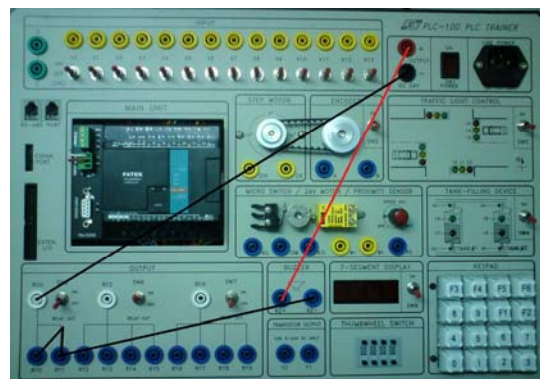


Fig. 2 Sound sensing circuitry

### 3.3 WORKING PRINCIPLE

In this project the PLC connected with the project. And when a train passes over the pressure sensor it just get a pulse. This pulse is received by PLC. PLC count the pulse does the work accordingly. Again when trains leave the crossing it also acts in the same way.

#### 4 REMOTE MONITORING SYSTEMS

Remote monitoring system works thorough as real-time guard. A computer based monitoring system is applied to the crossing area. This could be monitored through internet from anywhere. That's why any unusual problem could be easily solved remotely. For remote monitoring system it needs different technical side. Sever side, camera side, streaming side, display computer and website combines the whole work.

##### 4.1 STREAMING

Streaming media is multimedia that is constantly received by and presented to an end-user while being delivered by a provider. Its verb form, "to stream", refers to the process of delivering media in this manner; the term refers to the delivery method of the medium rather than the medium itself. A client media player can begin playing the data (such as a movie) before the entire file has been transmitted. Distinguishing delivery method from the media distributed applies specifically to telecommunications networks, as most other delivery systems are either inherently streaming (e.g., radio, television) or inherently nonstreaming (e.g., books, video cassettes, audio CDs). For example, in the 1930s, muzak was among the earliest popularly available streaming media; nowadays Internet television is a common form of streamed media. The term "streaming media" can apply to media other than video and audio such as live closed captioning, stock ticker, and real-time text, which are all considered "streaming text".

Live streaming, delivering live over the Internet, involves a camera for the media, an encoder to digitize the content, a media publisher, and a content delivery network to distribute and deliver the content.

##### 4.2 SETUP

The total settings are containing with some software and web server.

##### 4.3 VIDEO CAPTURING UNIT

Capturing unit is the use of video cameras to transmit a signal to a specific place, on a limited set of monitors. It differs from broadcast television in that the signal is not openly transmitted, though it may employ point to point (P2P), point to multipoint, or mesh wireless links.



Fig :4.1 Capturing unit for real-time video

##### 4.4 STREAMING SYSTEM

Live stream works with the following system:

Stream output is the name of the feature of broadcasting that allows outputting any stream read by file or as a network stream instead of displaying it. Different kind of processing can be applied to the stream during this process (transcoding, re-scaling, filters, re-muxing...). Stream output includes different modules, each of them having different capabilities. One can chain modules to enhance the possibilities. Standard allows to send the stream via an access output module: for example, UDP, file, HTTP, ... You will probably want to use this module at the end of your chains.

transcode is used to transcode (decode and re-encode the stream using a different codec and/or bitrate) the audio and the video of the input stream. If the input or output access method doesn't allow pace control (network, capture devices), this done "on the fly", in real time. This can require quite a lot of CPU power, depending on the parameters set. Other streams, such as files and disks are transcoded as fast as the system allows it.

duplicate allows you to create a second chain, where the stream will be handled in an independent way.

display allows you to display the input stream, as VLC would normally do. Used with the duplicate module, this allows you to monitor the stream while processing it.

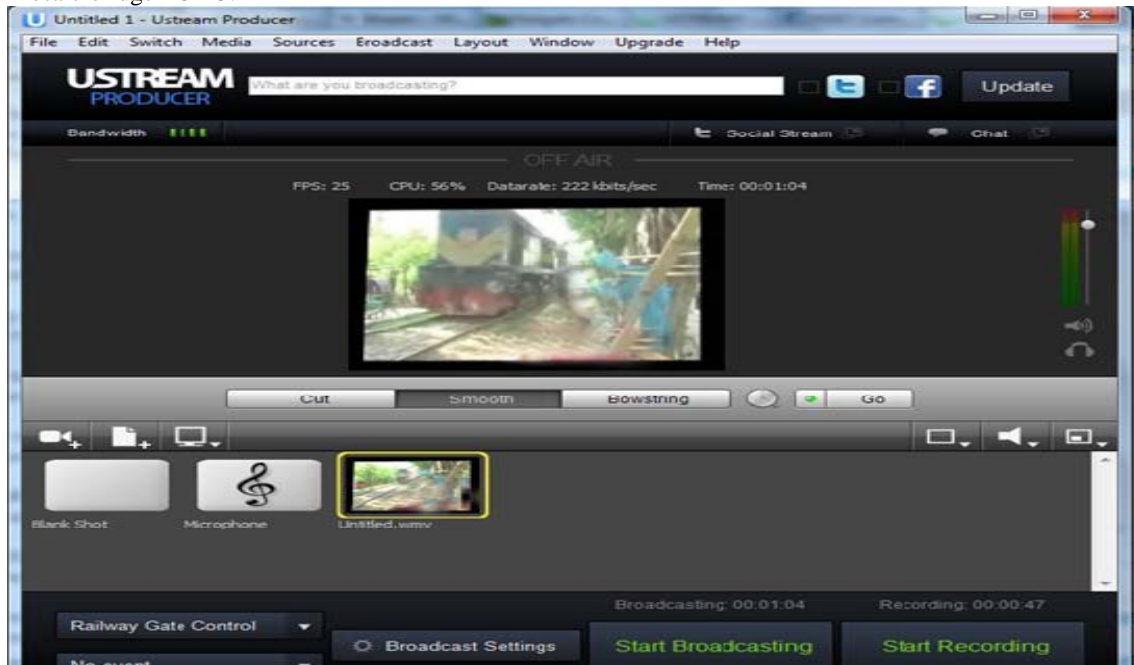
rtp streams over RTP (one UDP port for each elementary stream). This module also allows RTSP support.

es allows you to make separate Elementary Streams (ES) out of an input stream. This can be used to save audio and video streams to separate files, for instance.

bridge-out TODO

bridge-in TODO

Mosaic-bridge TODO.



#### 4.5 REMOTE CONTROL ADMINISTRATOR & USER LOGIN

This website part is for using in control room. First the controller needs to get the user name and password from the system administrator. Then he will be eligible to access the videos. The video section also categories with different sections. Such as, one unit in one section and rest units in others. One unit may contain 25-30 video players. That can control the amount of rail crossing. Presently the site is available at [bdallinfo.com/railway](http://bdallinfo.com/railway).



#### **4.6 ADMINISTRATOR AREA**

Administrators, commonly known as admins or sysops (system operators), are rail gate controller who have been granted the technical ability to perform certain special actions on controlling, including the ability to control train, block vehicles, allow pedestrians etc. tools.

This is the real view of controlling system. From the videos the operator can take any decision and can give any command from remote.

#### **5 CONCLUSIONS:**

The world has started experiencing more digital devices that has made observation and response according to situation demand much easier. By using this application we hope that railway accidents in Bangladesh could be reduced in a significant number.

#### **References**

- [1]. Robert L. Boylestad, "Introductory Circuit Analysis", Division of Bell & Howell Company, 1995
- [2] V.K. Mehta and Rohit Mehta, "Principle Of Electronics", S.Chand & Company Ltd, 2008
- [3] B.L Theraja and A.K Theraja, "A text Book Of Electrical Technology (AC & DC Machines)", S.Chand & Company Ltd. 2002
- [4] Russel M Kerchner and George F Corcoran, "Alternating-Current Circuits", Fourth Edition, John Wiley & Sons Int. 2006
- [5] A.K Shawney, "Measurement & Instrumentation",
- [6] V.K. Mehta and Rohit Mehta, "Principle Of Power System", S.Chand & Company, 2010
- [7] J. Wilson & J.F.B. Hawkes, "Optoelectronics An Introduction", Prentice-Hall Int, Second Edition, 2000
- [8] S.B. Morris, "Programmable Logic Controllers", New Jersey, Prantice Hall, Inc., 1995
- [9] F.D. Petruzella, Programmable Logic Controllers 3th Ed, Singapore, McGraw – Hill International Edition, 2005.
- [10] C.K. Meng, Y. Away, N.F. Elias & A.S. Prabuwo, The Real-Time Visual Inspection System For Bottling Machine, 2000
- [11] Bolton, W. Mechatronics: Electronic Control Systems in Mechanical and Electrical Engineering, 3rd edition Pearson Education, 2004.
- [12] <http://en.wikipedia.org/wiki/File:transformer-load>
- [13] <http://program-plc.blogspot.com>
- [14] [http://en.wikipedia.org/wiki/Programmable\\_logic\\_controller](http://en.wikipedia.org/wiki/Programmable_logic_controller)
- [15] <http://www.plcmanual.com>

## Harvesting Energy from Sound and Vibration

Arifur Rahman<sup>1</sup> and M. E. Hoque<sup>2</sup>  
Department of Mechanical Engineering  
Rajshahi University of Engineering & Technology  
Tel. & Fax: (+880) 721-750319.  
E-mail: [saimon.bis@gmail.com](mailto:saimon.bis@gmail.com)<sup>1</sup>, [emdadulhoque@gmail.com](mailto:emdadulhoque@gmail.com)<sup>2</sup>.

### Abstract

Recently, scientist and researcher are trying to seeking new source of energy because energy is needed everywhere and every time. Vibration and sound are one kind of unconventional mechanical energy source which is lost everywhere. Our main goal is to utilize and save this lost energy. In this industrialization, every heavy machines and industrial appliances produce sound and vibration at a time. This paper shows the process of harvesting from these lost energy by using piezoelectric material. Piezoelectric materials have a crystalline structure that provides them with the ability to transform mechanical strain energy into electrical charge and, vice versa, to convert an applied electrical potential into mechanical strain. This property provides these materials with the ability to absorb mechanical energy from their surroundings, usually ambient vibration, and transform it into electrical energy that can be used to power other devices as well as storing in battery.

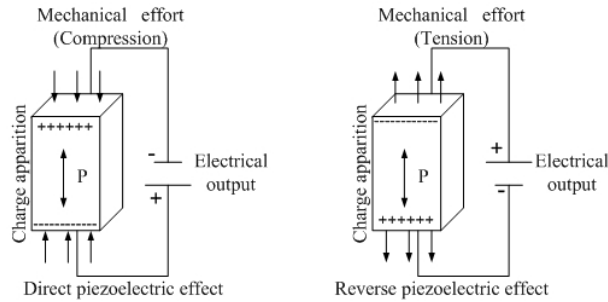
**Keywords:** Vibration, sound, piezoelectric material, harvesting energy, electrical energy.

### 1. Introduction

The increasing desire for completely self-powered electronics has caused the amount of research into power harvesting devices to become progressively larger over the last decade. One early study into power harvesting was investigated the ability to generate energy from the expansion and contraction of the rib cage during breathing. A prototype of the power harvesting system was constructed using polyvinylidene fluoride (PVDF) film and was implemented *in vivo* on a mongrel dog. The prototype was demonstrated to produce a peak voltage of 18V, which corresponded to a power of about 17 $\mu$ W. The discovery of a strong piezoelectric effect in polyvinylidene fluoride (PVDF) polymer, by Kawai in 1969 [1], further added many applications where properties such as mechanical flexibility are desired. With the research into power harvesting devices growing, it was determined that the power found from this system is not so high that is why its power is basically used for portable electronic devices as a self-powered device or it can be saved in battery for later usage [2]. With the recent advances in wireless and MEMS technology, sensors can be placed in exotic and remote locations. Since these devices are wireless it becomes necessary that they have their own power supply. The power supply in most cases is the conventional battery; however, problems can occur when using batteries because of their finite life span. Furthermore, in the case of sensors located on civil structures it is often advantageous to embed them, making access impossible. In this paper, a device has been developed by using fundamental characteristics of piezoelectric effect to utilize and convert the mechanical vibration to electric power.

### 2. Fundamentals of piezoelectric material

The conversion of mechanical energy into electrical one is generally achieved by converters alternator type or commonly known dynamo. But there are other physical phenomena including piezoelectricity that can also convert mechanical movements into electricity. The piezoelectric effect exists in two domains, the first is the direct piezoelectric effect that describes the material's ability to transform mechanical strain into electrical charge and the second form is the converse effect, which has the ability to convert an applied electrical potential into mechanical strain energy as shown in Fig. 1. The piezoelectric materials that exist naturally as quartz were not interesting properties for the production of electricity, however artificial piezoelectric materials such as PZT (Lead Zirconate Titanate) present advantageous characteristics. The piezoelectric strain coefficients describe the relationship between the applied electric field and the mechanical strain produced. Characteristic features [3] of soft piezo ceramic materials are comparably high domain mobility and resulting "soft ferroelectric" behavior, i.e. it is relatively easy to polarize which is used for sound conversion and "Hard" PZT materials can be subjected to high electrical and mechanical stresses which is used for vibration.



**Fig. 1.** Piezoelectric effect

### 3. Sound and noise as energy

Sound is a form of mechanical energy produced by vibrations. A wave is a disturbance that transfers energy through matter or space. It travels in longitudinal (compression) waves and moves much slower than the speed of light. In engineering, noise is defined as a signal that interferes with the detection of or quality of another signal [4]. Basically, noise is unwanted sound. It is a pollutant and a hazard to human health and hearing. Table 1 shows the different sound levels which are usually used. The high intensity sound or noise is shown in table 2 and has sufficient energy for conversion. There are several terms of measuring sound considered as main factors of EMS like types of sound source, sound intensity, pressure power, power level, velocity, types of wave, Frequency and pitch.

**Table 1.** Loudness of sound in decibel. **Table 2.** Some sound sources with power [5].

Sound	Loudness (dbs)	Hearing damage
Average Home	40-50	No
Loud Music	90-100	After long exposure
Rock concert	115-120	Progressive
Jet engine	120-170	pain

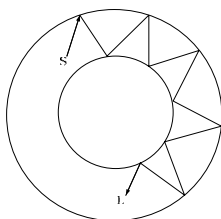
Situation And Sound source	Sound power Pac watt	Sound power Level $L_w$ db re $10^{-12}$ W
Rocket engine	1000000	180
Turbojet engine	10000	160
Siren	1000	150
Rock concert	100	140
Machinegun	10	130

### Energy equation of progressive wave [6]

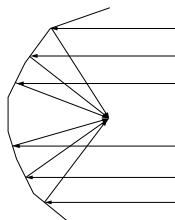
For a particle vibrating simple harmonically, the general equation of displacement,  $Y = a \sin(\omega t + \alpha)$ . Here  $y$  is the displacement and  $a$  is the amplitude and  $\alpha$  is the epoch of the vibrating particle and  $\omega$  is the angular velocity. The total (kinetic + potential) energy of a vibrating particle,  $E = 2\pi^2 m a^2 n^2$ . This energy is supplied by source that is, Energy transfer per unit area per second =  $2\pi^2 \rho n^2 a^2$ .

### 4. Amplification of sound

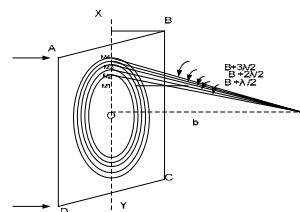
As the high output energy is dependent on the high deflection of piezoelectric material so it can be said that if the source sound intensity and pressure can be raised then energy will be high. There are several methods [7] of amplification of sound. The method of Fig. 2 and 3 is called whispering galleries and Fig. 4 represents the intensity of sound at a point due to a plane wave front. In this method, basically sound waves are redirected at a point which is usable in this experiment to raise sound intensity.



**Fig. 2**



**Fig. 3**



**Fig. 4**



## 5. Mechanical vibration

Vibration is the motion of a particle or a body or system of connected bodies displaced from a position of equilibrium. Most vibrations are undesirable in machines and structures because they produce increased stresses, energy losses, induce fatigue. Vibration occurs when a system is displaced from a position of stable equilibrium. The system tends to return to equilibrium position under the action of restoring forces. The system keeps moving back and forth across its position of equilibrium.

### Energy and power expressions of vibration [7]

This section will review some important ideas in energy and power in mechanical systems. If an increment of mechanical work on a particle of mass  $M$  is denoted as  $\Delta W$ , then this amount of work can be calculated using the force applied to the particle along the incremental change in path,  $dr$ , of the particle as follows:

$$\Delta W = F \cdot dr \quad (1)$$

where the  $\cdot$  denotes a dot product between the force and differential displacement vector. Because the kinetic energy,  $T$ , of a particle is equal to the rate of change in  $\Delta W$  with time, a convenient expression for  $T$  can be derived as follows:

$$\frac{dT}{dt} = \lim_{\Delta t \rightarrow 0} \frac{\Delta W}{\Delta t} = F \cdot \frac{dr}{dt} \quad (2)$$

## 6. Experimental setup and procedure

Figure 5 shows the block diagram of this harvesting process. The wave emits from sound source has no any specific direction. It spreads into several directions around the source. That is why it is very tough to accumulate all sound pressure in a point. In this paper a device has been designed which can focus several waves within its range in a point and increases the sound intensity at a focus point shown in Fig.6 and 7. Its helps to better displacement of piezo material which is kept into focus point as well as better output voltage. Figure 7 shows the dimensions of the design of focusing cone. Sound wave from different direction can be reflected by sound reflector face and the reflected wave is focused on the piezo material. Thus the intensity of sound has been increased by using this device and more energy can be converted.

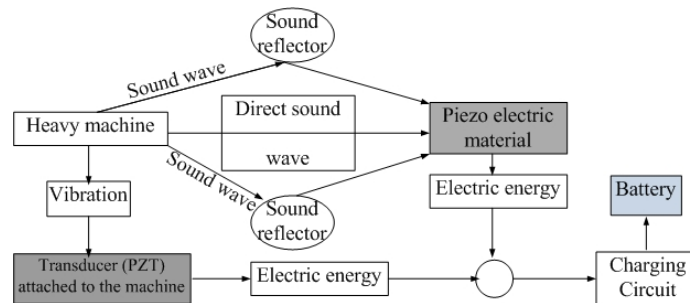


Fig. 5. Block diagram of harvesting energy vibration and sound source.

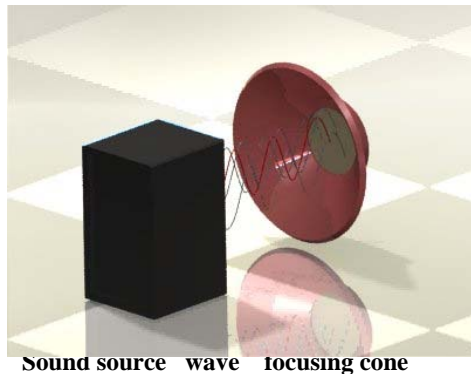


Fig. 6. Striking the piezo material by sound pressure (Solid works drawing)

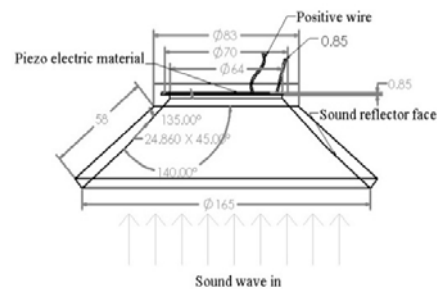
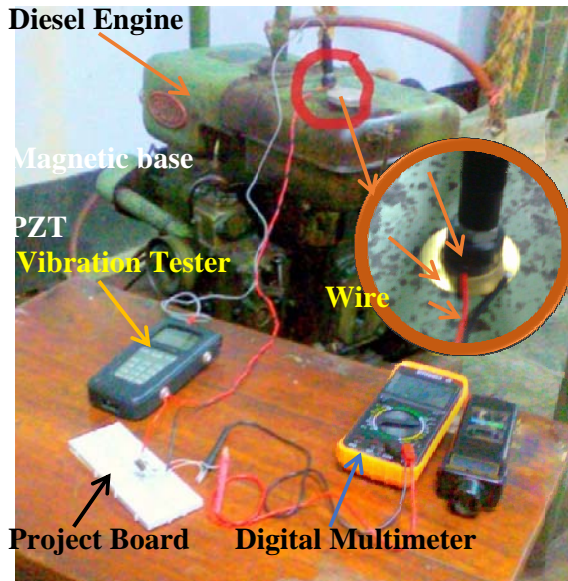


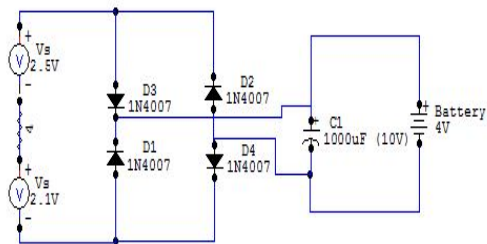
Fig. 7. Piezoelectric device (focusing cone) for converting sound to electric energy.

Figure 8 shows experimental set up which depicts that a heavy machine like diesel engine releases mechanical energy means of sound and vibration at a time. These two energy is our target for transducing. Sound waves which emit from machine spread around the ambient so it needs to be concentrated in a point to increase its intensity which is described in theory previous. For this reason, our designed focusing cone is used to capture sound wave and to redirect the sound wave in a specific point on piezoelectric material for getting higher sound pressure. This focusing cone is placed in front of machine in several positions so that it can capture several sound waves. When the higher intensity sound strikes piezoelectric material in focusing cone, then it produce comparatively high electric energy.

At the same time machine creates vibration which is undesirable and loss of energy. Figure 8 also shows the 7.5 Hp Beco Diesel Engine as a vibration source running at 1100 rpm. A vibration tester was used to measure the displacement, velocity, acceleration of the vibration. Piezoelectric material which is attached on the machine produces voltage. These two voltages found from sound and vibration is sum up through charging circuit (Fig. 9) and finally stored on battery.



**Fig. 8.** Experimental setup on 7.5 Hp Beco Diesel Engine.



**Fig. 9.** Circuit diagram of charging battery.

## 7. Analysis of charging circuit and connection

Due to stress and strain caused by vibration to the piezoelectric material, dual polarity of charge results in an alternating current (AC), which is then converted into direct current (DC) by a full bridge rectifier. The rectified current is then used to charge a capacitor or a battery, which can hold energy. The maximum power transfer technique will be used to design the circuit for this energy conversion. AC-DC converter [8] is used to maximize the power transfer to the load. The reason to use AC-DC converter is to convert a variable input voltage into a constant output voltage. Figure 9 shows the circuit diagram including full bridge rectifier. The optimal power transfer is achieved when the operating rectifier output voltage is half the open circuit voltage; this assumption allows the effective loss factor of the system to be dependent only on the coupling coefficient. If the device number can be increased then the output voltage may be found in satisfaction level in spite of dropping some voltage.

### Parallel and series connection of piezoelectric film

Since the power output from a single piezo-film was extremely low, combination of few piezofilms was investigated. Two possible connections were tested - parallel and series connections. The parallel connection did not show significant increase in the voltage output. With series connection, additional piezo-film results in increased of voltage output but not in linear proportion [9]. This may be due to the non-linear modification of internal impedance of the system. Further investigation is required to explain this non-linearity occurrence. If this is understood, an artificial modification could be added into the system to achieve the ultimate goal of producing high voltage output with high current density.

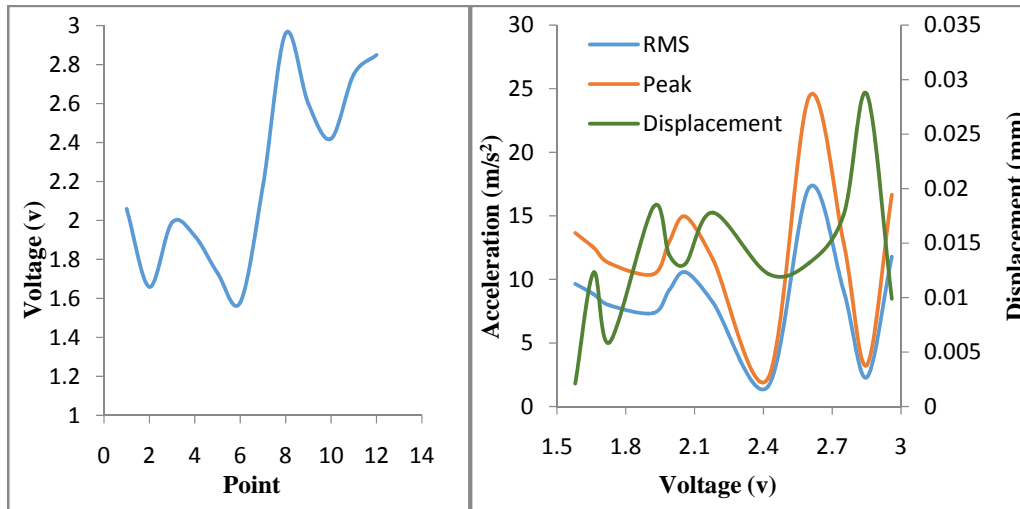
## 8. Experimental results and discussion

The output voltage which is the result of deflection of piezoelectric material fluctuates in the range about 1.5-3.0 volt. At the same time the amount of current is very low in mA ranges that are the power harvested from this experiment is small in amount. The material was placed in several positions on diesel engine. As the vibration rate of engine is not same at different places so the voltage found varies with respect to position. Table 3 shows the acceleration of rms and peak value, velocity, displacement and voltage. Data from table has been presented in graph which depicts clearly. In fig. 10(a), high voltage 2.96v is found at point 8 on the machine as well as the high voltage is recorded at high acceleration at the same point on the machine.

**Table 3.** Acceleration, velocity, displacement and voltage on different point of diesel engine.

point	Acceleration $m/s^2$		Velocity $cm/s$	Displacement $mm$	Voltage $v$
	Rms	Peak			
1	10.57	14.95	0.489	0.0131	2.06
2	8.84	12.50	0.191	0.0123	1.66
3	9.17	12.98	0.489	0.0139	1.99
4	7.36	10.41	0.431	0.0183	1.92
5	7.96	11.26	0.204	0.0059	1.73
6	9.65	13.65	0.189	0.0021	1.58
7	8.18	11.57	0.335	0.0178	2.18
8	11.78	16.66	0.462	0.0099	2.96
9	1.56	2.20	0.179	0.0122	2.42
10	9.11	12.89	0.471	0.0176	2.75
11	2.30	3.25	0.191	0.0287	2.85

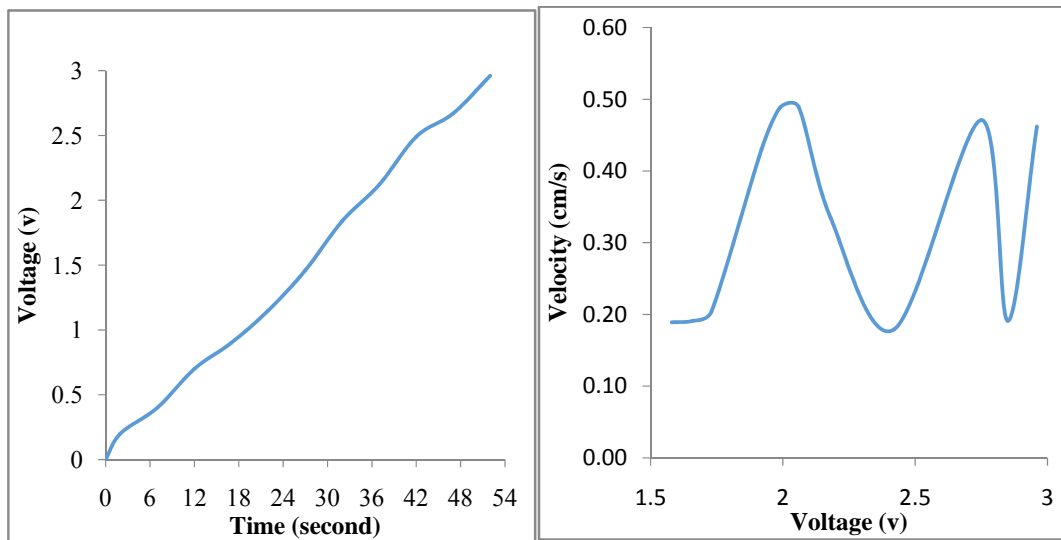
It is very clear from Fig. 10(b) that acceleration and displacement over voltage fluctuates very rapidly. In the region of voltage 2.6 to 3, Acceleration and displacement is high. From data table, at point 8 the voltage is high and at this point the voltage is gradually increasing with respect to time as shown in Fig. 11(a). There is no any abrupt fluctuation of voltage at the same time it is nonlinear voltage. Figure 11(b) follows the ideal curve of velocity and maximum velocity found in this experiment is 0.489 cm/s. The data recorded only on the basis of vibration. The harvesting energy from sound is very sensitive and complex. The method is mentioned above about sound and a prototype is also modeled which can transduce sound into electric energy. Finally this two energy is sum up in a circuit and stored in battery or used in MEMS. The major limitations facing researchers in the field of powerharvesting revolve around the fact that the power generated by piezoelectric materials is far too small to power mostelectronics.



(a) Voltage vs Point

(b) Acceleration and Displacement vs Voltage

**Fig. 10.** Output voltage at different point on the diesel engine.



(a) Voltage vs time at point 8

(b) Velocity vs voltage

**Fig. 11.** Output voltage representation over time at a fixed point and velocity at different point.

Therefore, methods of increasing the amount of energy generated by the power harvesting device or developing new and innovative methods of accumulating the energy are the key technologies that will allow power harvesting to become a source of power for portable electronics and wireless sensors. However, the rechargeable battery can be charged and then used to run any number of electronic devices for an extended period of time while being continuously charged by ambient motion. Innovations in power storage such as the use of rechargeable batteries with piezoelectric materials must be discovered before power harvesting technology will see widespread use.

## 9. Conclusion

In this paper a system has been developed which can transduce vibration and sound into electrical energy. In this project, the converted energy is measured in a voltage by proper experiment. The maximum voltage was found 2.96 volt. This paper shows the result found from only vibration which was practically done in lab on diesel engine. Different machines vibrate at different level and release energy at also different level. So this technology can be used in higher vibration sources for transducing higher energy. However, the research topic is also related to sound. For this reason a prototype model has been designed for converting sound energy to electric energy. This research has developed a model and process to generate power through the vibration and sound of any heavy machine using piezoelectric elements. The electrical energy harvested from ambient vibration and sound can then be used to power other devices or stored for later use. Despite some limitation of arrangements and materials the model was verified using experimental results and proved to be very accurate independent of excitation frequency. Further research is also necessary to implement both sound and vibration converting technology largely and integrate them in a structure for better future success of this project.

## 10. References

- [1] H. Kawai, "The piezoelectricity of PVDF". *Jpn. J. Appl. Phys.* **8**, 975–976 (1969).
- [2] Henry A. Sodano and Daniel J. Inman, Gyuhae Park, "Comparison of Piezoelectric Energy Harvesting Devices for Recharging Batteries", *LA-UR-04-5720, Journal of Intelligent Material Systems and Structures*, 16(10), 799-807, 2005.
- [3] Piezoelectric ceramic products, Piezotechnology, PI Ceramic ([www.piceramic.com](http://www.piceramic.com)).
- [4] M. J. Crocker, *Handbook of Acoustics*, John Wiley, New York, 1998.
- [5] [http://en.wikipedia.org/wiki/Sound\\_power](http://en.wikipedia.org/wiki/Sound_power) (1st July 2013 )
- [6] N. Subrahmanyam, Brij Lal, A Textbook Of Sound, Second revised edition, Chapter 4, Forced Vibrations and Chapter 9, Reflection, Refraction And Diffraction.
- [7] Prof. D. E. Adams, *Mechanical Vibrations*.
- [8] U K Singh and R H Middleton, "Piezoelectric Power Scavenging of Mechanical Vibration Energy", Australian Mining Technology Conference 2 - 4 October 2007.
- [9] Jedol Dayou, Man-Sang, C., Dalimin, M. N. and Wang, S. "Generating electricity using piezoelectric material", *borneo science* 24: march 2009.